



POLITECNICO
MILANO 1863

SCUOLA DI INGEGNERIA INDUSTRIALE
E DELL'INFORMAZIONE

Technical feasibility assessment for guarantee high IAQ standards using solar energy in a rural school in Santa Lucia Atlántico (Colombia)

TESI DI LAUREA MAGISTRALE IN
ENERGY ENGINEERING
INGEGNERIA ENERGETICA

Author: Lorenzo Di Salvatore

Student ID: 10560610

Advisor: Marcello Aprile

Co-advisor: Antonio Bula

Academic Year: 2021-22

Abstract

This thesis has been developed in cooperation with the Universidad del Norte with the aim of studying an alternative method of cooling the primary school classrooms of Santa Lucia, Atlantico, Colombia through the use of renewable energy. The starting point of the project was to identify and define the ideal conditions of thermal well-being and air quality in a tropical climate, to ensure that students' short- and long-term academic performance can improve or maintain high standards. For this reason, a lengthy review of the academic literature was carried out in order to define pointily values of temperature, ventilation and humidity to be used as set point values in the air conditioning system. The second phase of the project was the analysis of the meteorological data measured on site by colleagues of the Colombian university to clarify what were the real potential of the place and any problems that might arise. The third phase of the project consisted in trying to faithfully recreate a digital model of the building in the IES-VE software. It was then proceeded to the study and consultation of the project documents of the school as plans, sections and some datasheets of the materials used. In addition, on-site inspections were carried out, both to clarify all the technical aspects of materials and measures missing in the documentation, and to become aware of the entire work. Once the digital twin was defined, have been implemented and studied 2 different ventilation systems, a traditional split system installed in each class and a centralized ventilation system supported by fan coils installed in each class. Through the simulations carried out by means of the IES-VE software, it was possible to extract for each system all the data related to the thermal and electrical loads of the components involved, simulating an entire year of operation with a precision interval of 6 minutes. The obtained database was then used as a starting point for the dimensioning, through an Excel model, of the power production system through photovoltaic panels associated with a storage system. After having made the necessary comparisons and ascertained how the current state of the building affects the entire sizing of the ventilation system, power production and storage, Improvements to the building envelope have been considered to reduce thermal loads and consequently the battery storage system. It concludes by observing how the implementation of renewable energy on a school like the one in Santa Lucia can have a transversal socio-economic impact going to influence many aspects from a short and long term prospective.

Key-words: Renewables energy, Pv system, ventilation system, IAQ, Thermal Comfort

Abstract in italiano

Il presente elaborato di tesi è stato sviluppato in cooperazione con l'Universidad del Norte con l'obiettivo di andare a studiare un metodo alternativo di raffrescamento delle aule scolastiche della scuola primaria in Santa Lucia, Atlantico, Colombia attraverso l'uso di energia rinnovabile. Il punto di partenza del progetto è stato individuare e definire quali fossero le condizioni ideali, di benessere termico e di qualità dell'aria in un clima tropicale, per fare in modo che le performance accademiche di breve e lungo periodo degli studenti possano migliorare o mantenere standard elevati. Per questo motivo, una lunga revisione della letteratura accademica è stata effettuata in modo da poter definire valori puntuali di temperatura, ventilazione e umidità da usare come valori di set point nel sistema di condizionamento. La seconda fase del progetto è stata l'analisi dei dati meteorologici misurati in loco dai colleghi dell'università colombiana per chiarire quali fossero le reali potenzialità del luogo e le eventuali problematiche che potrebbero insorgere. La terza fase del progetto è consistita nel cercare di ricreare fedelmente un modello digitale dell'edificio nel software IES-VE. Si è quindi proceduto allo studio e alla consultazione dei documenti progettuali della scuola come planimetrie, sezioni e alcuni datasheet dei materiali usati. In aggiunta sono stati effettuati sopralluoghi in loco, sia per chiarire tutti gli aspetti tecnici di materiali e misure mancanti nella documentazione, sia per prendere coscienza dell'intera opera. Una volta definito il digital twin, si è passato all'implementazione e allo studio di 2 differenti sistemi di ventilazione, un tradizionale sistema split installato in ogni classe e un sistema di ventilazione centralizzato supportato da fan coil installati in ogni classe. Attraverso le simulazioni effettuate per mezzo del software IES-VE si è potuto estrarre per ciascun sistema tutti i dati relativi ai carichi termici e elettrici dei componenti coinvolti, andando a simulare un intero anno di funzionamento con un intervallo di precisione di 6 minuti. Il database ottenuto è stato poi utilizzato come punto di partenza per il dimensionamento, attraverso un modello Excel, del sistema di produzione di potenza tramite pannelli fotovoltaici associato ad un sistema di accumulo. Dopo aver effettuato i dovuti confronti e constatato come lo stato attuale dell'edificio influenzi l'intero dimensionamento del sistema di ventilazione, produzione di potenza e accumulo, sono stati presi in considerazione interventi di miglioramento dell'involucro edilizio per ridurre i carichi termici e conseguentemente il sistema di accumulo a batteria. Si conclude

osservando come l'implementazione di energie rinnovabili su una scuola come quella di Santa Lucia possa avere un impatto socioeconomico trasversale andando a toccare numerosi aspetti di breve e lungo periodo.

Parole chiave: Energie rinnovabili, Impianto fotovoltaico, impianto di ventilazione, IAQ, Comfort termico

Contents

Abstract	i
Abstract in italiano.....	iii
Contents	5
Introduction.....	8
1 Why considering improving comfort conditions in a rural school?.....	10
1.1. Analysis of the link between scholastic performances and IAQ and thermal comfort	10
1.1.1. Internal Air Quality	10
1.1.2. Thermal Comfort	16
1.2. Impact of schools on rural communities	22
1.3. Correlation between thermal comfort and cooling technologies in tropical climates.....	24
1.4. Overall conclusion on thermal condition, IAQ and cooling technologies influence on academic performance	27
2 Location and weather conditions evaluation	29
2.1. Dry Bulb Temperature	31
2.2. Relative Humidity.....	32
2.3. Irradiance levels	33
2.4. Wind speed measurement	34
3 Building structure and IES-VE digital twin constrains description.....	37
3.1. Spaces.....	37
3.2. IES-VE PRM structure and calculation model used	38
3.2.1. Physical Model Used by the Software	41
3.3. Shape and Orientation.....	45
3.4. Opaque And Transparent Envelope Properties	47
3.5. Internal Gains	48
3.5.1. Air infiltration	49
3.5.2. Internal loads.....	50

3.6.	Centralized AHU with fan Coil Architecture & Cooling Thermal Loads	52
3.6.1.	System Configuration.....	53
3.6.2.	System Technical Specification	55
3.6.3.	System Energy Loads	59
3.7.	Split System & Cooling Thermal Loads.....	61
3.7.1.	System Configuration.....	62
3.7.2.	System Technical Specification	65
3.7.3.	System Energy Loads	70
3.7.4.	Comparison between AHU & Split system	72
4	PV system.....	75
4.1.	Location and main characteristics of the system.....	75
4.2.	Electric loads definition.....	79
4.3.	Electric generation and consumption	80
4.4.	Batteries sizing.....	84
4.4.1.	Battery sizing for All-air system	85
4.4.2.	Battery sizing for split system.....	89
4.5.	Converter selection and matching.....	92
4.6.	Storage systems comparison due to the adoption of two different cooling systems	96
5	Building Envelope Improvements and Consequences	98
5.1.	Building Envelop Stratigraphy Improvements	98
5.1.1.	External Wall Stratigraphy Improvement.....	98
5.1.2.	Roof Stratigraphy Improvement	99
5.1.3.	External Windows Improvement	100
5.2.	New Split System Loads & Battery System Configuration.....	102
5.2.1.	System Energy Loads	102
5.3.	New HVAC System Loads & Battery System Configuration.....	105
5.3.1.	System Energy Loads	105
5.4.	Final Comparison.....	107
6	Conclusion	108

Bibliography	109
List of Figures	115
List if Tables.....	118
Acknowledgments	119

Introduction

This thesis has been developed in cooperation with the Universidad del Norte with the aim of studying an alternative method for cooling the primary school classrooms in Santa Lucia, Atlantic, Colombia through the use of renewable energy. The school in question has already been the subject of other studies by the department of mechanics of Universidad del Norte, specifically, a cooling system was investigated using radiant panels that used water stored in the tanks present in the school to cool the classrooms. The result of the study improved thermal comfort, but never maintained acceptable and constant temperature levels throughout the day and academic year. On the other hand, the system adopted took advantage of the simple natural ventilation of the classrooms and the room where the tank with water is located to reduce temperatures, resulting in a very economical and easy implementation. This study, however, goes to investigate more thoroughly the possibilities of adopting a more sophisticated cooling system, that through the production of electricity can make the intervention more sustainable and generate a positive social impact even on the inhabitants of the municipality of Santa Lucia, rethinking the school also as a real energy hub and a vector for the electrification of the houses of the city. The thesis is divided into several chapters that starting from the analysis of scientific literature to identify the correct set point values to be used in the cooling system, focuses on the creation of a digital model of the school that will then be used to simulate the behaviour of the 2 ventilation systems taken into account and obtain the relative thermal and electrical loads to be used for the sizing of the photovoltaic system and the its storage system. Some improvements on the building envelope will also be considered.

The elaborate starts with a deep investigation on the already existing literature with the goals to firstly determine why IAQ and thermal comfort ASHRAE standards are not suitable for their use in Tropical Climates as defined and secondly to understand the correlation between ambient and indoor conditions on the academic performances in order to create a perfectly suited air cooling control system that will provide, additionally to high thermal comfort levels, also the perfect environment to enhance the short and long term academic performances. Furthermore, it was partially taken under consideration also the social and economical impact of this kind of investments on a schools' facility.

Once it was defined what it is expected to obtain inside each classroom and for how long during the year, the next goal of the study involved the determination of the energy demand of the building considering the new defined conditions. It was decided to use the software IES-VE to extrapolate the daily energy load data because it allows a detailed definition of the whole input data of the building and have a robust simulation environment. In comparison with the previous investigation made by Universidad del Norte, in which only a classroom was object of simulation and the results have been extended for the remaining classrooms, in this study the whole education facility has been recreated and evaluated in a

virtual environment and it allowed a more realistic simulation of the building envelope conditions, additionally including the solar shading influence and internal wall conductivity. To create the digital twin of the education facility, the first step consisted in the conversion of the printed version of the school planimetry into a digital one through the use of AutoCAD software. Additionally, also in site visits of the school facilities have been performed to clarify the missing information and to represent as much realistic as possible the building. Once the planimetry of level one and two of the school were ready, they were uploaded into IES-VE virtual environment together with the occupancy profiles, internal gain values and cooling system architecture and detailed control system operative range.

Once it was possible to obtain the electric load profile of each energy asking equipment with a 6-minute timespan, this dataset have been imported in an excel model able to compare the energy production and demand of the facility and had the main goal to define what was necessary to make the school completely reliant on renewable energy through the support of a BESS system, one of the principal goal of the study. Furthermore, the excel model also included a section to evaluate the energy production of the photovoltaic system through a set of equations able to track the whole yearly solar position and take into account all the possible losses.

In conclusion, once all data has been available for an analysis, a comparison between the traditional split and all-air system have been performed with the main aim to highlight the pro and cons of the technologies in function of the initial goal of the study, IAQ and thermal comfort. As a final analysis, it was performed an evaluation on how the external envelope could be improved with relatively cheap and easily accessible material on the Colombian market in order to reduce the overall energy consumptions.

Additionally to the previous explained method, the work between me and the mechanical department of Universidad del Norte was regulated by, weekly meetings, on site visits and chronogram to define the work advance.

After the explanation of the goals and method used in the investigation, the original aspects that characterize the study are: the decision to don't take as valid the international standards for IAQ and thermal comfort in tropical climates but to pick them from previous investigations that had the opportunity to also perform survey on the topic; to evaluate energy demand and production with locally measured weather data and a faithful digital twin of the building; to evaluate energy demand with a very detailed time frame; to take under consideration the social impact of renewable energy on a rural city.

1 Why considering improving comfort conditions in a rural school?

1.1. Analysis of the link between scholastic performances and IAQ and thermal comfort

In order to define how the academic performance are influenced by internal air quality (IAQ) and thermal comfort, it is important to understand their exact definition and the variables that influence them. After a brief explanation, we are going to analyze, for both of them, the discovering of scientific literature regarding the link with academic performance.

1.1.1. Internal Air Quality

According to the norm UNI 10339 with the term indoor air quality we intend the characteristic of the air treated by an aeraulic system that answers to the following purity requirements: "It doesn't contain concentration of harmful contaminant that could cause damage to health and cause unease for the occupants ". Buildings with poor air quality have produced many occupant health complaints/ illnesses /conditions that have been recorded and labeled "sick building syndrome" (SBS). SBS is discomfort/ illness caused by indoor air. Symptoms are often comparable to a cold or influenza, such as headaches, drowsiness, eye irritation, and nose and throat infection. The main difference between SBS and a cold is that the SBS symptoms last much longer than cold symptoms and disappear after the occupant leaves the building.

Approximately 30% of new or remodeled buildings produce health complaints as reported by Environmental Protection Agency (EPA). Indoor air contaminant levels can be several magnitudes greater than the outdoor air contaminant levels due to the contaminant releases from building materials, occupants, or different building processes. Table 1-1 shows a few contaminant sources, permitted levels, and possible health effects according to EPA standards. Regardless of permitted levels, the actual response to a contaminant is based on the individual.

Contaminants	Sources	Permitted Levels	Health Effects
CO ₂	Human, combustion	1000 ppm	Stuffing
CO	Combustion, ETS	15 ppm	Body chemistry
SO _x	Combustion		Irritation, asthma
NO _x	Combustion	100 µg/m ³	Not very clear
Ra	Soil	4 picocuries/L	Lung cancer
VOCs (formaldehyde)	Combustion, pesticides, building materials, etc.	0.1 ppm	Eyes and mucous membrane irritation
Particulate (0.01 micro-insects)	Outdoor air, activities, ETS, furnishings, pets, etc		Lung diseases Cancer (ETS)

Table 1-1 Contaminant levels permitted according to EPA standards

Indoor contaminants could be particles or gases and vapors. Particles could be allergens, molds, bacteria, dust, fumes, smoke, or mist and fog. Contaminant gases could be inorganic or organic. Harmful inorganic gases, such as radon (a radioactive gas), have the potential to cause lung cancer due to the particle deposition in lungs. Harmful organic vapors may cause major respiratory irritation and may be perceived as unpleasant odors. In the worst-case scenario, harmful vapors could be completely odorless. Many paints waxes, varnishes, and cleaning products are rich in organic solvents that evaporate even without use.

The primary sources of indoor air-quality problems found by the investigations of the National Institute for Occupational Safety & Health (NIOSH) are:

- Inadequate ventilation, 52%
- Contaminant from inside the building, 16%
- Contaminant from outside the building, 10%
- Microbial contamination, 5%
- Contamination from building fabric, 4%
- Unknown sources, 13%

Appropriate design and maintenance of HVAC system can eliminate the majority of indoor air-quality problems. ANSI/ASHRAE Standard 62-2001 has a prescriptive ventilation rate procedure that defines adequate ventilation. The standard uses CO₂ as an indicator of adequate IAQ because CO₂ is a “marker” for human contaminants. The standard assumes that if CO₂ is kept at a required level, then other contaminants are also successfully diluted. Typically required fresh air quantities are 8–10 L/ (s person). The rest of the air may be recirculated in order to save energy used by the HVAC system.

To solve IAQ problems, building owners or managers could use one of the following three strategies: (1) eliminate or modify the contaminant source, (2) dilute the contaminant with outdoor air and air distribution, or (3) use air cleaning (filtering). Even though these strategies sound straightforward, they may not be easy to implement. For example, for mold

and fungi prevention, it is important to properly design HVAC systems for humidity control and it is just as crucial to have a properly constructed building envelope. Finally, the use of different types of filters and regular replacement of filters can significantly reduce IAQ problems. Typically, two or more types of filters are combined to achieve proper removal of contaminants.

According to the academic literature, the relation between IAQ and academic performances have been strongly investigated and some interesting consideration could be made. For example, a series of experiments by Wargocki et al. (1) (2) (3), summarized by Wyon (4), examined the effects of indoor air quality on the cognitive skills that are essential for office work.

In this experiment, indoor air quality was altered by decreasing the pollution load, i.e. by physically removing a hidden pollution source without informing the subjects, while maintaining an outdoor air supply rate of 10 L/s per person. The major pollution source was a carpet that had been used for 20 years in an office and was present behind a partition in a quantity corresponding to the floor area of the office in which the exposures took place, although low background emissions and the bio effluents emitted by the subjects themselves were always present. 30 subjects performed different cognitive tests and typing and addition tasks to simulate typical office work throughout 4.5 h exposures. The indoor air quality caused 70% to be dissatisfied with the air quality when the used carpet was present and 25% when it was absent. The presence of the used carpet caused subjects to type 6.5% more slowly, to make 18% more typing errors, and to experience more headache.

The original study of Wargocki et al. (1) was repeated in the same office by Bako-Biro et al. (5) with a different pollution source. Instead of carpet, there were 6 Personal Computers (PCs) with Cathode Ray Tube Visual Display Units (CRT/VDU) that had been in operation for about 500 h, corresponding to approximately 3 months of normal office use. 40% of the subjects reported that they were dissatisfied with the air quality when the PCs were present behind the screen, while only 10% were dissatisfied when the PCs were absent. Although the differences between conditions in terms of typing speed were small, more subjects typed slowly, and all subjects made more typing errors when the PCs were present. Combining the observed effects on the speed and accuracy of typing and the decrease in speed of proofreading, it could be shown that overall text-processing would be performed 9% more slowly if PCs were present.

According to another research (6), indoor air quality can also be modified by changing the ventilation rate. The outdoor air supply rate was increased from 3 to 10 or to 30 L/s per person with the original pollution source, a used carpet, always present behind the partition. 60% were dissatisfied with the resulting indoor air quality at the lowest ventilation rate and 30% were dissatisfied at the highest rate. In conclusion, the performance of the text-typing task improved by about 1% for every two-fold increase in the outdoor air supply rate.

Furthermore, in these other research (7) (8) was possible to define a function between outdoor air supply rate and performance. According to the Figure 1-1, it could be shown

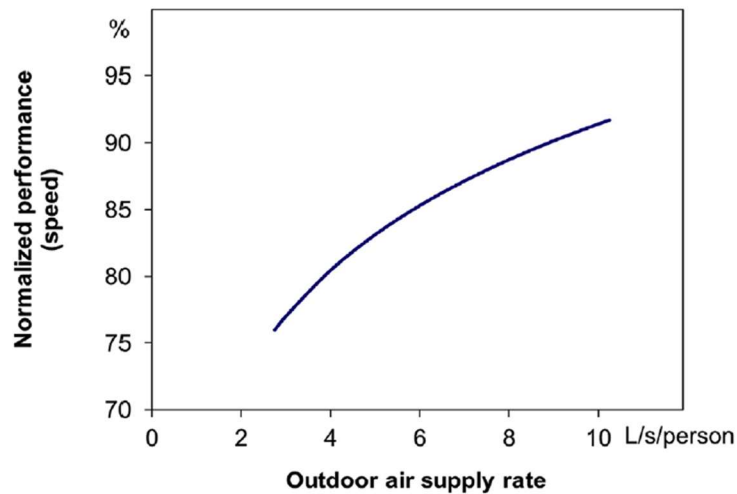


Figure 1-1-1: Experimental relationship between air supply rate x child and classroom performance of schoolwork

that doubling the outdoor air supply rate would improve the performance of schoolwork in terms of speed by about 8% overall, and by 14% for the tasks that were affected significantly, with only a negligible effect on errors.

Also in the scientific paper of Tess M. Stafford (6) was found that IAQ-renovations, and mold remediation improved the results of standardized math and reading test. The average mold project (~\$500; 000) improved test scores by 0.14–0.15 sds and pass rates by 3–4%, the average ventilation project (~\$300; 000) improved test scores by 0.07–0.11 sds and pass rates by 2–3% discovering that IAQ-renovations may be a cost-effective way to improve student test scores.

To conclude, according to the experiment made by A. Kabirikopaei (9) classrooms with unit ventilators were associated with lower mathematics scores when compared to classrooms with multi-zone systems. Instead, regarding reading score, higher ventilation rates in fall are associated with higher reading scores.

Until now it has been analyzed how to improve academic performances through IAQ. Now it will be analyzed how IAQ affect performance negatively. In the research of P. Wargocki (10), it is well illustrated fig. 1-2 all the mechanism on how air quality affects performances.

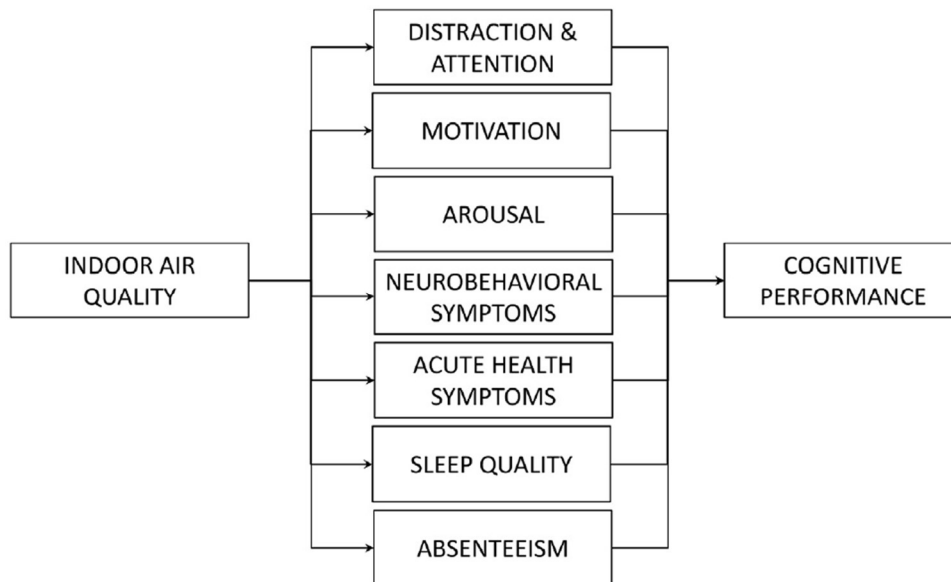


Figure 1-1-2: How IAQ affect cognitive performance

Poor indoor air quality can also be regarded as reducing performance if it increases sickness absence, as no work can be performed by absent workers/students. Milton et al. (11) showed that the risk of short-term sick leave associated with respiratory diseases caused by infection was significantly higher in offices in the USA with an outdoor air supply rate of 12 L/s per person compared to other offices ventilated with 24 L/s per person. Simons et al. (12) found high student absenteeism to be associated with poor ventilation in 2751 New York schools. Shendell et al. [34] found student absence decreased by 10 and 20% when the CO₂ concentration decreased by 1000 ppm in 434 American classrooms. A study by Gaihre et al. (13) in Scottish schools showed that an increase of 100 ppm of CO₂ corresponded to a 0.2% increase in absence rates (roughly one order of magnitude lower than the data of (14)) and corresponding to about to 0.5 day a year in the 190 days of a school year.

Poor indoor air quality at home may reduce next-day performance at work or at school by decreasing sleep quality or duration: in identical corridor rooms, 16 students slept with high or low rates of outdoor air supply that were achieved by operating or idling a simple fan mounted in the air-intake aperture (15). The resulting average CO₂ levels were about 850 ppm and 2400 ppm, respectively. The subjects reported that the air in their room seemed to be fresher, that they felt more refreshed and that their mental state was better in the condition in which the fan was operated. The objectively measured sleep efficiency (time spent asleep) was higher and their task performance the following morning was better when the fan had been operated.

Also accordingly to Mark J. Mendell (16) it can be hypothesized a casual links relating indoor IAQ in schools to performance and attendance of students as shown in the figure 1-3.

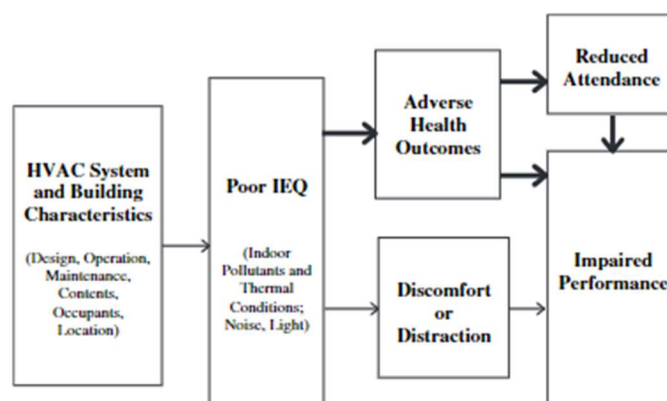


Figure 1-1-3: Casual link between academic performance and poor IAQ

The IEQ factors in turn could influence health outcomes of students (or teachers), which could influence students' performance directly or through effects on attendance. IEQ factors might also cause health effects that directly impair concentration or memory (e.g. neurologic effects) or cause other health effects that indirectly affect learning. For instance, indoor pollutants might exacerbate diseases such as irritated eyes, nose and throat, upper respiratory infections, nausea, dizziness, headaches and fatigue, or sleepiness that produce symptoms or absenteeism that in turn impair learning. For example, asthma is a principal cause of school absences from chronic illness, responsible for 20% of absences in elementary and high schools.

Another way to investigate what affect the academic outcomes is to analyse the school facility attributes that influence the most the well-being of students. Regarding cleaning technologies, in the research of Rosen, K. G., and G. Richardson (17) was found that improving air quality through electrostatic air cleaning technology reduces absenteeism. Their experiment, conducted in two Swedish day-care centres, one old and the other modern, collected data on absenteeism and air quality over three years. The air cleaning technology was operational during only the second of the three test years, and absenteeism fell during that period in both schools. But only in the older school did the change reach statistical significance (absenteeism dropped from 8.31 percent in year one to 3.75 percent in year two, but upon removing the air cleaners, the rate increased to 7.94 percent in year three).

Overall in literature, more research is needed to explain the positive relationship between particle concentration and student scores, but in a in a recent study on the effect of fine particles (PM_{2.5}) on college students' performance, it's concluded that every 10 µg/m³

increase in the PM_{2.5} concentration level can reduce the overall performance on mental tasks by 1% (18) . But at the same time student outcomes are positively affected by “active” learning experiences, activities that imply an increase airborne particle concentration. Student activity highly influenced the re-suspension of particles in classrooms, especially when ventilation rates were inadequate (19) . Also, educational activities such as hands-on learning in classrooms may be a significant source of indoor particles (20) . Classroom occupancy density and location of the school may also be important factors in the concentration of particles in a classroom. Highly dense classrooms in more polluted areas create consequently more particle concentrations in classrooms. To control particle concentrations in classrooms, appropriate ventilation systems and high-efficiency filters should be used in school buildings.

Analysing ventilation technology, the purpose of ventilating classrooms and school buildings, at minimum, is to remove or otherwise dilute contaminants that can build up inside. Such contaminants come from people breathing, from their skin, clothes, perfumes, shampoos, deodorants, from building materials and cleaning agents, pathogens, and from a host of other agents that, in sufficient concentrations, are harmful. One of the first symptoms of poor ventilation in a building is a build-up of carbon dioxide caused by human respiration. When carbon dioxide levels reach 1000 parts per million (about three times what is normally found in the atmosphere), headaches, drowsiness, and the inability to concentrate ensue. Myhrvold (21) found that increased carbon dioxide levels in classrooms owing to poor ventilation decreased student performance on concentration tests and increased students' complaints of health problems as compared to classes with lower carbon dioxide levels.

1.1.2. Thermal Comfort

Instead, with reference to the definition of thermal comfort, we can say that the primary purpose of HVAC systems is to maintain thermal comfort for building occupants. ANSI/ASHRAE Standard 55-1992 defines thermal comfort as the mind state that expresses satisfaction with thermal environment by 80% or more of the building occupant’s through a subjective evaluation.

The human body behaves similar to a heat engine, obeying the first law of thermodynamics. The chemical energy contained in food is converted into thermal energy through the process of metabolism. This thermal energy is used partially to perform work, while the other part has to be released to the surroundings to enable the normal functioning of the human body. The first law of thermodynamics for the human body has the following form (Fanger, 1970):

$$M - W = Q_{skin} + Q_{respiration} = (C_{sk} + R_{sk} + E_{sk}) + (C_{res} + E_{res}) \quad (1.1)$$

where M is the rate of metabolic heat production (W/m^2 body surface area), W is the rate of mechanical work, Q represents the different heat losses, C the convective heat losses, R the radiative heat losses, and E the evaporative heat losses.

The metabolic heat production, losses and work are measured in W/m^2 body surface area or in metabolic “met” units (1 met = 58.2 W/m^2). Figure 1-1-4 gives metabolic heat production rates for typical tasks (ANSI/ASHRAE Standard 55-1992).

Activity	met	W/m^2
Reclining	0.8	46.6
Seated and quiet	1.0	58.2
Sedentary activity (office, dwelling, lab, school)	1.2	69.8
Standing, relaxed	1.2	69.8
Light activity, standing (shopping, lab, light industry)	1.6	93.1
Medium activity, standing (shop assistant, domestic work, machine work)	2.0	114.4
High activity (heavy machine work, garage work, if sustained)	3.0	174.6

Figure 1-1-4: Metabolic heat production according to ANSI/ASHRAE Standard 55-1992

The main heat-transfer mechanisms are convection, radiation, and evaporation. In general, the total heat transfer from the human body depends on environmental and personal factors. The environmental factors are air temperature (affects C), relative humidity (affects E), air velocity near the human body (affects C), and surface temperature of the enclosure and surrounding objects (affects R). The personal factors are activity rate and clothing (body insulation).

Several thermal comfort indices correlate the perception of thermal comfort with measured environmental parameters, i.e., dry bulb temperature, mean radiant temperature, and humidity levels. A rationally derived index, the operative temperature (T_o), empirical index and the effective temperature (ET^*), are used to plot an ASHRAE comfort zone for winter and summer conditions (see Figure 1-5).

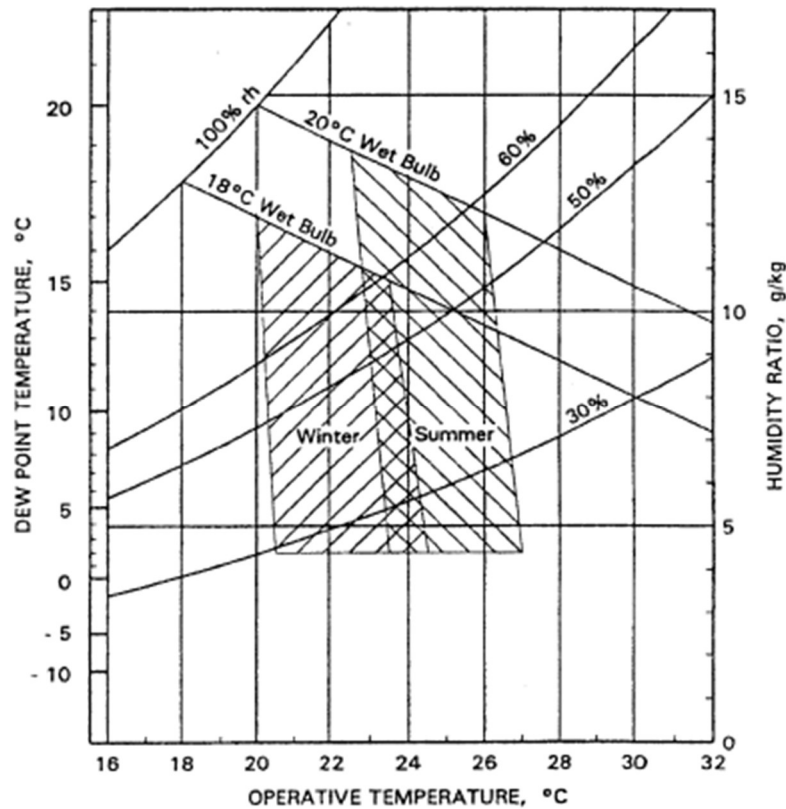


Figure 1-1-5: Comfort zone according to ASHRAE 55-1992

The “comfort zone” represents combinations of air temperature and relative humidity that most often produce thermal comfort for a seated North American adult in typical summer or winter clothing. An assumed level of dissatisfaction is 10% of all occupants. The slender lines bordering the comfort zone represent ET^* : for winter $ET^* = 20^\circ\text{C} - 23.5^\circ\text{C}$ and for summer $ET^* = 23^\circ\text{C} - 26^\circ\text{C}$. The ASHRAE comfort zone can be adjusted for different clothing levels, air velocities, activity levels, and human adaptation. Overall, HVAC systems are designed to produce an indoor air state within the ASHRAE comfort zone.

According to the academic literature, the relation between thermal comfort and academic performances have been strongly investigated and some interesting consideration could be made. With reference to (10) under moderately warm conditions, above neutrality, it is possible to avoid sweating by reducing metabolic heat production. This leads to a lowering of arousal, as people relax and generally try less hard to work fast. This is often a completely unconscious response to warmth. Aspects of mental performance with a low optimal level of arousal, such as memory (22) and creative thinking (23), are improved by exposure to a

few degrees above thermal neutrality, but they too are impaired at higher temperatures, closer to and above the sweating threshold. Tham and Willem (24) showed that increased accuracy in the Tsai-Partington test indicates raised arousal, which improves concentration and would thus be expected to benefit rule-based logical thinking. They exposed heat acclimatized subjects living in the Tropics to 20°C, 23°C and 26°C and observed higher arousal at 20°C, as indicated by measurements of stress biomarkers in saliva. Activation of the sympathetic nervous system and higher alertness are beneficial for tasks that require attention and the ability to sustain prolonged mental effort. Individual control of the thermal environment may be necessary if optimal performance of office work is to be achieved. Wyon (25) showed that individual control equivalent to ± 3 K would be expected to improve the performance of mental tasks requiring concentration by 2.7%. Wyon showed that this degree of individual control (± 3 K) would be expected to improve the group mean performance of routine office tasks by 7%. Fig. 1-6 shows the magnitude of the effects of temperature on performance that have been documented in the literature and an experimental relationship between thermal discomfort and the performance of office work.

Also a comprehensive set of experiments on the effects of classroom temperatures on the

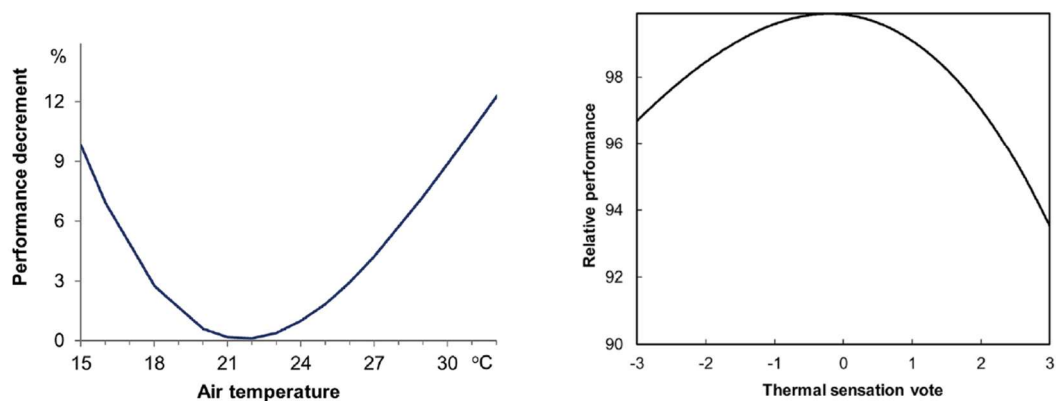


Figure 1-1-6 : Air temperature and thermal sensation vote relation with performance

performance of schoolwork was carried out in 50 years ago Sweden (26). In these experiments, three parallel classes of 9 and 10-year-old children were exposed for 2 h to each of three classroom temperatures: 20, 27 and 30°C, encountered in balanced order, and four classes of 11 and 12-year-old children were similarly exposed to 20 and 30°C in the morning and the afternoon. The children performed a number of school exercises, including numerical tasks (addition, multiplication, number checking) and language-based tasks (reading and comprehension, supplying synonyms and antonyms) so that their rate of working and the number of errors they made could be quantified. The children's performance of both types of task was significantly lower at 27°C and 30°C in comparison with 20°C. Performance tended to be lower, though not significantly lower, at 27°C than at 30°C, and the negative effects of raised classroom temperatures were significant in the afternoon, when the children were fatigued, but not in the morning. The magnitude of the negative effect of temperature on performance was for some tasks as great as 30%. When

the temperature was reduced to 20°C, the performance of 2 arithmetical and 2 language-based tests improved significantly.

Sarbu and Pacurar (27) examined the performance of 18 university students in a classroom over a period of 36 days. The classroom temperatures were manipulated by operating or idling the air cooling and changing the air-cooling set-point; they remained between 22°C and 29°C. The students repeatedly performed two attention tests: the concentrated attention test (Kraepelin test) and the distributive attention test (Prague test). These tests took 10 min and 7 min to complete, respectively. The results showed that the performance of students on both tests followed an inverted-U curve, similarly to what was observed in fig 1-6.

Haverinen-Shaghnessy and Shaughnessy (28) measured temperatures in 140 fifth-grade classrooms in 70 elementary schools for a week-long period and correlated them with a state-wide assessment of learning. Average indoor temperature was 23°C and it varied between about 20°C and 25°C. Modelling showed that there was a 12-13% increase in mathematics score for each 1 decrease of temperature (0.5%/degree). Park (29) analyzed more than 4.5 million school-leaving examination results from New York City high schools and found that taking the examination on a day when the ambient temperature was 32°C increased the risk of failing to pass by 12.3% compared with the results obtained when the examination was taken on a day when the ambient temperature was 22°C. He showed additionally that an increase in temperature of 1°C will reduce the examination score by 0.4% (1-7) which is quite similar to what was observed by Haverinen-Shaughnessy (28).

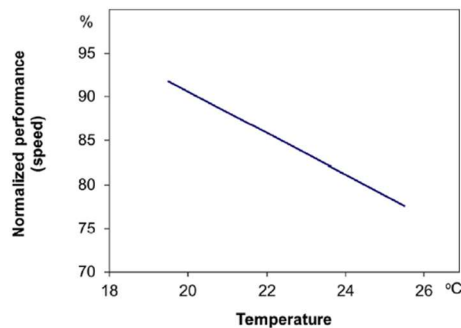


Figure 1-1-7: Temperature and academic performance correlation

Until now it has been analyzed how to improve academic performances through thermal condition. Now it will be analyzed how thermal condition affect performance negatively.

There are 6 different biological mechanisms that have been individualized by (30) in order to correlate thermal comfort with academic performances:

- (i) Thermal discomfort distracts attention;
- (ii) Warmth lowers arousal (the state of activation of an individual), exacerbates and increases the prevalence of building-related symptoms (SBS), causing distraction

and thus further negative effects on performance, and has a negative effect on cognition;

- (iii) Cold conditions decrease finger temperatures and thus have a negative effect on manual dexterity ;
- (iv) Rapid temperature swings have the same effects on office work as slightly raised room temperatures ;
- (v) Vertical thermal gradients reduce perceived air quality at head height and so lead to a reduction in room temperature that then causes complaints of cold at floor level that are due to vasoconstriction, not to the low temperatures at floor level ;
- (vi) Raised temperatures can result in increased carbon dioxide (CO₂) concentration in the blood, which may cause headaches ;

It should be assumed that thermal discomfort sensations due to cold or heat stress distract attention, and that the physiological responses to heat stress reduce arousal and therefore motivation to exert effort. More generally, the effects of thermal conditions appear to be mediated directly by the physiological changes that take place, including vasoconstriction in the cold, which reduces manual dexterity, and an increase in the blood gas level of CO₂ in response to heat, which causes headache and increased difficulty in thinking clearly. However, as indicated by Lan et al. (31) increasing temperatures and the physiological responses that then occur, including an increase in the blood gas concentration of CO₂, result in a range of negative health symptoms such as headaches or difficulty in concentrating and thinking clearly that can reasonably be expected to have direct negative effects on cognitive performance unless more effort is exerted to counteract them.

At support of these biological mechanism stated in the research (30) , there is the study made by M. Puteh (32) in a mechanically ventilated school building in Malaysia. It consists of a survey made by the Teaching and Learning Classroom Thermal Comfort Inventory (TLTCI). It is composed by 5 parts: i) demographic; ii) Climate change awareness; iii) Teaching and Learning Comfort Inventory; iv) Classroom Thermal Effect; v) Adaptability and Involvement.

The analysis of the classroom thermal comfort shows that 45.5% of the students participating in the survey feel that their classroom is hot and 48.3% said that they are not satisfied with the heat of their classroom. Findings also reveal that the classroom thermal conditions affected the health being. Many students complain that their skin becomes dry (13.3%), having difficulties in breathing (16.7%), asthmatic syndrome (20%), coughing, eye infection (30%), emotional problem (40%) and stress (68.3%). This research (32) could be considered a relevant one because the school is located in Malaysia, where the climate is tropical, hot and humid and the outdoor temperatures and the relative humidity ranges respectively between 23.7°C to 31.3 °C and 67% to 95%, with similarity to the climate of Santa Lucia, where the school of the case study is located.

1.2. Impact of schools on rural communities

Schools have a variety of important impacts on rural communities, beginning with providing education in rural areas. Schools are a hub of activity, celebrations, events and community engagement. In many cases, staff and students generate the events that give people a purpose to gather. Through this activity, schools shape and sometimes redefine perceptions of community identity and spirit. Schools have economic impacts on the community by often being the largest employer and by generating parent traffic to the community, where they may use other services in the community. Schools make the community more attractive to potential new residents. Stakeholders in rural communities perceive schools as critical anchors that enable and sustain rural culture. That culture in turn supports the agriculture industry and a mainly rurally based resource economy. For this reason, a modern school that could guarantee high thermal and air quality comfort could have huge impact on the sanitary system of the rural community and additionally a positive impact on the academic performance that could reflect on the economics of the community.

Accordingly to the international literature, There are only a few studies that relate the impact of schools on their communities. In a study by Kilpatrick, Johns, Mulford, Falk, & Prescott (33) that included an extensive literature review and case studies of five rural Australian school-community combinations, the following contributions of schools in rural communities were noted:

Outcomes for Youth:

- Educational: Increased attendance and retention in secondary school.
- Personal development: Increased self-esteem, confidence, leadership skills, volunteerism.
- Social/ civic: Increased retention in the community, increased involvement and knowledge of community networks and organizations.
- Employment/ career: Better opportunities and success.

Outcomes for the Community:

- Personal development: Increased self-confidence/ esteem through interaction and recognition by the school.
- Social: Increased levels of inter-generational trust.
- Community learning: School staff provides instruction, leadership and the school provides a venue for community learning programs and initiatives.
- Environmental: School and staff provide programming and leadership for environmental awareness and programs.

- Economic: School and the staff buy local and thereby support the local entrepreneurs and economy.
- Indigenous and Marginalized Communities: School staff provide leadership and work collaboratively with parents and community leaders to remove barriers, improve culturally inclusive programming and instruction and develop strong community partnerships.

Schools increase the attractiveness of a community for potential newcomers. Economic development professionals generally agree that presence of schools or proximity to schools constitutes a competitive advantage for attracting business investment (34) (35).

In a large-scale study of 233 American municipalities, (36) attempted to determine the role of economic development policies and the municipalities' attributes in determining economic prosperity. Among the many variables that correlated to economic prosperity they found that education policy, particularly capital investment in school infrastructure, construction, and the rates of graduation from local schools were related to economic prosperity.

Economic impact of a local school is also critical through the jobs and other economic spin-offs it creates. In many cases a rural community's school is the largest employer, or in the top three largest employers if there is a health centre, and/ or regional municipal office also located in the village or town. For example, a study of the impacts of public sector spending in rural Saskatchewan found that every public service job generated indirect employment of another 0.39 jobs. The employment earnings of public sector workers had an economic multiplier effect of 0.4434 so that each dollar of public sector earnings created another \$0.44 in spending (37)

Another impact of schools in rural communities is that they are a delivery point for health and other services. Schools are an ideal location for delivering these services because nearly all children between certain ages can be accessed through them. A variety of community health services could be provided (e.g. immunizations) and are a gateway for other family supports, counseling and community mental health services.

Regarding the link between IAQ or thermal comfort with socioeconomically disadvantaged students, two interesting scientific papers could be analysed. The research performed by Carolina M. Rodriguez and Marta D'Alessandro shows a correlation between ORC (Operation Report Card) that could be enhanced through good IAQ and racial class. They found that, for example, a one unit increase in ORC for Latinx students was associated with up to a 2.7% increase in math score at the 90th percentile of the score distribution but a 0.4% decrease at the same percentile for White students.

At support of this, in the Children's Environmental Health Network's (CEHN) 1997 conference (38) reported that children from racial minorities are more likely to encounter poor IAQ. The CEHN conference stated that Black and Hispanic neighborhoods have a

disproportionate number of toxic waste facilities in their neighborhoods and that 80% of Hispanics live in neighborhoods where air quality does not meet EPA standards. While this finding does not specifically focus on schools, the existence of poor air quality in these neighborhoods may parallel poor quality air indoors in schools. Statistics from the General Accounting Office report (39) on school facilities in 1996 directly confirm that schools serving poor and minority students do suffer disproportionately from poor IAQ. Of schools where less than 40% of their students were eligible for free lunch, approximately 60% reported unsatisfactory IAQ, but of schools where more than 40% students were eligible for free or reduced-cost lunch, almost 23% percent reported having unsatisfactory IAQ.

1.3. Correlation between thermal comfort and cooling technologies in tropical climates

The aim of this chapter is to analyze the main literatures discoveries related to the link between cooling technologies and thermal comfort of students in order to understand how the temperature perception of students in tropical climates and with different cooling systems is different from the one stated in the international standards.

Accordingly to this research (40), it was investigated and compared the IAQ and thermal comfort in classrooms of four buildings of an educational institute located in Islamabad, Pakistan, having different types of heating ventilation and air conditioning system. The first school with only natural ventilation, the second one with natural ventilation and local AC (split system) and the last two with centralized HVAC systems. (40). It is reported that in Representatives of European Heating and Ventilating Associations (REHVA) Guidebook 13 limiting value for CO₂ level is 1500 ppm [32] while according to American Society of Heating, Refrigeration and Air Conditioning Engineers (ASHRAE) standards 62.1–2016 (for ventilation), limiting indoor CO₂ concentration should not be 700 ppm above the outdoor CO₂ levels (300–500 ppm) and the relative humidity should be maintained below 65%. Similarly, according to ASHRAE Standards 55–2013 (Thermal Comfort), temperature may range between 22.5°C and 25.5 °C for thermal comfort. The study concludes that the quality of indoor air is largely dependent on type of ventilation system present. CO₂ concentration levels were found highest in the buildings with non-centralized HVAC systems. Comparison with standards also showed exceeding levels of CO₂ concentration from ASHRAE standards frequently during the occupational period of study duration. In buildings with centralized HVAC system, CO₂ levels were found to be lower, with lesser exceedance frequency beyond safe limits during the occupational period.

In another study similar to (40), Stephen Siu Yu Lau (41), make a comparison between 3 different three different ventilation strategies (i.e. air-conditioning [AC], hybrid [HB], and natural ventilations [NV]) installed at the NUS university campus located in Singapore, where the the weather is hot and humid throughout the year with few seasonal fluctuations.

The daily average temperature ranges from 24.4 °C to 30.2 °C and the average relative humidity ranges from 68.8% to 96%, similar to our case study in Santa Lucia, Atlantico.

The paper defines as NV the possibility to ventilate the classroom through operable windows or openings directly connected to the out-door environment. For HB it is considered NV plus the adoption of mechanical ventilation involving, for example, ceilings or wall-mounted fans. Data were collected from 1043 survey questionnaires; concurrently, on-site measurements in three consecutive years were analysed. The Griffith method was used to calculate the comfort temperature or neutral temperature. It was founded that the neutral operative temperatures predicted using the linear regression analysis were 26.7 °C, 29.5 °C, and 27.8 °C for AC, HB, and NV spaces, respectively. The mean comfort operative temperatures based on Griffiths' method were 25 °C, 28.7 °C, and 29 °C for AC, HB, and NV spaces, respectively. The relatively high comfort temperatures for HB and NV spaces obtained in this study are in good agreement with some of the existing studies conducted in tropical and subtropical regions. The neutral operative temperature in AC space (26.7 °C) suggests that the typical setpoint of 24 °C for the AC system on the NUS campus could be increased by two degrees without affecting the average comfort level of the occupants. Together with extensive implementation of HB ventilation, reductions in energy used for cooling could be significant campus wide. Furthermore, the results of the ANOVA test indicate that higher air velocity was associated with greater satisfaction and higher overall thermal comfort levels, highlighting the benefits of increased air speed, particularly in HB or NV spaces.

To conclude, Stephen Siu Yu Lau (41) findings support the conclusion that in warm climates, increasing air movement using fans could increase the comfort temperature, bringing it closer to the mean operative temperature.

Also the in the research performed by C.Cândido (42) in northeast Brazil, it was observed that users could adapt to an air temperature up to 26 °C with a minimal air velocity of at least 0.4 m/s. That study suggested that the user acceptance of higher air velocities increased to compensate for elevated temperature and humidity.

Additionally, in another research performed in Brazil (43), exactly in João Pessoa (7,11°S; 34,86°W) where the climate is predominantly humid tropical, it was investigated the thermal comfort of children from 9 to 11 years old with the scope of identify the preferred and comfortable ranges of thermal parameters for AC from the opinions of the children who use these spaces. The environmental measurements in the classrooms resulted in a mean air temperature of 26.76°C and a mean radiant temperature of 26.65°C. Based on the analysis of the relationship between thermal context and the children's votes for thermal sensation and preference, the mean radiant temperature of 26.81°C was the reference for thermal neutrality and the condition for children not wanting to change the temperature. Regarding the sensation of comfort, 34.01% of the children voted for discomfort due to low temperatures and 30.93% voted to high temperatures. In the correlation analysis between

the thermal sensation and preference, students were likely to prefer lower temperatures in the room, as they reported sensations of low temperature and neutrality. It was reported that 48.46% of the children would prefer the temperature in the classroom to be lower, and 93% of them preferred an air-conditioned environment.

Another study performed by Alison G. Kwok (44) in Hawaii, where the climate is classified as Tropical zone by Köppen climate classification it was founded that the point where the maximum number of people voted "neutral," which occurred at 26.8°C in naturally ventilated classrooms and at 27.4°C, in air-conditioned classrooms. The first significant conclusion of this study is that people in naturally ventilated schools are comfortable in conditions that are outside of the comfort zone specifications of Standard 55. That's important because the amount of energy and resources spent to achieve comfort zone conditions will be lower saving long-term energy costs. The second conclusion is a significant number of people experiencing a variation of $\pm 2, 3^\circ\text{C}$ of temperature still found these conditions to be acceptable. However, preferred temperatures were 2.5°C cooler (24.3°C) than the observed naturally ventilated neutrality and 4°C cooler (23.4°C) than observed air-conditioned neutrality.

On the contrary, Zaki et al. (45) investigated the university students' comfort temperature and adaptive behavior in Malaysia and Japan with mechanical cooling and natural ventilation operative modes. In Japan, the mean comfort operative temperature in natural ventilation operation mode was 25.1°C, while in Malaysia, it was 25.6°C. As for mechanical cooling operation inside the classrooms, the mean comfort operative temperature was 26.2°C in Japan and 25.6°C in Malaysia. One of the main conclusions of this study was the validity of applying thermal comfort standards in hot-humid climates.

Another strategy to choose the best comfort temperature in tropical climates was proposed in the research (46) where the researcher used an artificial neural network to define it. They took under consideration these variables: outdoor running mean temperature, relative humidity, air velocity, weight, clothing insulation, and activity level. They found that their artificial neural networks is 50 times better than conventional methods to define comfort temperature. After considering 2 different study periods for an educational building during the 2017 warmer season and 2018 it was found that in AC buildings the indoor environmental conditions caused occupants to express a cold sensation, with a mean TSV (Thermal Sensation Vote) of -0.8 in the first period and -0.4 for the second period. In NV mode, the surveyed expressed feeling slightly warm with a mean TSV of 0.5 during the first period; the warm sensation was higher in the second period with a mean TSV of 1.5. In conclusion, the studied buildings in AC mode show an overcooling, representing higher energy consumption with limited thermal comfort levels. Likewise, passive cooling methods were not enough to achieve thermal comfort. For both modes, implementing strategies to improve thermal comfort and save energy is the right choice.

1.4. Overall conclusion on thermal condition, IAQ and cooling technologies influence on academic performance

According to the research analyzed, the operative cooling temperature suggested by international standards have to be adapted to the personal thermal sensation of the students thorough a survey with the aim to define the neutral and preferred temperature of the residents. Consequently, for the investigated case study of Santa Lucia the cooling system will try to be in compliance with the international standards regarding CO₂ levels and relative humidity but for operative temperature further investigation with a survey on the thermal comfort of the children of the school of Santa Lucia will be needed to define the correct operative temperature. Anyway, the choice of the operative temperature will take in account the fact that in tropical climates the neutral temperature perceived by students was discovered to be higher of the temperature range proposed by international standards. For ASHRAE Standards 55–2013, temperature may range between 22.5°C and 25.5 °C for thermal comfort but from the founding of (42) (43) (44) in tropical climates the neutral temperature percieved by occupants range between 26.5°C – 26.9°C. On the contrary, as founded in the research (44), significant number of people experiencing a variation of $\pm 2, 3^{\circ}\text{C}$ of temperature still found these conditions to be acceptable, so a wrong set point temperature could have reasoning on the energy expenditure but less impact on the comfort of the students.

Regarding the air diffusion system, according to (47) displacement ventilation and ceiling diffuser are recommended solution for classroom ventilation in order to guarantee the best heat removal efficiency and HB is the best compromise to have good thermal comfort and energy saving according to (41).

Regarding the ventilation rate, REHVA Guidebook 13 suggest a limiting value for CO₂ level of 1500 ppm [32] while according to ASHRAE standards 62.1–2016 limiting indoor CO₂ concentration should not be 700 ppm above the outdoor CO₂ levels (300–500 ppm). For this reason, the typical required fresh air quantity suggested is 8–10 L/ (s person). Instead, according to (6) (7) (8) (11) (11) (9) a positive relationship between high ventilation rate and increased academic performance or reduced absenteeism was founded so, with reference to academic literature, a good value that could be choose to maximize this correlation is 10-12 L/s per person or CO₂ sensor could be installed to regulate the fresh air supply.

Furthermore, air cleaning strategy to guarantee the best IAQ will be also needed. Accordingly to (17), improving air quality through electrostatic air cleaning technology reduces absenteeism and for (18) every 10 $\mu\text{g}/\text{m}^3$ increase in the PM_{2.5} concentration level can reduce the overall performance on mental tasks by 1%. At support of this results also the research (40) suggested that buildings with centralized HVAC system could keep CO₂

concentration with lesser exceedance frequency beyond safe limits during the occupational period.

Therefore, the investigation on the best system that guarantee thermal comfort, good IAQ and minimum energy spending will be analyzed for our study case in Santa Lucia after the calculation of the building cooling loads but from the literature analysis the operative parameters and cooling system architecture to take under consideration are:

- Ventilation rate of 10-12 L/s per person or CO₂ levels under 1000 ppm
- Set point temperature range 26.5°C – 26.9°C
- Relative humidity levels below 65% according to ASHRAE standards 62.1-2016
- Electrostatic air cleaning technology with centralized HVAC system preferred
- Displacement or Ceiling diffuser are recommended
- Hybrid ventilation (natural ventilation + mechanical ventilation) is the best compromise between thermal comfort and energy expenditure
- Individual temperature control by classroom occupants of ± 3 K

After this conclusion, a mechanical ventilation system will be needed for sure but the coexistence with natural ventilation have to be evaluated. Furthermore, the adoption of a radiant cooling system could be implemented to save energy expenditure and the coupling with mechanical ventilation system could avoid the condensation problem that affect this kind of technology in hot and humid climates.

2 Location and weather conditions evaluation

The “Institución Educativa Santa Lucía” is located at latitude 10.321°N and longitude -74.95 °E in the department called Atlántico, in the coast of Colombia.



Figure 2-2-2: Localization of Santa Lucía in Colombia



Figure 2-2-1: Top view of Institución Educativa Santa Lucía

The town where the school is it is called Santa Lucía. It has an extension of 50 km^2 and has a population of 11944 people. It is the nineteenth largest agglomeration in the department of Atlántico. The municipality has a population density of approximately 238.94 inhabitants/km. The alphabetization rate in the population over 5 years of age is 84.4%. Public services have considerable coverage, since 93.8% of homes have electricity service, 85.7% have sewage service and only 9.2% have telephone communication.

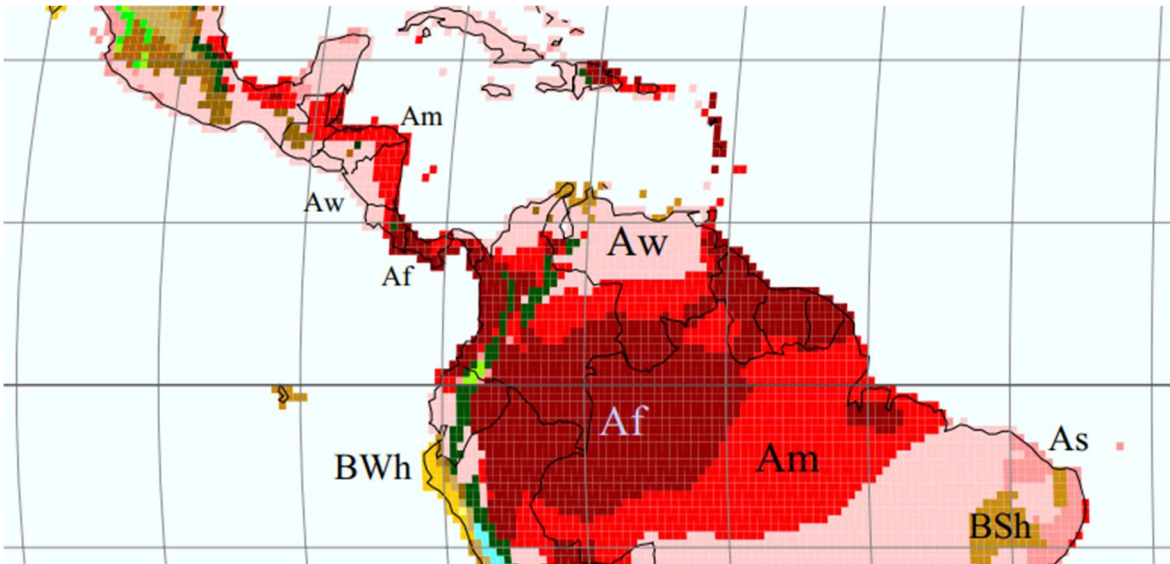


Figure 2-2-3: Köppen-Geiger classification

According with the climate classification of Köppen-Geiger, as it possible to see in the figure 2-3 , the department of Atlántico it is classified as Aw, a tropical savanna climate. This kind of climates is characterized by a pronounced dry season, with the driest month having precipitation less than 60 mm (2.4 in) and less than $100 - \left(\frac{\text{Total Annual Precipitation (mm)}}{25} \right)$ of average monthly precipitation.

Instead for the ASHRAE 90.1, that is a modified Köppen-Geiger system that identify 8 classes using heating and cooling degree-days with base temperatures of 18 °C and 10 °C respectively, furtherly subdivided according 3 humidity classes defined in agreement with the Köppen-Geiger (A: humid, B: dry; C: marine). According to this, Santa Lucia is classified as 1A, very hot-humid climate because more than 5000 days in the year the temperature is 10°C higher. This classification will be useful during the analysis of the properties of the building envelope because (48) define the minimum requirement for this climate zone.

To begin the analysis of the climates condition, it is important to specify that the dataset used it is relative to the meteorological measurement performed at the airport of the city of Barranquilla “Ernesto Cortissoz” and are not measurement performed in loco. With a good grade of approximation, it is possible to state that the environmental condition in Santa Lucia are approximately the same of the one perceived in the Cortissoz Airport. The time frame took under consideration by weather measurement goes from 2004 to 2018 and the average values are taken under consideration.

2.1. Dry Bulb Temperature

Beginning with the analysis of the dry bulb temperature (fig 2-4) values remain stable through the year with small temperature variation range through the day. It is possible to see that in the first 4 months and the last 4 months of the year the temperature is slightly lower of the median value of 27.9°C. The 4/5 central months of the year from May to September are the hottest one. In fact, on the 30th of September, it is registered the maximum temperature of the year of 36.3°C.

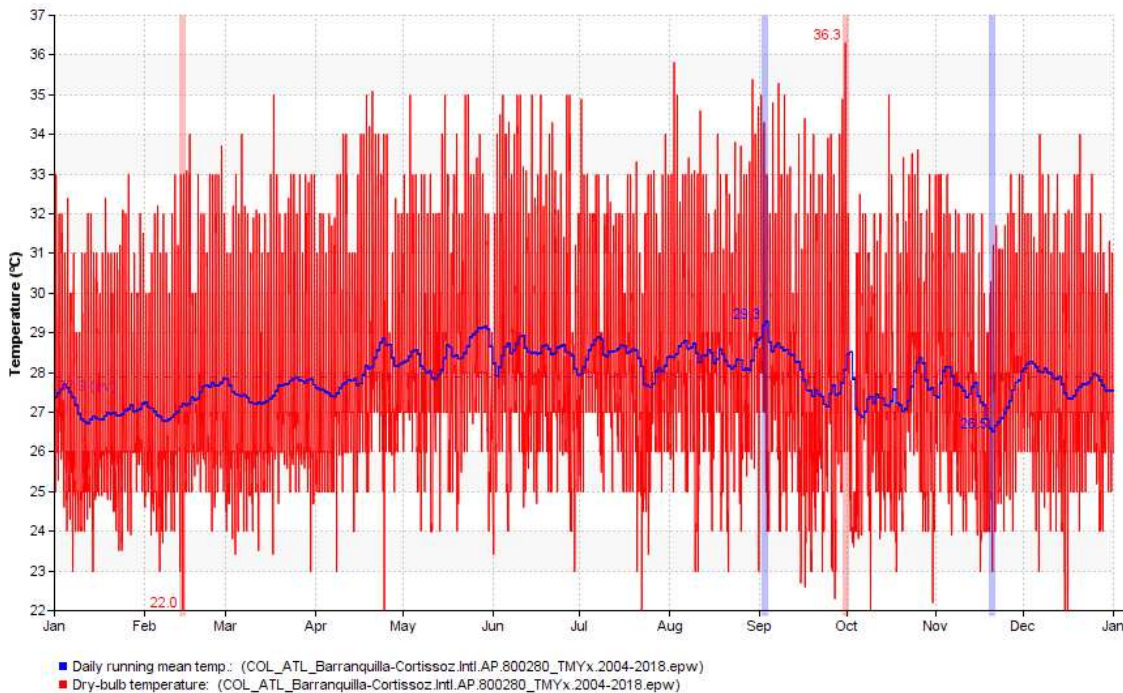


Figure 2-2-4: Dry-bulb temperature

Observing a typical week of May from 17 to 23 (Fig.2-5) it is possible to note how the thermic excursion does not exceed 10°C as a maximum value. This is an important information for the cooling system because it will have to work with huge loads but with stable operative temperatures, also during the year, that will guarantee optimal efficiencies if a good dimensioning is done.

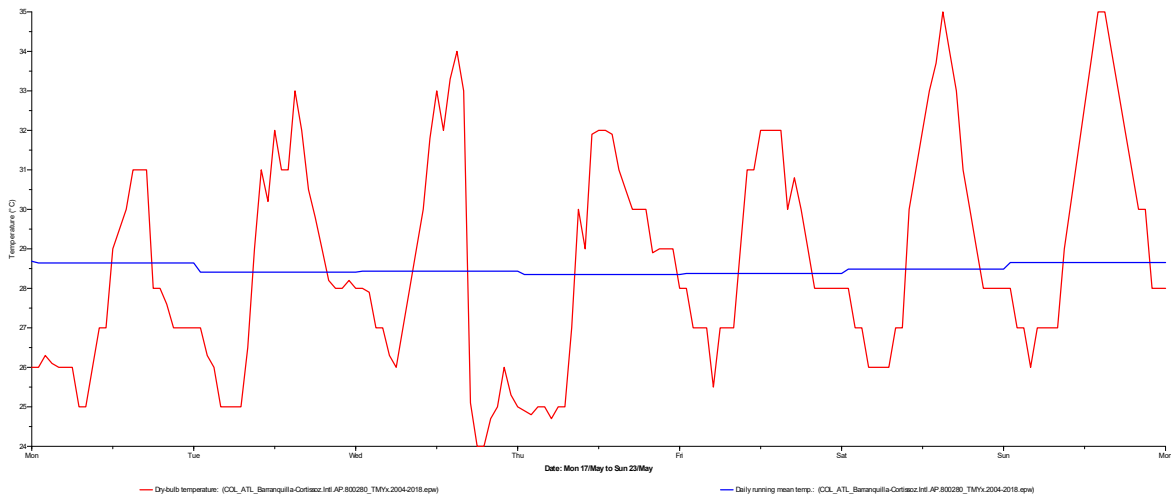


Figure 2-2-5: Dry bulb temperature from 17/05 to 23/05

2.2. Relative Humidity

Regarding the relative humidity, as a tropical climate, the values are really high on average. In this case, it is assessed near to 82% with the lowest value at 44%. The 100% of external humidity level it is reached 565 times in 8760 hours during the year. According to the color gradient chart (fig. 2-6) it is possible to appreciate the trend during the year and during the day of the humidity level.

From August to November it is a critical period, the levels are really high with a median value of 86.7%. Instead, analyzing the daily trend it is possible to appreciate how the highest value are recorded in the first hours of morning and night and then in the middle of the day relative humidity attests to lower values but anyway high for the humidity standards that

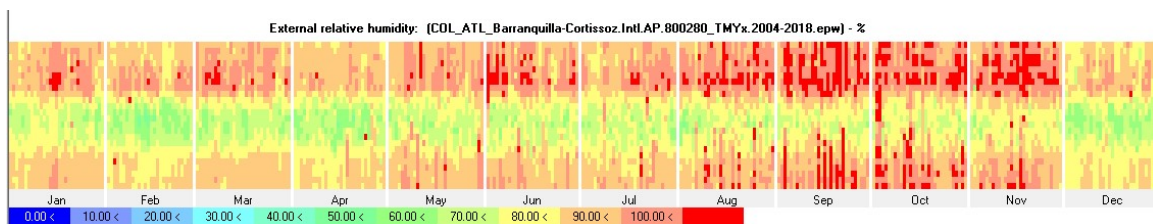


Figure 2-2-6: Relative humidity color gradient chart

have to be reached.

In order to guarantee the correct percentage of humidity inside the building, the dehumidification phase will be really important for the whole year, therefore the effect of latent heat recovery must be well evaluated.

Furthermore, because the scope of this work will include the evaluation for the usage of renewables energies, a brief analysis of the availability of solar and wind energy will be made.

2.3. Irradiance levels

Regarding the global irradiance level, it is registered a peak level of 1009.832 W/m^2 . In the figure 2-7 is possible to appreciate the two main component of the global irradiance, the

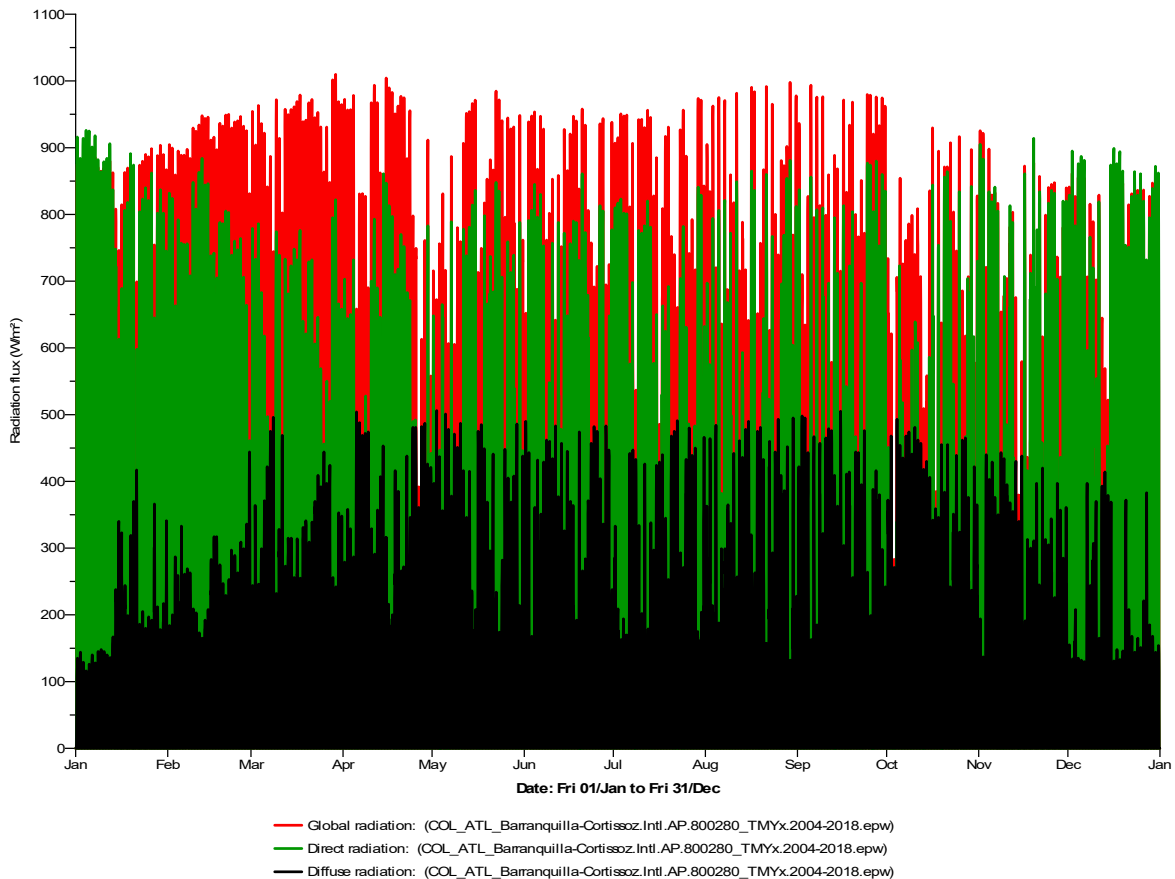


Figure 2-2-7: Global, Direct, Diffused Radiation level

direct radiation and the diffuse radiation. Regarding the diffused radiation level, they seem quite high and with reference to the global radiation values it seems not negligible, but a higher ratio between diffuse and global radiation represents a higher occurrence of clouds, higher atmospheric pollution or higher water vapor content. In fact, this aspect is confirmed by the data of relative humidity analyzed before. As it is increased the water vapor content in the air, as the reflected refractive radiation increase. In such a case, the intensity of the solar radiation received by the photovoltaic cell is reduced, which is reflected in the productivity of the cell.

At support of this, also according to the chart on Global Photovoltaic Power Potential made by World Bank Group that measure the electric power producible with a power plant of 1

kW, the position of Colombia in the chart is lower than Portugal also if the global radiation value of Colombia is higher. To conclude, the irradiance quality is not the optimal one because the ratio between diffuse and global radiation is high but good levels of energy production could be reached. According to a simulation made with the free tool of European commission, "PVGIS 5.2" (49) the estimated yearly PV energy production found was 1538.86 kWh and the yearly in-plane irradiation was 2105.08 kWh/m² but a set of hypotheses have been made. The PV technology was monocrystalline silicon and the power installed was 1 kWp. The entire system loss imposed was 14% and the PV module slope and Azimuth angle were set at their optimum values, respectively at 14° and -22°, to maximize power production. From this evaluation we can state that the quality of the global irradiance is not the best but the approximative energy production calculation supports the idea to exploit this source of renewable energy.

2.4. Wind speed measurement

Regarding the wind data measured, they are reported in the figure 2-8.

The values during the year are characterized mainly by two main different periods, for the first 4 months a seasonal wind characterize the wind velocity and it is assessed at a reference value $\cong 5$ m/s (18 km/h). It is possible to appreciate a drastic change of the wind velocity in

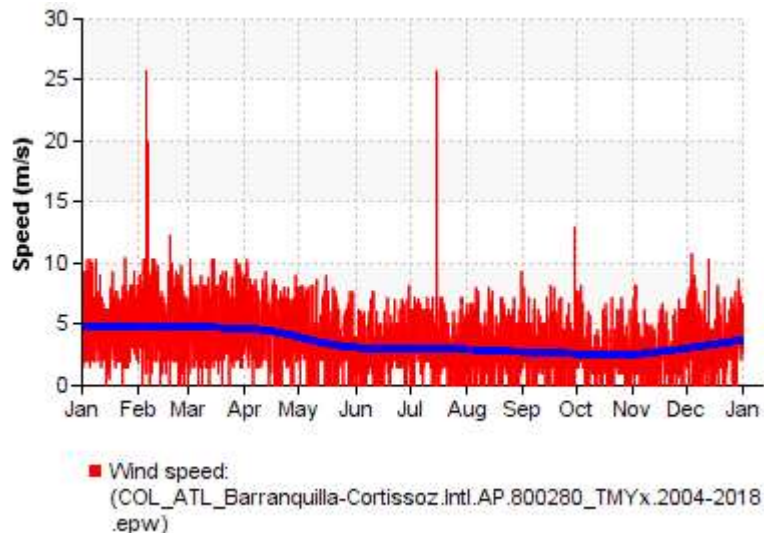


Figure 2-2-8: Daily wind data measurement

the other 8 months. The mean value is near to 3 m/s (10,8 km/h) with a decrease of 40% from the previous 4 months. Analyzing this data with the wind speed distribution diagram (fig. 2-9) it is possible to understand that a further installation of a wind turbine model have to

be evaluated taking under consideration that for 2216 hour in a year, the wind speed is around 3 m/s and the maximum value reached it is rarely more than 9 m/s.

Furthermore, the annual wind direction is also an important parameter to be evaluated. As possible to see in fig. 2-10 and 2-11 the main wind speed direction and relative high speed wind is mainly related to the NE direction and nearly 60% of the wind direction is between North and Est.

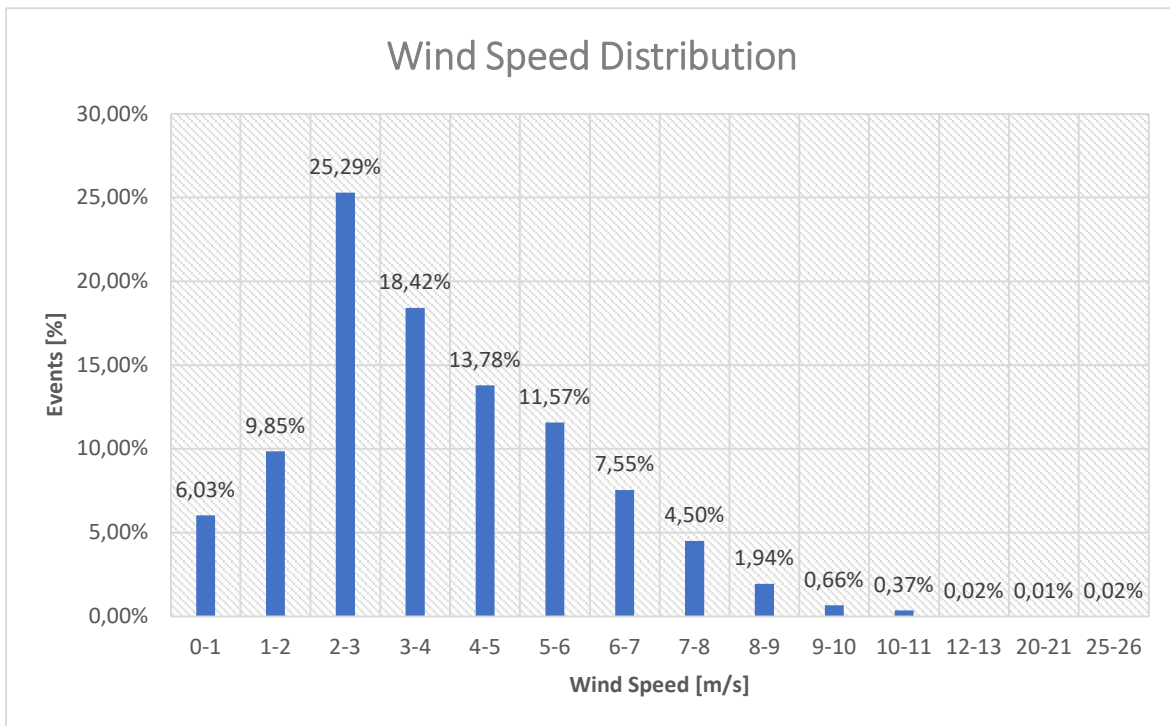


Figure 2-2-9: Wind Speed Distribution

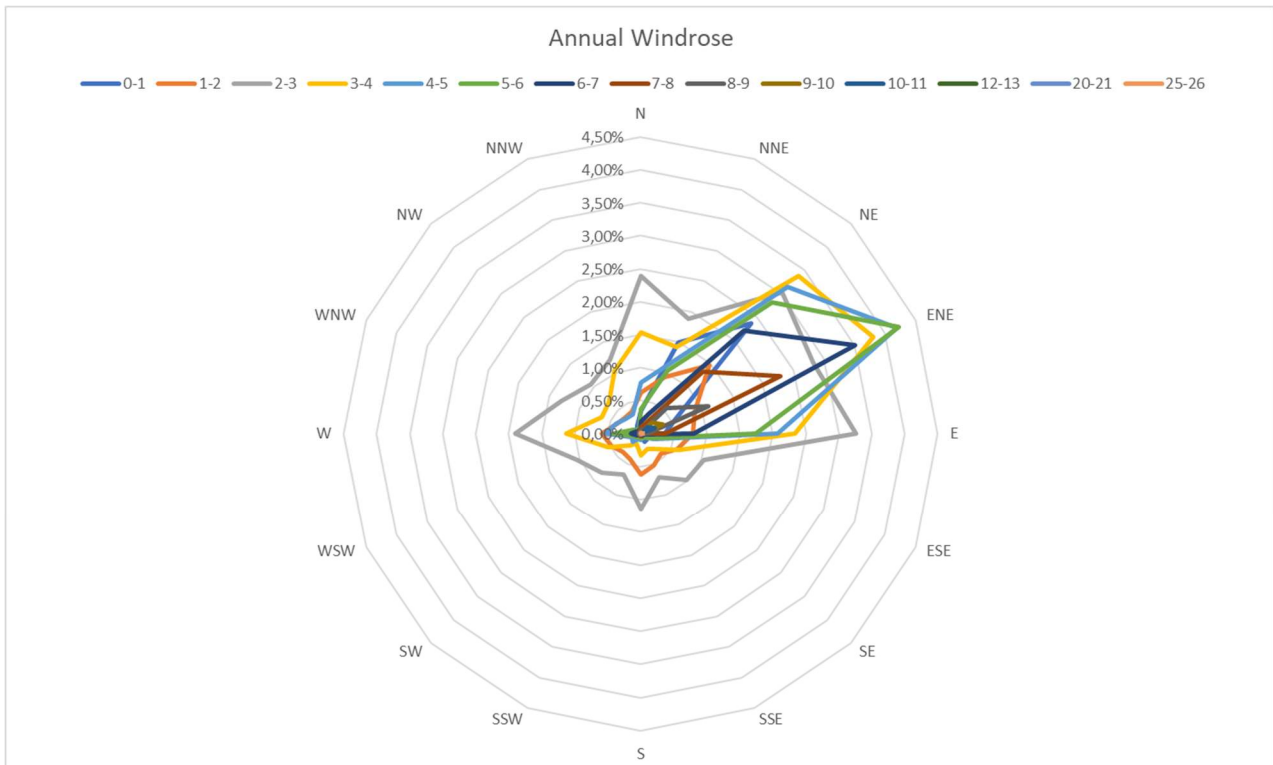


Figure 2-2-11: Annual Windrose

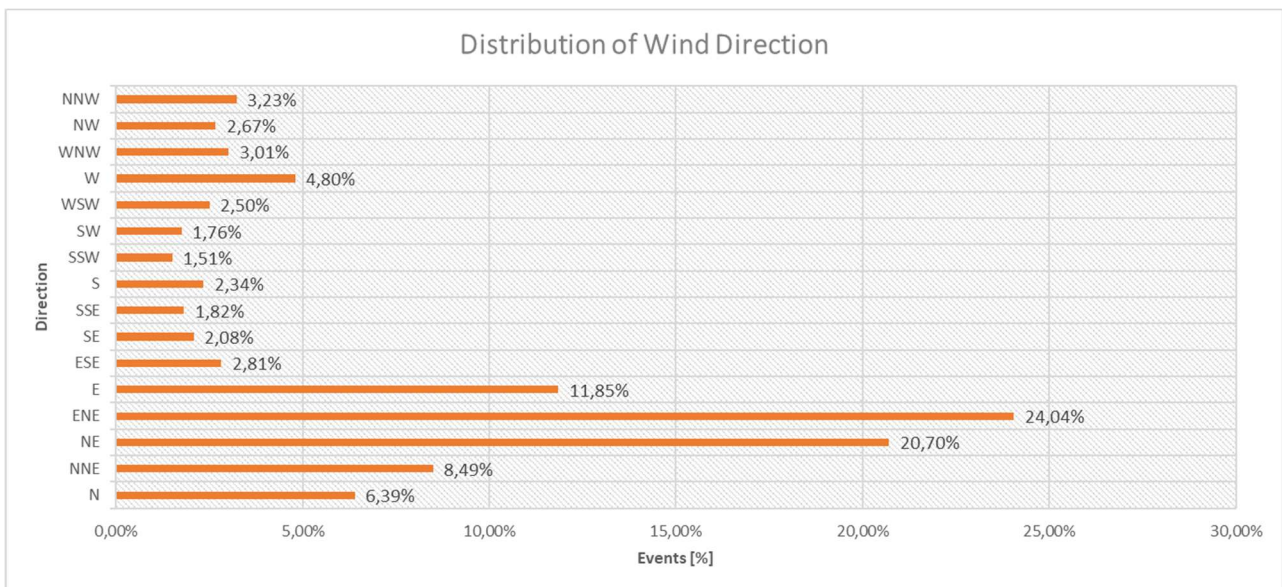


Figure 2-2-10: Distribution of Wind Direction

3 Building structure and IES-VE digital twin constrains description

3.1. Spaces

The Institución Educativa Santa Lucia it is locaed in calle Cra. 3 Calle 5 3 - 120, Santa Lucía, Atlántico, Colombia. The building structure has an estimated surface area of 5534 m2 conformed by six blocks of two floors each. It has 28 classrooms, 6 bathrooms, 3 laboratories, a library, a coffee shop, a sports field, and green zones. Only the teacher rooms have two air conditioning inverter systems of 12000 Btu each, all the other spaces lack of any kind of air-cooling system.



Figure 3-3-1: Top view of Institución Educativa Santa Lucia



Figure 3-3-2: Outside view of a classroom

Here are displayed the planimetries of the two building levels that had to be recreated from scratch from the pdf of the building planimetry.

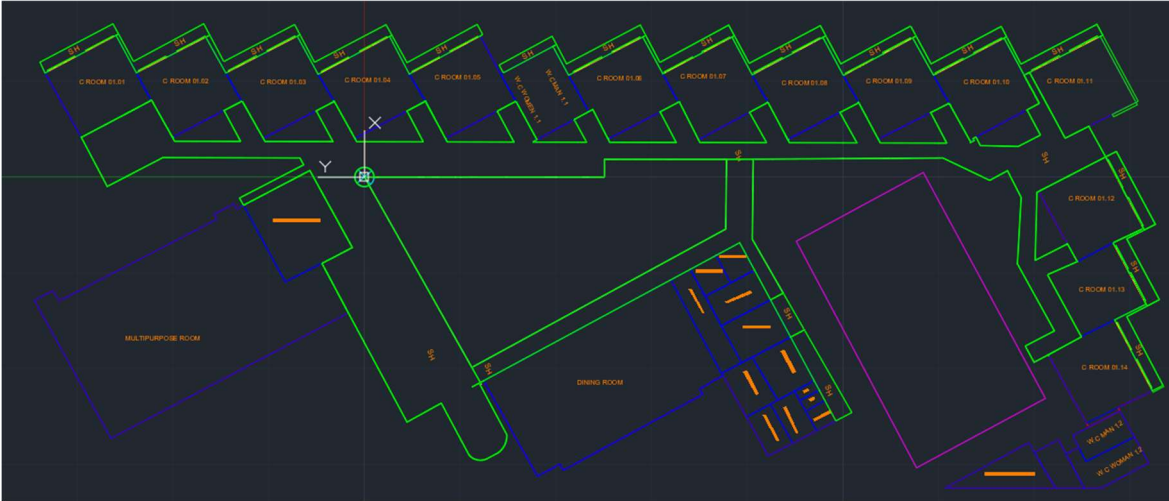


Figure 3-3-4: Dwg of first floor

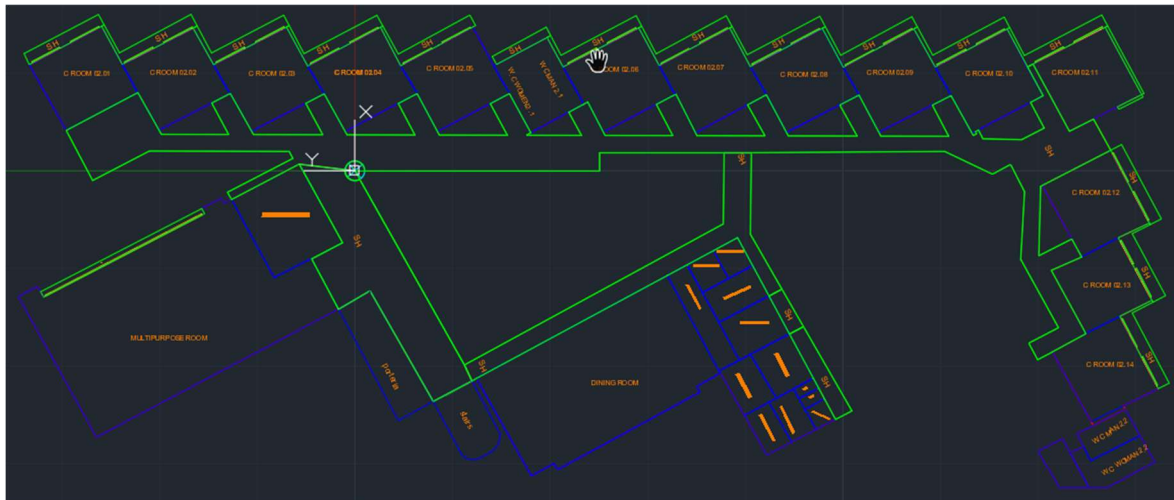


Figure 3-3-3: Dwg of second floor

3.2. IES-VE PRM structure and calculation model used

The IES Virtual Environment (VE) is a suite of building performance analysis applications. It can be used by designers to test different options, identify passive solutions, compare low-carbon & renewable technologies, and draw conclusions on energy use, CO₂ emissions and occupant comfort.

To setup and evaluate the digital twin, the Performance Rating Method (PRM) of ASHRAE Standard 90.1-2010 have been chosen. The PRM can be used to demonstrate compliance with the standard and to rate the energy efficiency of commercial and high-rise residential buildings with designs that exceed the requirements of Standard 90.1.

The PRM workflow is detailed under the following five headings:

1. Model Data (Preliminary Setup)

Preliminary data is required to define the PRM models. This includes tasks such as, building geometry creation, specifying orientation, etc.

The primary actions in this section are:

- **User Details:**
Provide username, company name, etc
- **Site, Location and Climate:**
Usage of APlocate to define the site location and weather detail
- **Building Geometry:**
Creation of the building geometry using standard methods while also providing advice on zoning strategy. Also, definition of the building orientation and any obstruction data.
- **Room / Zone Names:**
Provides advice on the naming strategy for the various rooms (zones) in the building
- **Prototype data (ASHRAE Baseline):**
Import prototype data which contains ASHRAE 90.1 information and sensible defaults where ASHRAE baseline information is not applicable
- **Room / Zone Groups:**
Use the VE room group creator to assign rooms to pre-defined prototype room groups
- **Solar Shading:**
Use suncast to carry out a full solar analysis

2. Model Data (Proposed Model)

When the preliminary data setup is complete, the user is then required to derive the proposed model and assign proposed elements to the preliminary model.

The primary actions in this section are:

- **Envelope Thermo-physical Properties:**
APcdb is used to create and assign proposed constructions to the model
- **Room / Zone Template Data:**
As the model has been organised appropriately in the preliminary setup the prototype information can now be easily assigned to each room via the 'space types' room groups. Initially the data that's assigned to proposed model is ASHRAE baseline information. The user is given the opportunity to edit this information by reviewing the thermal templates. Input data for external lighting and elevators / escalators is also required
- **HVAC systems:**

Once the model has been populated with thermal information, a sizing run is performed. The user is then required to create a proposed system in ApacheHVAC and populate it with information from the sizing run.

- **Renewable Energy Systems:**
The renewables dialog is used to define either PV panels, Wind generators or CHP generators
- **Utility Tariffs:**
A utility tariff is defined in terms of \$(kWh) for electricity, gas, coal and oil

3. Model Data (Baseline)

The baseline model variants are derived from the proposed model. Four models are required 0°, 90°, 180° and 270°. The baselines models are updated with ASHRAE 90.1 specific information based on climate zone, etc.

The primary actions in this section are:

- **Create:**
This automatically creates the baseline variant and applies the correct glazing percentages and constructions.
- **Envelope Thermo-physical Properties:**
This gives the user the facility to review what constructions have been applied to the model
- **Room / Zone Template Data:**
Baseline templates are created and assigned. These are a copy of the proposed templates created earlier. The user is given the opportunity to review this information by interrogating the thermal templates
- **HVAC systems:**
As with the proposed model the user is required to create a baseline system in ApacheHVAC and populate it with information from the sizing run

4. Simulation

When the model creation process is complete the simulations are ready to be performed. This section of the navigator allows the user to run single simulations to test either the proposed or baseline case, or a simulation batch run which will automatically run all five simulations.

The baseline models are run automatically, however data is required for the proposed simulation. This data will determine the parameters for all five runs e.g. the results file name, the duration of simulation, etc.

5. Results Output and Analysis (LEED EA c1)

When the simulations are complete the results data is used to populate the PRM reportage which is presented in a format similar to LEED EAc1 Letter Template. Results can be viewed for the entire report or for specific tables within the report.

3.2.1. Physical Model Used by the Software

This section briefly introduces the calculation models used by the software. These are obviously dynamic models, with a minimum time interval of the order of a minute. The information was extracted from the IES-VE guidelines (50)

Conduction

For the modelling of conductive heat exchange, the software uses the finite difference method to solve the heat equation.

Assumptions considered:

- The conduction through each element is assumed to be 1D one-dimensional
- The thermophysical properties λ , ρ , c are considered uniform in the space within the reference solid body

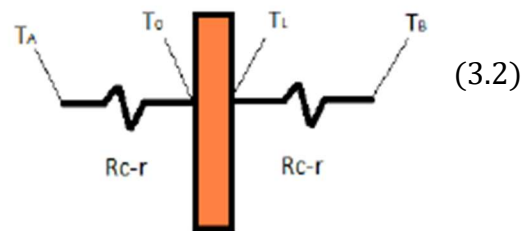
With these assumptions, the heat equation can be written as:

$$\rho c \frac{dT}{dt} = \lambda \frac{d^2T}{dx^2} \quad (3.1)$$

Where " ρ " is the air density [kg / m^3], " λ " is the conductivity coefficient of the solid [$\text{W} / \text{m}^2\text{K}$], " c " is the specific heat at constant air pressure [J / kgK].

A condition of continuity of the thermal flux vector at the boundary is then considered. The boundary conditions are:

1. At time $t = 0$ $T(x, 0) = T_0 \forall x$
2. For $x = 0$ $-\lambda \frac{dT}{dx_{x=0}} = h_{cr} [T_a(t) - T(0, t)]$
3. For $x = L$ $-\lambda \frac{dT}{dx_{x=L}} = h_{cr} [T_b(t) - T(L, t)]$



Where $Rc-r$ is the radiative conductive resistance, h_{cr} is the radiative conductive coefficient.

The finite difference method is based on a discretization of the space-time domain So:

$t = j * \Delta t$ where Δt is the time step and j is the number of intervals

$x = i * \Delta x$ where Δx is the spatial step and i is the number of intervals

Leaving aside the various steps, we then move on to a discretized equation:

$$\frac{\Delta T_i^j}{\Delta t} = \alpha \frac{\Delta^2 T_i^j}{\Delta x^2} \quad (3.3)$$

This operation is possible only if the conditions of Consistency, Stability and Convergence are valid. For the solution of the discretized equation, this is developed in Taylor series (already convergent in itself).

The derivation method used for spatial discretization is the central derivative:

$$\frac{\Delta^2 T}{\Delta x^2} = \frac{T_{i+1}^2 + T_{i-1}^2 - 2T_i^2}{\Delta x^2} \quad (3.4)$$

While for time discretization, if you want to use an explicit method, the forward derivative is used:

$$\frac{\Delta^2 T}{\Delta x^2} = \frac{T_i^{j+1} + T_i^j}{\Delta t} \quad (3.5)$$

Or, if you want to use an implicit method, the back derivative:

$$\frac{\Delta^2 T}{\Delta x^2} = \frac{T_i^j + T_i^{j-1}}{\Delta t} \quad (3.6)$$

These methodologies are combined to have an acceptable compromise between the advantages and disadvantages of the two methods: the explicit one is "faster" and, in order not to lose stability, it must have a much higher spatial step than the temporal one.

On the contrary, the implicit method is unconditionally stable, therefore it allows to analyse smaller time intervals, while requiring a greater number of calculation steps and thus occupying more memory. The method used by the program is the: "Crank Nicholson" combinations of both. To take into account the storage of heat in the indoor air, the following equation is used:

$$Q = (1 + F_f) * c * \rho * V * \frac{dT_a}{dt} \quad (3.7)$$

Where:

"C" and "ρ" are specific heat and air density. "V" and "Ta" are respectively the internal volume of the envelope and the internal air temperature. To consider the thermal inertia of the internal components, IES introduces a corrective factor "Ff".

Convection

As regards the heat exchange due to convection, the software calculates the convective heat exchange coefficient as follows: For the external convection the program uses the "McAdams relations" which estimate the convection coefficient as a function of the wind speed. For internal forced convection, on the other hand, different methods can be used:

- Use of fixed values of h_c specified by CIBSE.
- Use of fixed values present in the APcodb database.
- Variable convective exchange coefficients depending on the temperature difference, air speed and surface orientation, as calculated for the CIBSE procedure.
- Use of Alamdari & Hammond reports.

The last two alternatives proceed by updating the convection coefficient with an iterative method. A detailed description of the different methods will not be exposed as they are not the subject of this thesis.

Infiltrations and radiative exchange

As regards the contribution due to air infiltrations, the equation is followed for the calculation:

$$Q = mc_p(T_i - T_a) \quad (3.8)$$

Where:

"M" and "cp" are respectively the flow rate and the specific heat at constant pressure of the moving air, "Ti - Ta" is the difference between the air intake temperature and the ambient temperature.

The radiative exchange is distinguished in long wave radiation, that is the radiative exchange between surfaces or subjects with a temperature not very different from the ambient temperature, and short-wave radiation, where very different temperatures come into play such as the solar radiation incident on the walls. Regarding the long-wave

radiative heat exchange, the program uses a calculation method based on the mean radiant temperature, where the net flux on the i-th surface is represented by the formula:

$$\varphi_{net,1} = A_i h_i (\theta_i - \theta_{mr,i}) \quad (3.9)$$

Where:

A_i is the surface considered [m^2], h_i is the radiative heat transfer coefficient [$\frac{W}{m^2K}$], calculated as $\sum_{j=1}^n h_{i,j}^{rad}$,

$h_{i,j}^{rad}$ depends both on the surface temperatures and on the mutual radiation factors θ_i is the i-th surface temperature, $\theta_{mr,i}$ is the mean radiant temperature "seen" from the i-th surface defined as $\sum_{j=1}^n \frac{h_{i,j}}{h_i} \theta_j = 1$ where all the other surfaces are identified with the subscript j.

For the calculation of h_i and the average radiant temperature, the program introduces simplifications or considers all surfaces as grey bodies of equal emissivity. It then uses a method for the calculation of the average radiant temperature provided by CIBSE, not detailed in this thesis. The radiation exchanged by the water vapor particles with the walls is also considered through the Hottel approximation which calculates the emissivity of the air as a function of partial pressure and an equivalent length. As regards the solar radiation incident on the external walls, both the direct and diffuse radiation from the SunCast module is calculated, distributed over time for each surface, also taking into account the shading. For the purposes of this thesis we will not go into the calculation model used by this module.

Balance equations

Once all the different contributions due to the heat exchange have been calculated, ApacheSim uses a "Stirred tank" model assuming that the room temperature and humidity are uniform, for the resolution of the energy balance. The sensitive balance equation will consider the various aspects previously treated plus the contribution of sensitive heat due to internal loads:

$$C \frac{d\langle \theta \rangle_v}{dt} = \sum_{i=1}^{N_{s,inv}} m^{as} c_p^{au} (\langle \theta \rangle_{s,inj} - \langle \theta \rangle_v) + \sum_{i=1}^{N_{s,sup}} A_i h_{cr} (\langle \theta \rangle_{s,i} - \theta_{op,i}) + Q_{P\&C}^{cr,s} + Q_{Sys}^{cr,s} \quad (3.10)$$

Where:

"C" indicates the heat capacity of the humid indoor air [J / K], The first term after the same is the heat exchanged by infiltrations or the introduction of air into the environment. The second term indicates the convective-radiative heat exchange in the environment due to the

surfaces of the envelope. The third and fourth term are the internal loads produced by people and machinery, and those produced by the plant (sys).

the latent balance equation:

$$h_v^{H2O} \rho^{as} \frac{d \langle x \rangle_v}{dt} = \sum_{j=1}^{Ns,inv} m_{in,j}^{as} h_v^{H2O} (\langle x \rangle_{s,inj} - \langle x \rangle_v) + Q_{Sys}^{lat} + Q_{P\&C}^{lat} \quad (3.11)$$

Where:

The first term on the left of the equal represents the accumulation of water vapor in the ambient air. The first term after the equal represents the latent heat resulting from the air flows entering the envelope for each surface. The second term and third term represent the contributions of latent heat (adjective plus mass exchange) introduced by the plant and by people and machinery.

As we have seen there are different methods to determine the various terms of the equations, to be consistent with the legislation, in the simulation we will use the ASHRAE method selectable in the program settings.

3.3. Shape and Orientation

The building has been modelled according to the real dimension and orientation.

The orientation of the building was set at 265° from the north direction. The ratio between surface and volume of the building is 0,33 and the distribution of the windows related to the classrooms is distributed mainly on the north direction but also 6 classes are exposed to East.

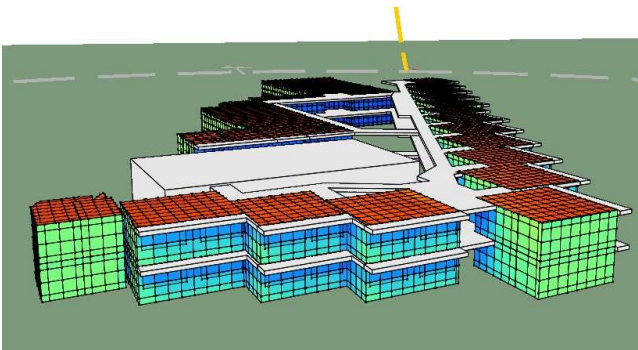


Figure 3-3-5: East solar exposure

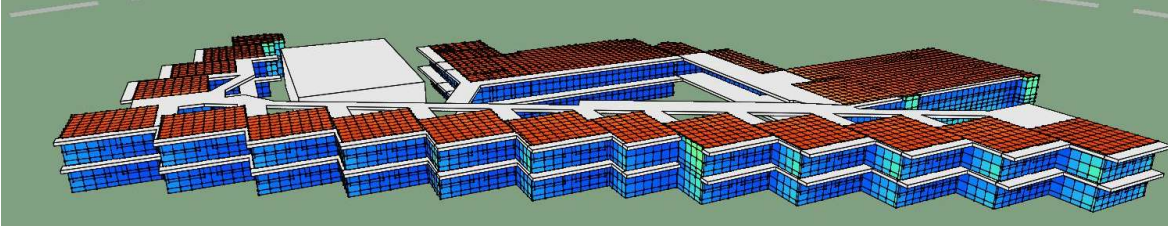


Figure 3-3-6: North solar exposure

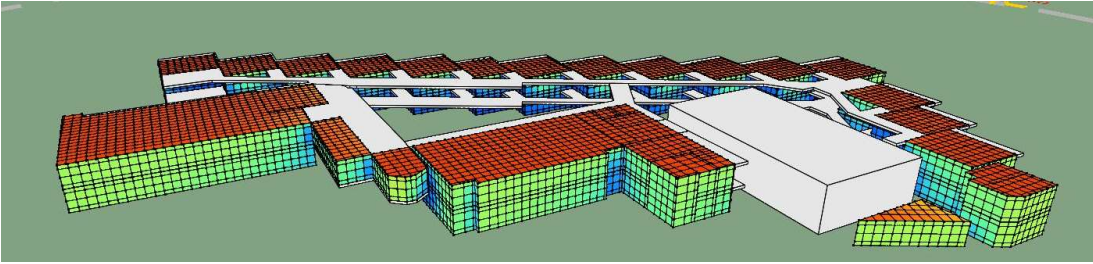


Figure 3-3-7: South solar exposure

According to the solar shading analysis, it is possible to predict which kind of building elements will be more affected by the solar impact and furthermore identify which kind of building sector have to be improved. It is possible to see from the solar exposure analysis how the orientation of the classroom (mainly north) together with the shading system on top of the windows and in the walking central part of the school, helps to avoid that a lot of the solar radiation on North and South side get inside the classrooms, heating up the environment as solar gain or trough irradiation of the external envelope.

It is possible to observe how the colour difference it is remarkable from north and south side of the whole school, for this reason it is possible to conclude that the orientation of the classroom and the whole building were made correctly and thanks to that are the less impacted by solar contribution.

Furthermore, the south school side will be really influenced by the solar impact but for the scope of this thesis, only the classroom will be analysed and equipped with the cooling system.

To conclude, it was also taken into account the presence of PV panels and it's shading effect ont on the roof in order to evaluate stratigraphy changes before and after.

3.4. Opaque And Transparent Envelope Properties

Firstly, in order to recreate in the most verisimilar way the case study building, the entire dwg file were recreated through the use of Autocad. Only the perimeter boundaries of the air-conditioned areas have been delineating.

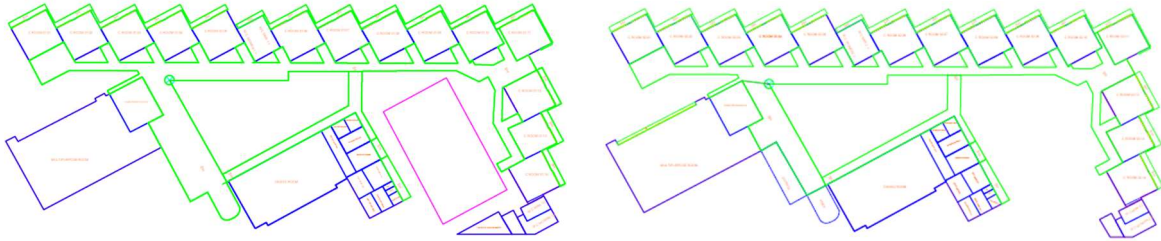


Figure 3-3-8: Planimetry of 1st and 2nd floor

Then by importing the profile built in Model IT, the three-dimensional model was built, creating the external envelope and dividing each floor by internal partitions for the creation of the individual rooms. Then, we proceeded to create the external shielding systems.

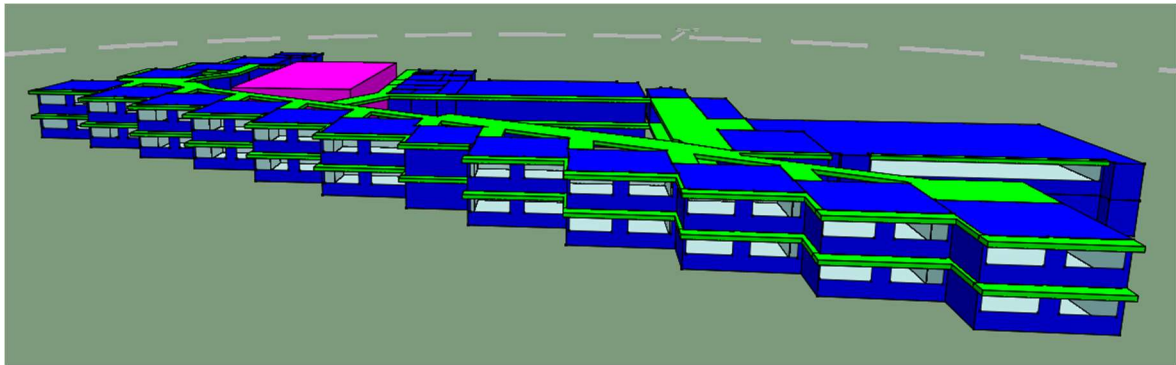


Figure 3-3-9: Building digital twin created by IES-VE

Once the envelope has been created, the geographical location of the building and its orientation have been defined using the APlocate function present in the Apache module. Selecting the project settlement area (Santa Lucia, Atlantico, Colombia), the climatic data were loaded from the airport database. Furthermore, in this section, it was possible to load the Colombian holiday calendar.

The next step was to insert the stratigraphy of the opaque envelope.

Since the components of the envelope must have the same characteristics as the real ones, the same project information has been applied to opaque and transparent elements.

The opaque envelope has a simple structure, it is constituted mainly by simple concrete. The thickness of the block has been set by 150 mm and here are reported the main physical properties of the block.

Material	Thickness mm	Conductivity W/(m·K)	Density kg/m ³	Specific Heat Capacity J/(kg·K)	Resistance m ² K/W	Vapour Resistivity GN·s/(kg·m)
[CBL] CONCRETE BLOCK (LIGHTWEIGHT)	150.0	0.1900	600.0	1000.0	0.7895	83.000

Figure 3-3-10: Concrete block properties

It as been used for the whole external walls and internal partition. Instead for the roof and internal ceiling floor the stratigraphy of the layers are respectively reported in the following images.

Material	Thickness mm	Conductivity W/(m·K)	Density kg/m ³	Specific Heat Capacity J/(kg·K)	Resistance m ² K/W
[STD_PHF] Insulation	3.0	0.0300	40.0	1450.0	0.1000
[STD_MEM] Membrane	0.1	1.0000	1100.0	1000.0	0.0001
[STD_CC1] Concrete Deck	100.0	2.0000	2400.0	1000.0	0.0500

Figure 3-3-11: Roof layer properties

Material	Thickness mm	Conductivity W/(m·K)	Density kg/m ³	Specific Heat Capacity J/(kg·K)	Resistance m ² K/W
[STD_CC2] Reinforced Concrete	100.0	2.3000	2300.0	1000.0	0.0435
Cavity	50.0	-	-	-	0.2100
[STD_FBA] Chipboard Flooring	20.0	0.1300	500.0	1600.0	0.1538

Figure 3-3-12: Internal ceiling roof properties

Regarding the transparent envelope elements, a traditional window has been installed.

Material	Thickness mm	Conductivity W/(m·K)	Angular Dependence	Gas	Convection Coefficient W/m ² ·K	Resistance m ² K/W	Transmittance	Outside Reflectance	Inside Reflectance	Refractive Index	Outside Emissivity	Inside Emissivity	Visible Light Specified
[STD_EXW] Outer Pane	6.0	1.0600	Fresnel	-	-	0.0057	0.409	0.289	0.414	1.526	0.837	0.042	No
Cavity	6.0	-	-	-	1.4033	0.6183	-	-	-	-	-	-	-
[STD_INW] Inner Pane	6.0	1.0600	Fresnel	-	-	0.0057	0.783	0.072	0.072	1.526	0.837	0.837	No

Figure 3-3-13: Windows properties

3.5. Internal Gains

The next step was the subdivision of the building into different zones, assigning each its specific set-points and related internal loads.

The ASHARE90.1-2010 proposes two methods: the "Building Area Method" and the "Space by Space Method", according to which to define the thermal zones. The first considers the entire building as a single thermal zone, this can only be done if there is a prevalent activity (for example, an office building without special use areas). The second involves the

repartition of the building into zones based on their functionality, internal loads and the system corresponding to them.

The building of this thesis has rooms with different thermal set-points and functionalities so the "Space by Space Method" were used also if the main focus of the study is to guarantee the satisfactory levels of IAQ and thermal comfort only inside the classroom.

Accordingly to the method used, different thermal zones have been created through the template manager of the Apache module of IES VE. Thanks to this tool, it was possible to define and attribute the thermal set-point conditions, internal loads and air infiltrations of the classrooms.

As a thermal set point, it was imposed a main set point value of 26.5 °C in accordance to the values discovered during the analysis of the scientific papers performed before. Instead for the humidity control, the minimum and the maximum saturation level have been set respectively 55% and 65%. The system will work in accordance to the occupancy profile set for the internal loads.

3.5.1. Air infiltration

With reference to air infiltrations, every classroom is equipped with openings, one under the windows, the other one on one vertical side and allow a natural exchange of air between the external environment and the classrooms (fig 3-14).



Figure 3-3-14: Openings dimension

In order to simulate their presence, an air infiltration element have been taken under consideration for each classroom. Many different scenarios have been evaluated. Starting

form the value of the weighted average annual wind speed and the surface openings on the walls was possible to come out with an air infiltration intake of $31.92 \text{ m}^3 / \text{s}$. It has been hypothesized that 50% of the surface of the measured rectangles are openings in order to have a conservative evaluation. Anyway, the first value of infiltration obtained with a average wind speed of 4.315 m/s is evidently too high. Also the room load calculation final results assess cooling loads values of 1010.16 W/m^2 . For this reason, many attempt have been done changing the wind speed value until 0.1 m/s . Comparing this last case with the case with no infiltration, we obtain respectively 68.41 W/m^2 and 47.04 W/m^2 cooling loads.

To conclude, the case with infiltration set to $0,1 \text{ m/s}$ could be a realistic and the less conservative one. However, the energy saving obtainable with minimum infiltration in comparison with 0.1 m/s case is 31.24% . For this reason, the dimensioning of the cooling system will be done considering all the openings closed because it is a preliminary intervention that will guarantee nearly a $1/3$ energy expenditure reduction.

3.5.2. Internal loads

For the creation of internal loads, the time profiles concerning occupation, lighting and equipment (computers, printers, etc.) usage have been set in accordance to the daily usage by students of the classrooms. Lessons starts at 7:00 and finishes at 17:00 with a one-hour break for lunch between 12:00 and 13:00 (fig 3-16).

For the occupancy, a $1,76 \text{ m}^2 / \text{person}$ was the value set as occupancy density in order to simulate the presence of 35 students in each classroom.

For the lighting load, the usage profile of the lights behaves according to the availability of solar natural light. The usage profile imposed in the software was "external lighting with photosensor control" and it aims to reduce to 0 the light usage when a level of 50 lux is guaranteed by sun. With this profile it is attempted to take under consideration only the moment of the day in a year when the sunlight is not available. The lighting technology adopted was fluorescent lighting with a power density of $13.347 \text{ W} / \text{m}^2$.

For the equipment, in this case only computer, the usage profile follows the same one imposed for lighting and occupancy. The power densities chosen was 10.764 W/m^2 and it was supposed the presence of 1 computer for each classroom.

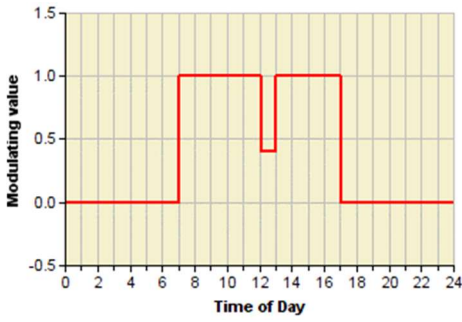


Figure 3-3-16: Daily occupancy profile

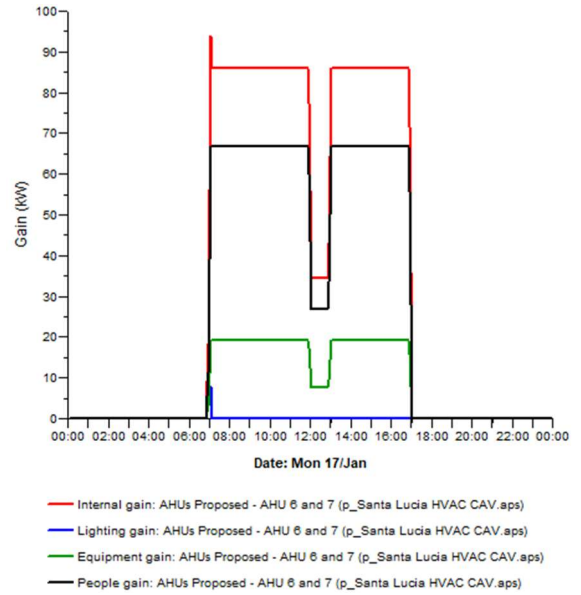


Figure 3-3-15: Daily Internal Daily Profile

To conclude, the daily internal gain profile of the rooms it is similar for each school day as shown in the fig 3-15. It is possible to appreciate how artificial lighting system it is used only for some minutes in the early hours of the morning (blue line). Regarding the people gain, it represents the main internal gain source inside the classrooms that have to be eliminated to keep the optimal room condition defined before together with the CO2 production of the students.

Additionally, to the daily profile, also the weekly and annual profile have been defined. Students go to the school from Monday to Friday, for this reason the system switch off completely during the weekend. Annually speaking, the academic calendar was taken under consideration in order to include all the festivity and closing days of the school.

School Holidays	Starts	Finishes
First Day of School	24 Jan 2022 (Mon)	
Easter Holidays	11 Apr 2022 (Mon)	17 Apr 2022 (Sun)
Semester 1 Holidays	20 Jun 2022 (Mon)	10 Jul 2022 (Sun)
October Holidays	10 Oct 2022 (Mon)	16 Oct 2022 (Sun)
Last Day of School	4 Dec 2022 (Sun)	

Figure 3-3-17: School Yearly Calendar

3.6. Centralized AHU with fan Coil Architecture & Cooling Thermal Loads

Once defined and assigned the thermal template to each zone of the building, 2 different HVAC system have been modelled in order to compare two different solutions. The first system proposed is an all-air system with room fan coil. Air is used as the media and transports thermal energy from the conditioned space to the HVAC plant. In these systems air is processed in the A/C plant namely AHU (Air Handling Unit). AHU consists of Dampers, Mixing chambers, Filters, Cooling/ Heating coils, Humidifiers, Fans/ Blowers etc. in a packaged cabinet. This processed air is then supplied to the conditioned spaces through Air Distribution system. Air Distribution system consists of Ducts, Dampers and Diffusers. This air extracts (or supplies in case of winter) the required amount of sensible and latent heat from the conditioned space. The duct that supplies the air to spaces is called Supply Air Duct (SAD). The return air from the conditioned space is conveyed back to the plant, where it again undergoes the required processing thus completing the cycle. The duct that returns the air from spaces to A/C plant is called Return Air Duct (RAD). Adequate Fresh air is always supplied by AHU to maintain Ventilation and Indoor Air Quality (IAQ). Furthermore, the fan coil units in the conditioned space works to mitigate the internal loads effects further processing the air in the conditioned space. In this case, the system architecture chosen was a single duct, constant volume, single zone system.

In a single duct system, there is only one supply duct, through which either hot air or cold air flows, but not both simultaneously. In a constant volume system, the volumetric flow rate of supply air is always maintained constant. The control is based on temperature and Relative humidity (% RH) measured at a single point. Here a zone refers to a space conditions controlled by one thermostat. However, the single zone may consist of a single room or one floor or whole building with several rooms. The cooling/ heating capacity in the single zone, constant volume systems is varied by varying the supply air temperature and humidity, while keeping the supply airflow rate constant. Volume control dampers (VCD) are used to balance the Return air and Fresh air flows.

The decision to choose this architecture was dictated several factors. The orientation of the classroom is basically the same and it is not affected by a huge gradient of solar gain between the different classrooms. Furthermore, the room loads are comparable between all the classrooms also because the number of students inside is fixed to 35 persons and the dimension of the room are similar. The ventilation rate required for each room is fixed to 11 l/s/pp as the temperature and humidity set point that are respectively set to 26.5 °C and 55%-65% for each classroom. To conclude, having only one supply duct that cannot bring in the same moment hot and cold air is not a problem because the building has to be cooled the whole year due to the high humidity and temperature of the tropical climate. Furthermore, having similar loads between the rooms help to have a fixed consumption of the system during the year and the possible implementation of a sensible recovery system

could help to save more energy. Additionally, from an economy of scale of point of view, having a centralized system that produce the cooling needs helps to avoid the installation of numerous terminal units inside the conditioned spaces and auxiliary equipment has fans or pumps.

Analysing the drawbacks of Centralized AHU with fan Coils, since systems are quite large in size, require separate spaces like AHU Room. It reduces use of effective floor space. Particularly in high rise buildings, it is difficult to provide long runs of ducts, as AHUs are located either on roof or basement. Luckily, our building has only 1 floor more additionally to the basement floor and the continuity of the structure guarantee an optimal installation of the cooling ducts. Another drawback could be the difficulty for the installation in existing buildings, as large space is required in false ceiling to lay the ducts. Fortunately, each classroom of the school has relatively high ceilings and no installation problem could be faced.

3.6.1. System Configuration

Giving a look to the system architecture, in the figures 3-18 and 3-19 we can appreciate the configuration of the multizone constant air volume system. Part of the components present have been not used for the calculation of the loads. For example, for the economizer duct, no air will be addressed to this side of the system because during the simulation were find some problems to regulate the indoor temperature. The energy recovery heat exchanger has been used and it was decided to implement a plate air to air heat exchanger with a 60% efficiency of sensible heat recover.

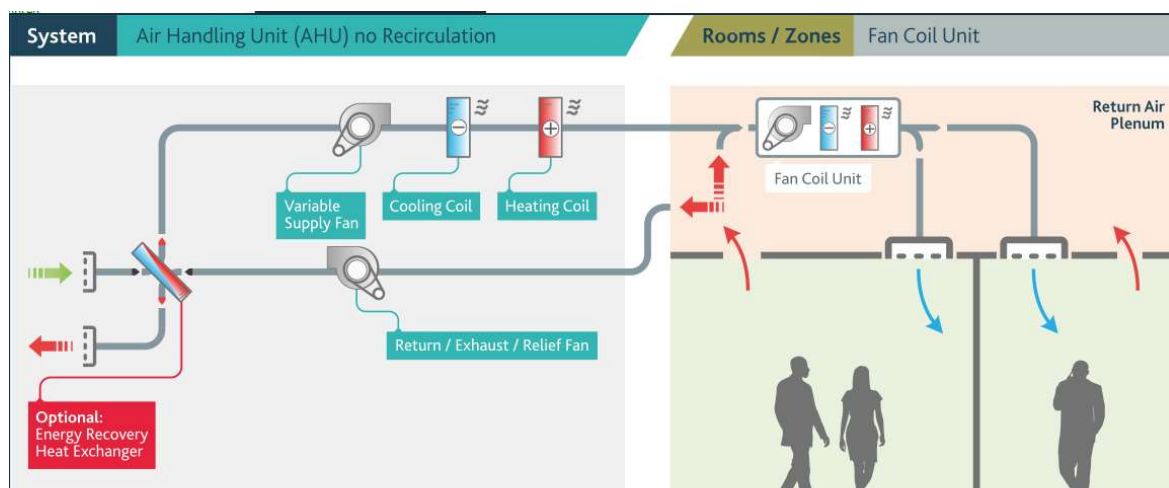


Figure 3-3-18: Air Handling Unit with Recirculation

It was decided to use 100% outside supply air in order to minimize the CO₂ content inside the room and address the constant fresh air needed for the ventilation.

All the sensors installed in the system (fig. 3-19) are setted to guarantee to the rooms a strict temperature and humidity range of 26.5°C – 26.9°C and 55% - 65% and to avoid the use of the economized duct.

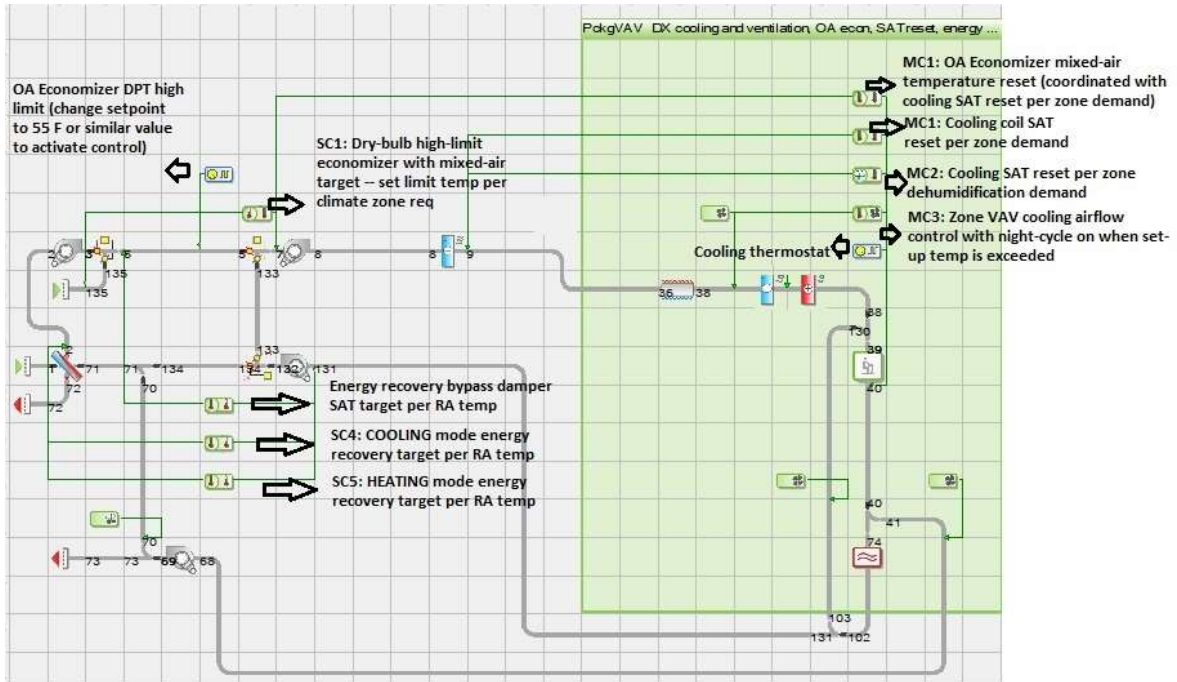


Figure 3-3-19: AHU System Architecture

It is difficult to explain the combination of the all sensors but basically the main interventions was related on the set up the MC1, MC2 and MC3 sensors of a constant profile according to the fig 3-20 in parallel with the system usage.

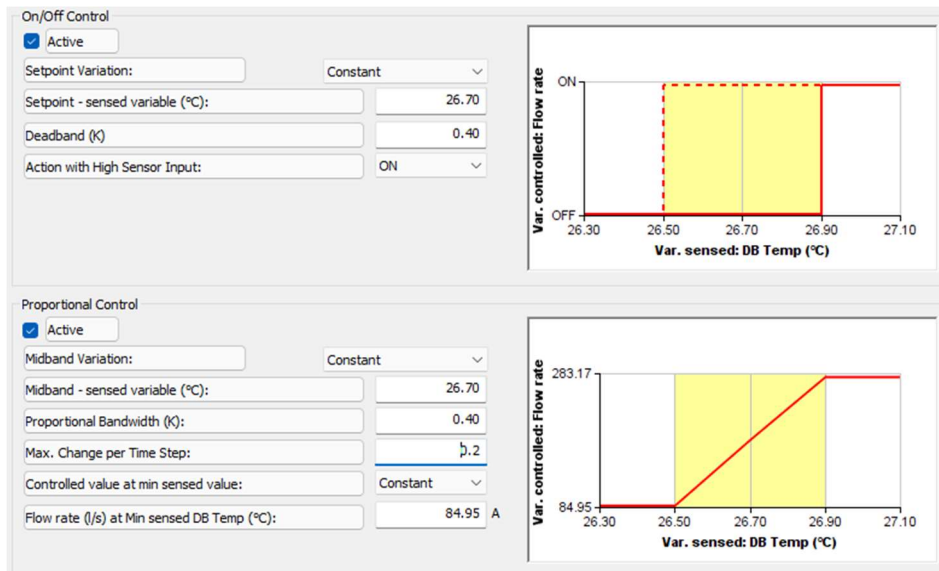


Figure 3-3-20: Sensor logic

As it is possible to appreciate in the figure 3-21 the air temperature (red line) and humidity values (black line) inside the classrooms in a casual day of the year are kept between these ranges (blue line = cooling set point). Instead, for the weekend and festivity days the cooling system is completely switched off and it the air temperature and humidity levels rise with no control.

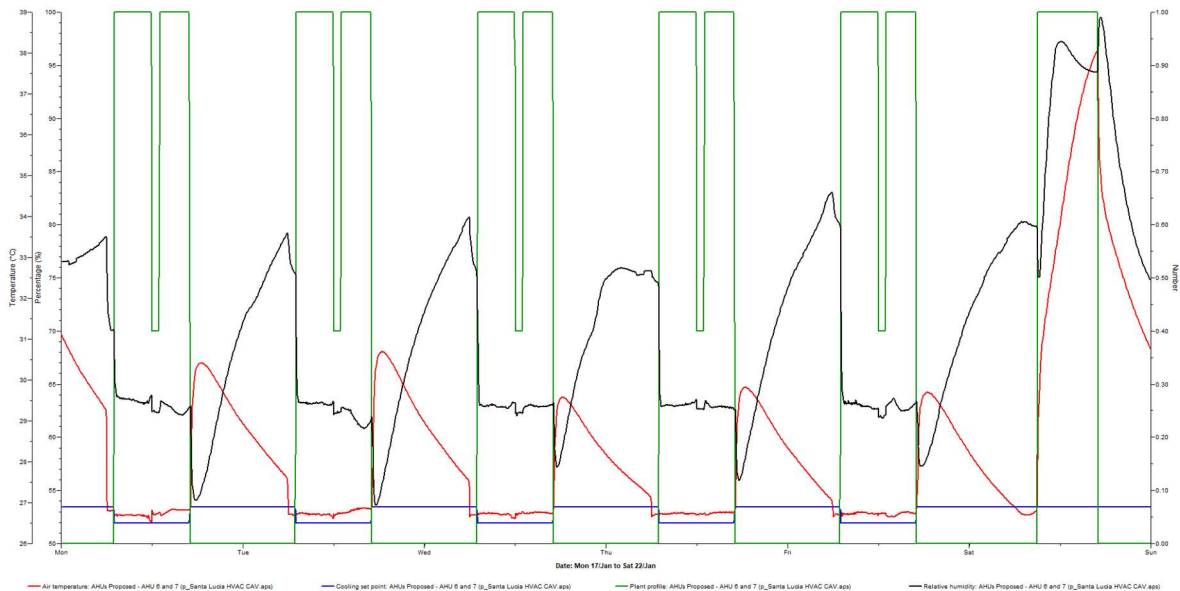


Figure 3-3-21: Week Air Temperature & Humidity inside the classrooms

3.6.2. System Technical Specification

3.6.2.1. Water to Water Heat Pump

Regarding the cooling production, it was decided to install a water to water heat pump big enough to guarantee the sensible and latent cooling coil load. Many different cooling system could be chosen, but in order to use renewable electricity produced by solar panels, it was decided to adopt machines able to function directly with electricity supply.

The haetpump will go to manage the water coming from the main cooling coil in the AHU and the fan coils inside each classroom.

The main charateristic of the HP are here shown in fig. 3-22. The rated COP and EER are respectively 3,28 and 9.5 . For this project the design COP is 3,57. All the system have been designed with an oversizing factor of +15% in order to have a conservative approach. Overall, the cooling design capacity was calculated by the software and it is 865.321 kW. To conlude, are also diplayed the the operative temperature of the condenser and evaporative side of the refrigerant cycle.

Reference: EWC Chiller with default values and VSD sec'd pump, 2-sp clg tower fan

General
 Meter: Electricity: Meter 1

Operational model
 Chiller model description

Performance curve set: Generic Hermetic screw - 1 compressor View/Edit/Library

Minimum chilled-water flow fraction: 0.50
 Minimum condenser water flow fraction: 0.40
 Minimum part-load ratio for continuous operation: 0.05
 Compressor heat gain to condenser water loop (fraction): 1.00

Design condition Reference condition

Chiller:	Cooling capacity, Q_{des} :	111.312 kW	
	Coefficient of performance, COP _{des} :	5.32	
Condenser water:	Entering temp, T _{ectdes} :	30.02 °C	V _c /Q _{des} : 0.05 l/s/kW
	Flow rate, V _c :	5.69 l/s	DeltaT _{cdes} : 5.56 K
Chilled water:	Supply temp, T _{letdes} :	6.67 °C	V _e /Q _{des} : 0.04 l/s/kW
	Flow rate, V _e :	3.99 l/s	DeltaT _{edes} : 6.67 K

Figure 3-22: HP Characteristics

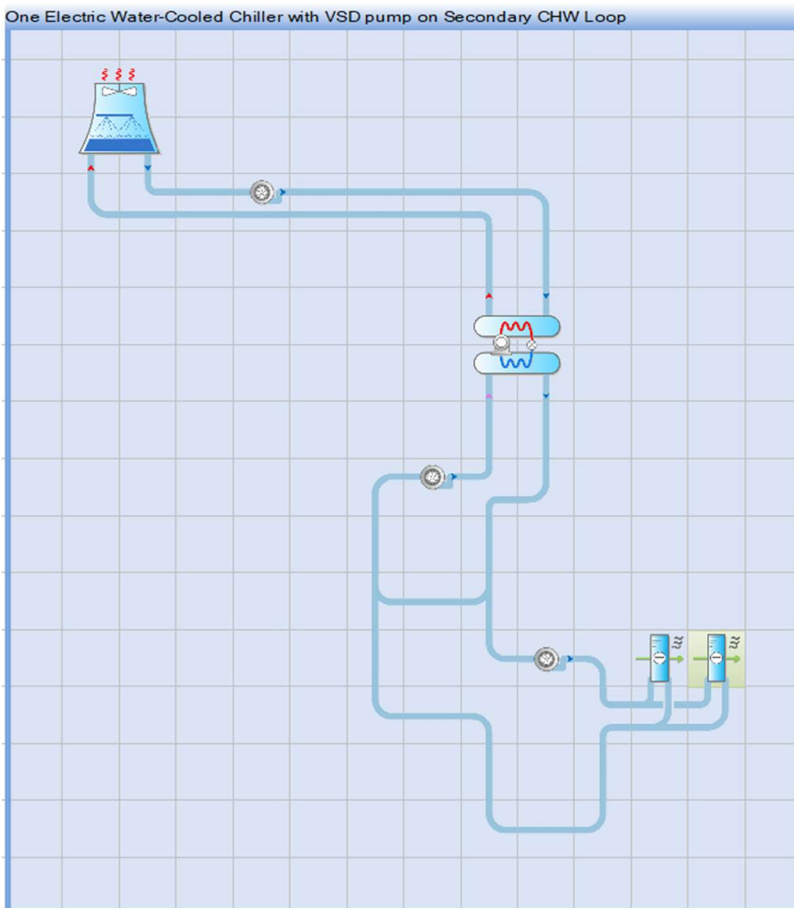


Figure 3-23: Water Loop Scheme

Chilled water loop Pre-cooling Chiller set Heat rejection Thermal storage

General

Design outdoor dry-bulb temperature: 29.22 °C A

Design outdoor wet-bulb temperature: 26.13 °C A

Condenser water loop

Heat rejection device: Cooling tower

Waterside economizer

Condenser water loop Cooling tower Fluid cooler Waterside economizer

Design parameters

Heat rejection, Qhrdes: 133.781 kW

Design leaving temperature: 30.02 °C

Approach: User entered 3.82 K

Range: 5.62 K

Minimum flow fraction: 0.40

Adjust minimum flow for operating chillers

Fan power, Wfan: 1.408 kW

Fan electric input ratio, Wfan/Qhrdes: 0.0105

Fan control: Two-speed fan

Fan meter: Electricity: Meter 1

Low-speed fan flow fraction: 0.50

Low-speed fan power fraction: 0.30

Figure 3-24: Cooling power Characteristics

3.6.2.2. Supply & Return Fan

Analysing the air moving system, the air handling system is composed by 4 different fans as shown in fig 3-25. According to the numbers, the fan n°1 and n°3 are devoted to handle the return air from the rooms to the energy recovery heat exchanger and then to the supply fan. Instead, the fan n°2 is devoted to supply air to the coils and then to all the rooms of the building. To conclude, the fan n°4 it is the marginal one it terms of power and flow rate handled because it is devoted to manage the exhaust air that is mainly used in the heat exchanger recovery system and then mainly managed by the fan n°3. The technical characteristics of the fans are shown in the figure 3-26 where it is possible to appreciate how the fan power loads changes at variable flow rates and how the motor efficiency behaves to these changes. With reference to the figure 3-26, it is referred to the fan n°2, but all the fans installed have the same technical characteristics but differ for the value of design fan power because different design total pressure have to be win in order to handle the return and supply air.

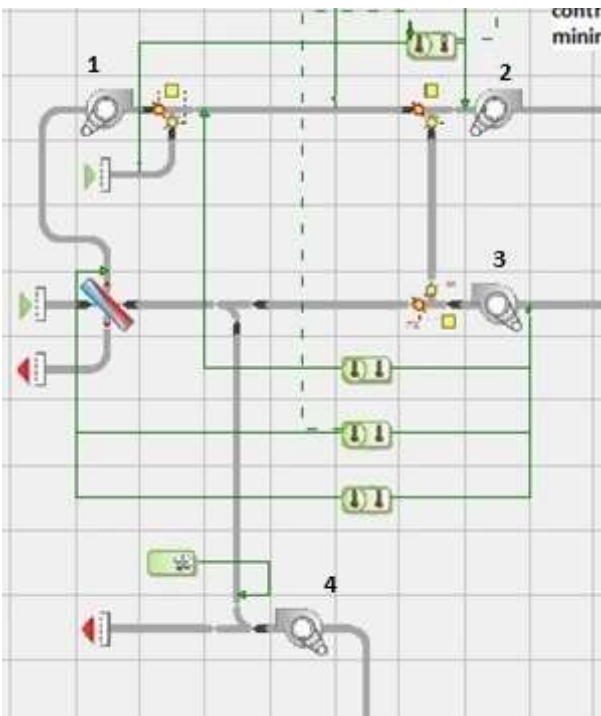


Figure 3-3-25: Fan system

Reference: S2: SA Fan
 Link: Supply fan Re-apply

Settings

Design flow rate: Autosize 6714.04 l/s A
 Oversizing factor: 1.00
 Design total pressure: 498.16 Pa
 Fan efficiency at design flow rate: 82.22 %
 Motor efficiency at design flow rate: 90.00 %
 Motor airstream heat pickup factor: 100.00 %
 Design fan power: 4.520 kW
 Electricity meter: Electricity: Meter 1
 Fan category: Interior central

Characteristic

Variable volume
 Airflow modulation performance curve: Variable-speed drive (VSD) fan

	Flow fraction (%)	Fraction of design motor power (%)	Motor efficiency (%)	Fan power (kW)
1	20.00	11.00	86.15	0.497
2	40.00	22.00	91.54	0.994
3	60.00	37.00	93.46	1.672
4	80.00	61.00	92.69	2.757
5	100.00	100.00	90.00	4.520

Add Insert Remove

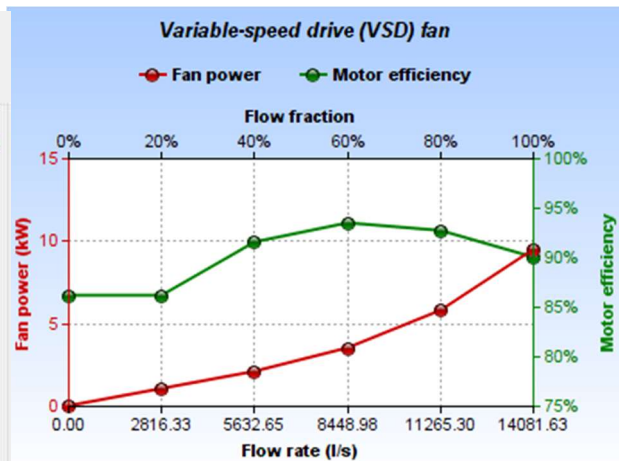


Figure 3-3-26: Technical characteristic of the fan

The fan component does not actively influence the flow rate; the values entered here do not determine airflow through the system. These values are used solely to calculate the consequential energy consumption and effect on air temperature at a given flow rate. Pressure, in this case, refers to the total static pressure (internal plus external) to be

overcome by the fan. Efficiency includes both the mechanical efficiency of the fan and the electrical efficiency of the motor and associated power electronics.

3.6.3. System Energy Loads

This chapter is dedicated to deeply analysis of all the possible loads involved in the daily operation of the school with the centralized AHU. The simulation is made with a time span of 6 minutes (the smallest possible from the software) for the whole year taking into account the real occupancy profile of the building.

Firstly, in the fig 3-27 it is possible to appreciate the energy breakdown of the annual energy expenditure of the whole building. The space cooling account for the bigger part with a 66,49% followed by the ventilation fans for 15,69% and Heat rejection fan energy 5,64%. The smallest energy spending contribution is given by internal lighting 0,1%, due to the mainly usage of the natural light. Overall, the entire system has an energy expenditure of 236141,14 kWh per year.

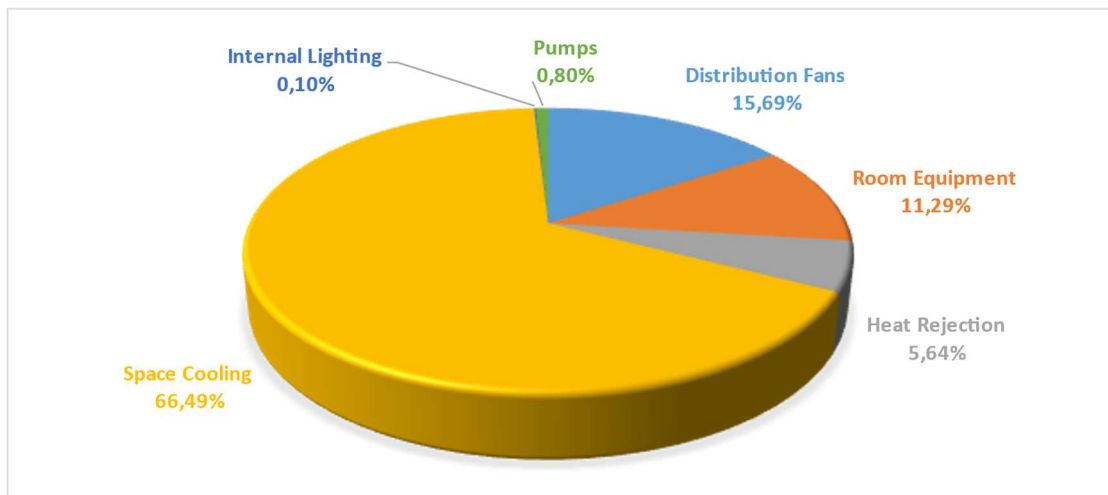


Figure 3-3-27: Energy Consumption Breakdown

Secondly, for the cooling loads (fig 3-28) it is interesting to appreciate how the proportion between sensible and latent loads is completely in favour of the second one due to the huge humidity present in this geographical area. In total the latent load account for the 61 % and the sensible one account for 39%. Furthermore, the loads have a quite predictable behaviour, increasing in the central part of the year and diminishing in the last and first month of the year but overall are quite constant thanks to the building orientation and shading system, quite constant meteorological conditions through the whole year, fixed internal gain and thermal and IAQ goals that the system have to reach and keep constant every operative day. According to the graph it is possible to appreciate how the sensible load is quite constant,

although the latent load varies sensibly in the second part of the year affecting the cooling total load that reach the peak value the 30th of September at 15:00. This peculiarity of the loads allows the dimension or selection of a cooler machine perfectly suited and optimized for the scope.

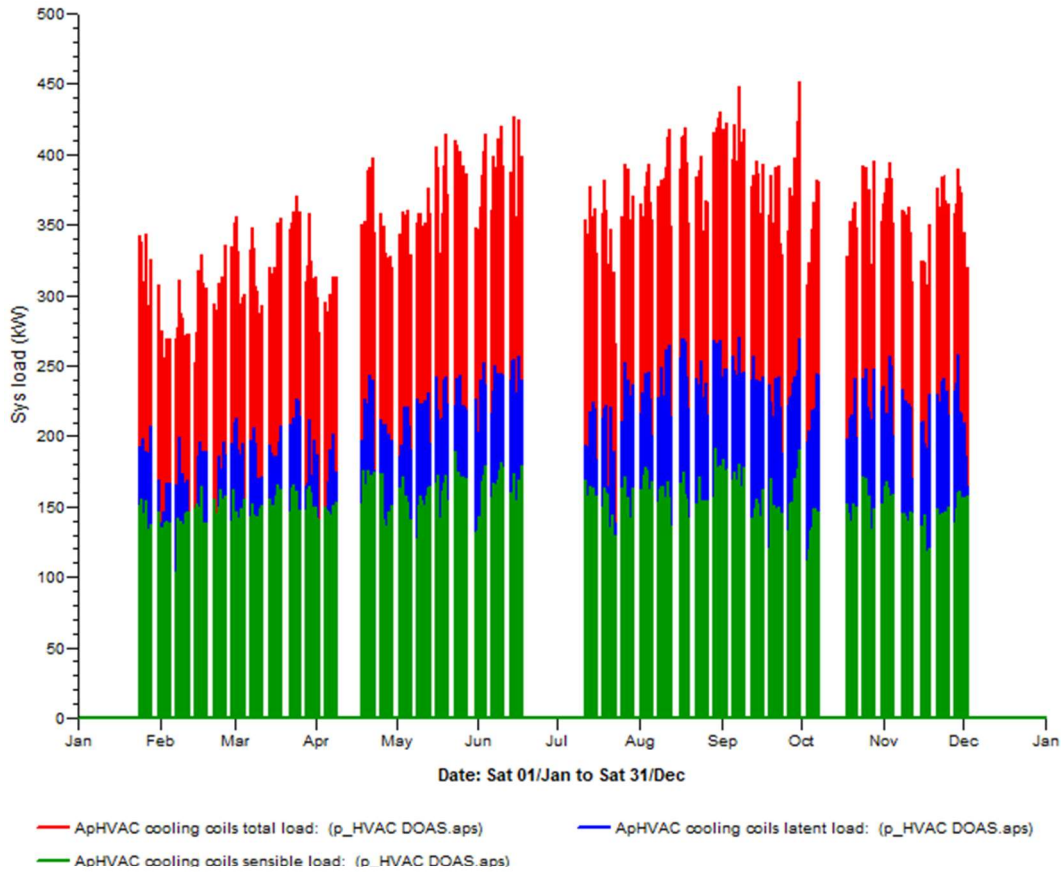


Figure 3-3-28: Total, Sensible and Latent Cooling Loads

In conclusion, it is possible to appreciate in fig 3-29 the compounded electrical consumption of the whole components of the building. It is taken as a reference for the further dimensioning of the PV system that will be analysed in the next chapter. As seen in the cooling loads graph, also in this graph is possible to notice that the electric peak for the HP is coinciding with the cooling loads peak of the 30th of September. The yellow line spikes of the lighting electricity consumption evidence how the lighting system is switched on only in some days/hour of the year when the solar light is not enough. Regarding the equipment energy it is constant and in line of the occupancy profile of the building. Furthermore, the distribution fan energy modulates in function of the ventilation demand of the rooms and is relatively stable for the whole operation period of the AHU. To conclude also the heat rejection fan energy necessary to cool down the condenser side of the HP is displayed.

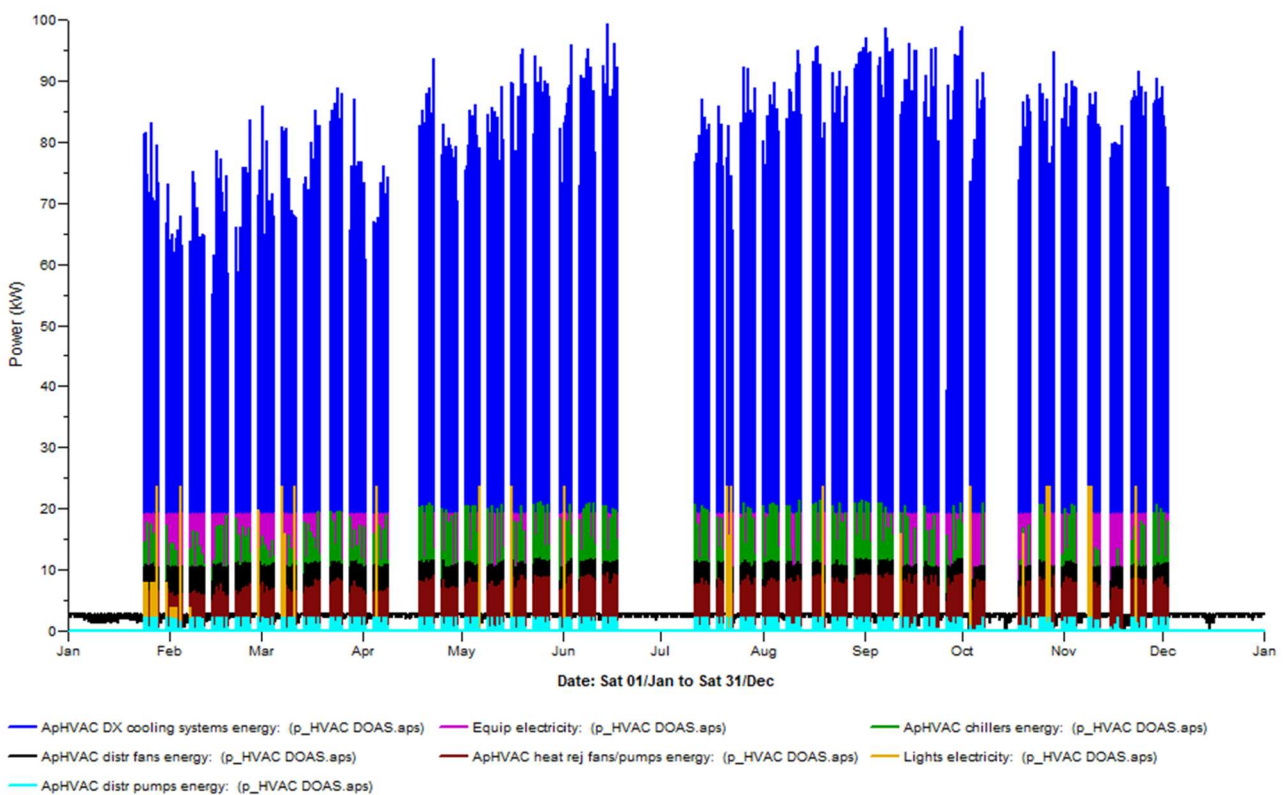


Figure 3-3-29: Electrical Consumption Breakdown

3.7. Split System & Cooling Thermal Loads

In order to give an alternative to the all-air system due to the installation problem that could exist for the implementation of this system, it has been proposed the adoption of a commercial and traditional air conditioning split system for each of the existing classrooms.

The aim of this chapter is to show the main peculiarity of the system, its load and a final comparison with the all-air system in order to evaluate the pro and cons of the two.

3.7.1. System Configuration

Each packaged terminal air conditioner is installed in each classroom, so the system account for 28 different terminals. The schematization of the system template is shown in fig 3-30 and account for a supply and exhaust channel for the outdoor air and a packaged unit equipped with air mixing damper, fan, heating coil and cooling coil.

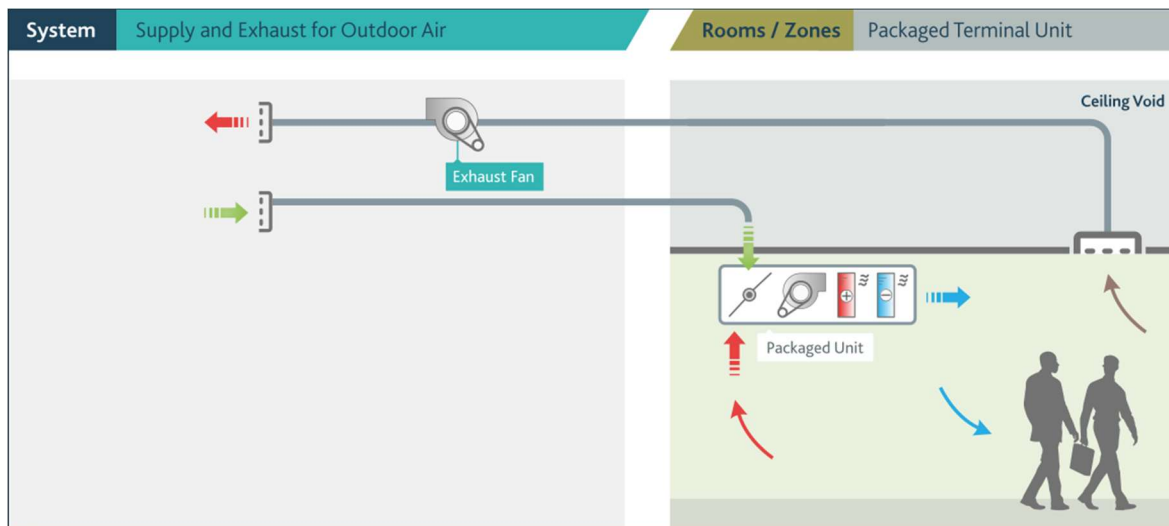


Figure 3-3-30: Packaged Terminal Air Conditioning System

In order to avoid the main issue that is possible to have with the adoption of all-air system and to simulate a traditional split system, the supply and exhaust channel for the outdoor air were not used. In order to avoid simplify to a traditional split system, the air mixing damper of the packaged unit has been set up to keep the close position for the whole operative period of the system. Regarding the heating coil, its use is mainly destined to heating purposes but in this case, it switch on only for a few minutes during the day to regulate the temperature of the air going into the room that have to respect the strict range settled. In fact its dimensions in terms of heating capacity is really small, 0.141 kW using an oversizing factor of 25%.

Furthermore, to guarantee the proper value of CO₂ inside the classrooms, it was imposed a natural ventilation air exchange of 4 l/s/person that allow to keep CO₂ levels under the 1200 ppm limit. Additionally, in order to guarantee the correct ranges of temperatures (26,5 - 26,9°C) and humidity (55% - 65%) a system of sensor have been implemented to the standard template. In the fig 3-31 is possible to see the system architecture complete with all the sensors used. From the template, from sensor n°1 to n°5 were already present in the system, the sensor n°6 and n°7 were added consequently to guarantee the correct thermal ranges. Regarding the sensor n°1 it was regulating the damper aperture, for this reason it was switched off. The two thermostat named with number 3 and 5 were linked to the

cooling coil air temperature output and was set to 26.5°C. The controllers n°2 and n°4 go to modulate the ventilation rate according to the air temperature observed at the output of the cooling coils. The 2 new sensors added, the n°6 and n°7 are respectively engaged to control the humidity and temperature levels inside the room and their control logic is shown in fig 3-32 in order to demonstrate when the system switch on or off in function of these two main parameters.

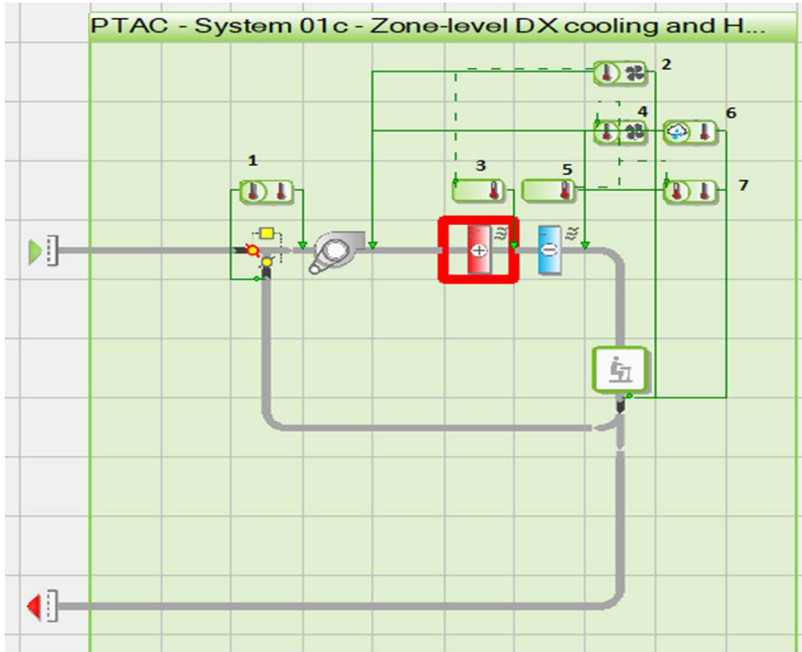


Figure 3-3-31: Packaged Air Conditioning System Architecture

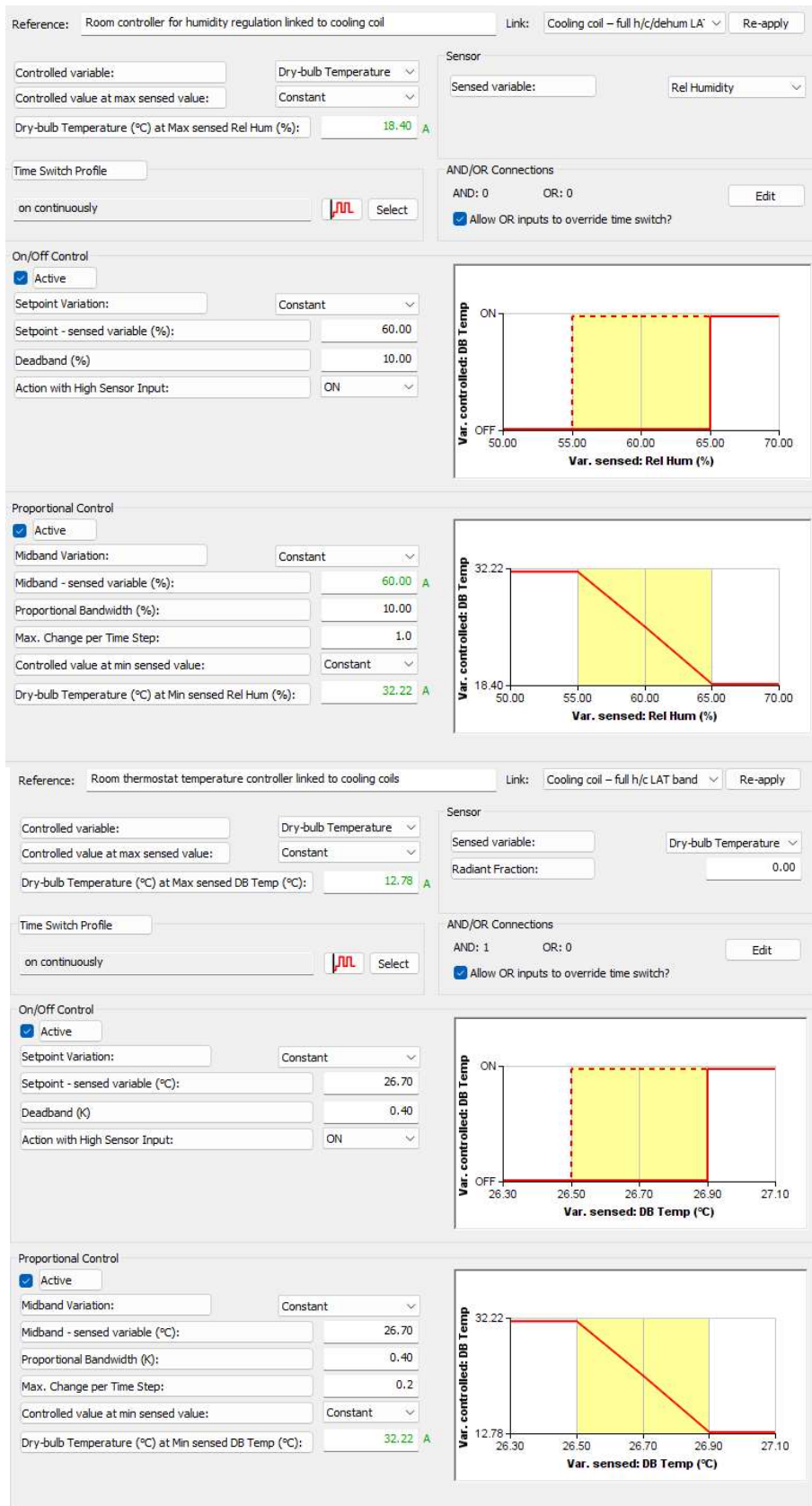


Figure 3-3-32: Control logic of humidity and temperature sensors

3.7.2. System Technical Specification

For the same reason written in the same chapter but for the all-air system, the cooling coil it as been linked to a DX Cooler in order to easly account the electrical consumption needed by the system. The condenser side of the Dx cooler is cooled by an air fan.

The machine here proposed was picked from the library of the IES VE software and all the technical specification of the direct expansion cooler are considered reasonable in order to quantify the electric energy needed for the whole system, that is the main objective of the creation of the digital twin of the school.

There are 15 pre-defined DX Cooling types, and is possible to replace, copy, and or edit any of these:

- 9 for Packaged Air-Conditioning systems and Packaged single-zone heat pumps (PSZ-HP)
- 6 for Packaged Terminal Air-Conditioning (PTAC) Packaged Terminal Heat Pumps (PTHP)

These pre-defined systems differ in terms of size ranges and associated COPs. The COP values in the predefined DX Cooling types match ASHRAE 90.1-2007 requirements, as adjusted per CA Title-24 ACM Manual methods to remove the supply fan power from the EER that was determined for a packaged unit at ARI conditions. For reference, the EER with SA fan power and the intermediate value EER_{nf} (EER with no fan, per the Title24 ACM Manual calculation) are included in the name of each type. EER_{nf} is then converted to COP without the fan, which is the input used in the DX Cooling dialog.

The DX cooling model simulates the refrigerant side of a DX cooling system. The DX cooling airside is modelled with a version of the current ApacheHVAC simple cooling coil model dedicated to DX cooling, using the total available DX cooling capacity calculated by the DX cooling model. This model uses default or user-defined DX cooling performance characteristics at rated conditions and three performance curves to determine DX cooling performance at off-rated conditions. The three DX cooling performance curves are:

- DX cooling capacity (temperature dependence) curve
- DX cooling electric input ratio (EIR) (temp dependence) curve
- DX cooling electric input ratio (EIR) (part-load dependence) curve

The DX cooling model includes the compressor and outdoor (condenser) fan power and thus energy consumption. In this case the condenser is cooled with an air fan and not with an evaporative cooler. It does not include the indoor (supply) fan power. Supply fans for DX cooling systems must be modelled separately as an ApacheHVAC fan component. Energy consumption by condenser fans is included in the DX units' Electric Input Ratio (EIR) and associated performance curves. A condenser fan Electric Input Ratio (EIR_{fan/pump}), representing the ratio of condenser fan power consumption to the total DX

unit power consumption, is used to split the calculated energy consumption into separate results for compressor vs. condenser fan.

The rated condition is the basis for the calculation of DX cooling performance at simulation time. The rated condition is normally the ARI rating condition or equivalent in locations where other equipment rating standards apply. The default rated condition data are based on the standard ARI conditions (ARI Standard 340/360-2007 and ARI Standard 210/240-2008). These include the following:

- Outdoor (condenser) section entering air:
 - dry-bulb temperature 35 °C
 - wet-bulb temperature 23.9 °C
- Indoor (evaporator) section entering air:
 - dry-bulb temperature 26.7 °C
 - wet-bulb temperature 19.4 °C

The design condition, on the other hand, is the condition at the time of peak design cooling load.

The main characteristic of the DX Cooler are here shown in fig. 3-33. The rated COP and EER are respectively 3,54 and 10,2 . For this project the design COP is 3,54. All the cooling coils have been designed with an oversizing factor of +15% in order to have a conservative approach. Overall, the cooling coil design capacity was calculated by the software and it is 14.936 kW for each device present in each classroom. To conclude, are also displayed the the operative temperature of the condenser and evaporative side of the refrigerant cycle that are kept as standard values from the standard ARI conditions (ARI Standard 340/360-2007 and ARI Standard 210/240-2008).

Reference:	M2: PTAC - DX Cooling coil	
Link:	PTAC/PTHP cooling coil	Re-apply
Coil type:	Direct-expansion (DX) cooling coil (1-to-1)	
DX equipment:	DX Cooling - PTAC 7-15 kBtu/h - COP 3.54 EERnf 12.1 (EER 10.2 per 9	

Design sizing parameters		
Contact factor:	0.75	
Oversizing factor:	1.15	
Rated capacity, Q _{rat} :	13.595 kW	D
Design capacity, Q _{des} :	14.936 kW	A
Design coefficient of performance, COP _{des} :	3.74	A
Design outdoor DBT:	34.33 °C	A

Rated condition		
DX cooling:	Coefficient of performance, COP _{rat} :	3.540
Condenser:	Outdoor air dry-bulb temperature, T _{odbrat} :	35.000 °C
Evaporator:	Entering coil wet-bulb temperature, T _{ewbrat} :	19.444 °C

Figure 3-3-33: DX Cooler characteristic

In the next images, fig 3-33-1 fig 3-33-2 are shown the characteristic curves function of the DX cooling electric input and cooling capacity in function of temperature (T entering coil wet bulb, T entering condenser) and part load operativity. The software uses respectively 6 and 3 different coefficients in order to simulate all the possible operative conditions of the system starting from the nominal conditions.

Name: DX cooling for PSZ/PVAV/PMZ/PVVT systems
 Description: DX cooling for Packaged Single Zone/NAV/Multi-Zone/Variable volume V

DX cooling electric input ratio (temp dependence) $f_{EIRtt}(Tewb, Tect)$
 A biquadratic function of
 $tewb = Tewb - Tdatum$
 $tect = Tect - Tdatum$
 where
 Tewb = entering coil wet bulb temperature
 Tect = entering condenser temperature, Todb or Towb
 Tdatum = datum temperature
 $f_{EIRtt}(Tewb, Tect) = (C00 + C10tewb + C20tewb^2 + C01tect + C02tect^2 + C11tewbtect) / Cnorm$

Datum temperature Tdatum (0°C or 0°F) -17.778 °C

C00 -1.06393100 C10 0.05518517 1/K C20 -0.00041116 1/K²
 C01 0.02775834 1/K C02 0.00016113 1/K² C11 -0.00067910 1/K²

Cnorm is adjusted to make $f_{EIRtt}(Tewbrat, Tectrat) = 1$
 Applicable Ranges
 Minimum Tewb 15.000 °C Maximum Tewb 24.000 °C
 Minimum Tect 24.000 °C Maximum Tect 46.000 °C

Name: DX cooling for PSZ/PVAV/PMZ/PVVT systems
 Description: DX cooling for Packaged Single Zone/NAV/Multi-Zone/Variable volume V

DX cooling electric input ratio (part-load dependence) $f_{EIRp}(p)$
 A cubic function of
 $p = \text{part-load fraction}$

$f_{EIRp}(p) = (C0 + C1p + C2p^2 + C3p^3) / Cnorm$

C0 0.20123007 C1 -0.03121750 C2 1.95049790 C3 -1.12051040

Cnorm is adjusted to make $f_{EIRp}(1) = 1$
 Applicable Ranges
 Minimum p 0.100 Maximum p 1.000

Name: DX cooling for PSZ/PVAV/PMZ/PVVT systems
 Description: DX cooling for Packaged Single Zone/NAV/Multi-Zone/Variable volume V

DX cooling capacity (temp dependence) $f_{CAPtt}(Tewb, Tect)$
 A biquadratic function of
 $tewb = Tewb - Tdatum$
 $tect = Tect - Tdatum$
 where
 Tewb = entering coil wet bulb temperature
 Tect = entering condenser temperature, Todb or Towb
 Tdatum = datum temperature
 $f_{CAPtt}(Tewb, Tect) = (C00 + C10tewb + C20tewb^2 + C01tect + C02tect^2 + C11tewbtect) / Cnorm$

Datum temperature Tdatum (0°C or 0°F) -17.778 °C

C00 0.87403018 C10 -0.00205488 1/K C20 0.00055436 1/K²
 C01 -0.00532260 1/K C02 0.00003298 1/K² C11 -0.00019171 1/K²

Cnorm is adjusted to make $f_{CAPtt}(Tewbrat, Tectrat) = 1$
 Applicable Ranges
 Minimum Tewb 15.000 °C Maximum Tewb 24.000 °C
 Minimum Tect 24.000 °C Maximum Tect 46.000 °C

Figure 3-3-33-1: DX Cooling capacity in function of temperature

Figure 3-3-33-2: DX Cooling electric input ratio in function of T and part load operativity

Regarding the ventilation system, here it is present only a moving air device for each packaged unit installed in each classroom. The technical characteristics are shown in the fig 3-34 where it is possible to appreciate how the fan power loads changes at variable flow rates and how the motor efficiency behaves to these changes. Pressure, in this case, refers to the total static pressure (internal plus external) to be overcome by the fan. Efficiency includes both the mechanical efficiency of the fan and the electrical efficiency of the motor and associated power electronics. As said, it has to handle only indoor room air.

Reference: M4: PTAC Fan

Link: Package terminal unit fan Re-apply

Settings

Design flow rate: Autosize 867.16 l/s A

Over sizing factor: 1.00

Design total pressure: 249.08 Pa

Fan efficiency at design flow rate: 49.00 %

Motor efficiency at design flow rate: 90.00 %

Motor airstream heat pickup factor: 100.00 %

Design fan power: 0.490 kW

Electricity meter: Electricity: Meter 1

Fan category: Interior local

Characteristic

Variable volume

Airflow modulation performance curve: Variable-speed drive (VSD) fan

	Flow fraction (%)	Fraction of design motor power (%)	Motor efficiency (%)	Fan power (kW)
1 - (T)	20.00	11.00	86.15	0.054
2 - (T)	40.00	22.00	91.54	0.108
3 - (T)	60.00	37.00	93.46	0.181
4 - (T)	80.00	61.00	92.69	0.299
5 - (T)	100.00	100.00	90.00	0.490

Add Insert Remove

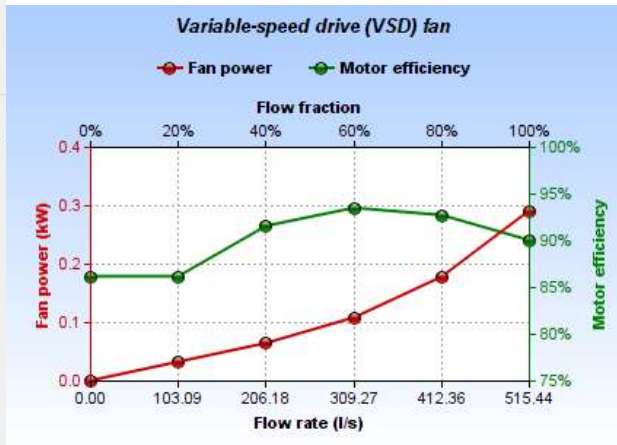


Figure 3-3-34: Technical characteristic of the fan

3.7.3. System Energy Loads

This chapter is dedicated to deeply analysis of all the possible loads involved in the daily operation of the school with the traditional split system. The simulation is made with a time span of 6 minutes (the smallest possible from the software) for the whole year taking into account the real occupancy profile of the building.

Firstly, in the fig 3-35 it is possible to appreciate the energy breakdown of the annual energy expenditure of the whole building. The space cooling account for the bigger part with a 66,69% followed by the ventilation fans for 19,47% and Heat rejection fan energy 4,26%. The smallest energy spending contribution is given by internal lighting 0,12%, due to the mainly usage of the natural light. Overall, the entire system has an energy expenditure of 190255,2 kWh per year.

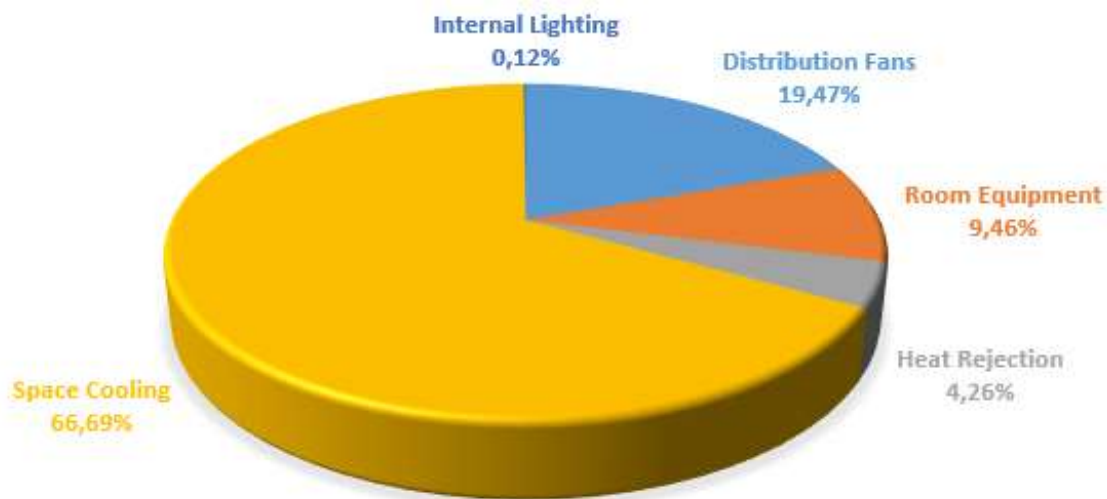


Figure 3-3-35: Energy Consumption Breakdown

Secondly, for the cooling loads (fig 3-36) it is interesting to appreciate how the proportion between sensible and latent loads is completely in favour of the first one. In total the latent load account for the 41,18 % instead the sensible one for the remaining 58,82%. Furthermore, the loads have a quite constant and predictable behaviour during the whole year thanks to the building orientation and shading system, quite constant meteorological conditions through the whole year, fixed internal gain and thermal and IAQ goals that the system have to reach and keep constant every operative day. According to the graph it is possible to appreciate how the total load is quite constant, although the latent load varies sensibly in the second part of the year. No visible peak loads point out from the load graph, but the 24th of October is observable the day with the highest total cooling load with a maximum value of 536,941 kW. Instead, regarding sensible and latent cooling load, the highest peak are respectively observed the 23th of May (279,8739 kW) and 5th of September (299,67 kW). This peculiarity of the loads allows the dimension or selection of a cooler machine perfectly suited and optimized for the scope.

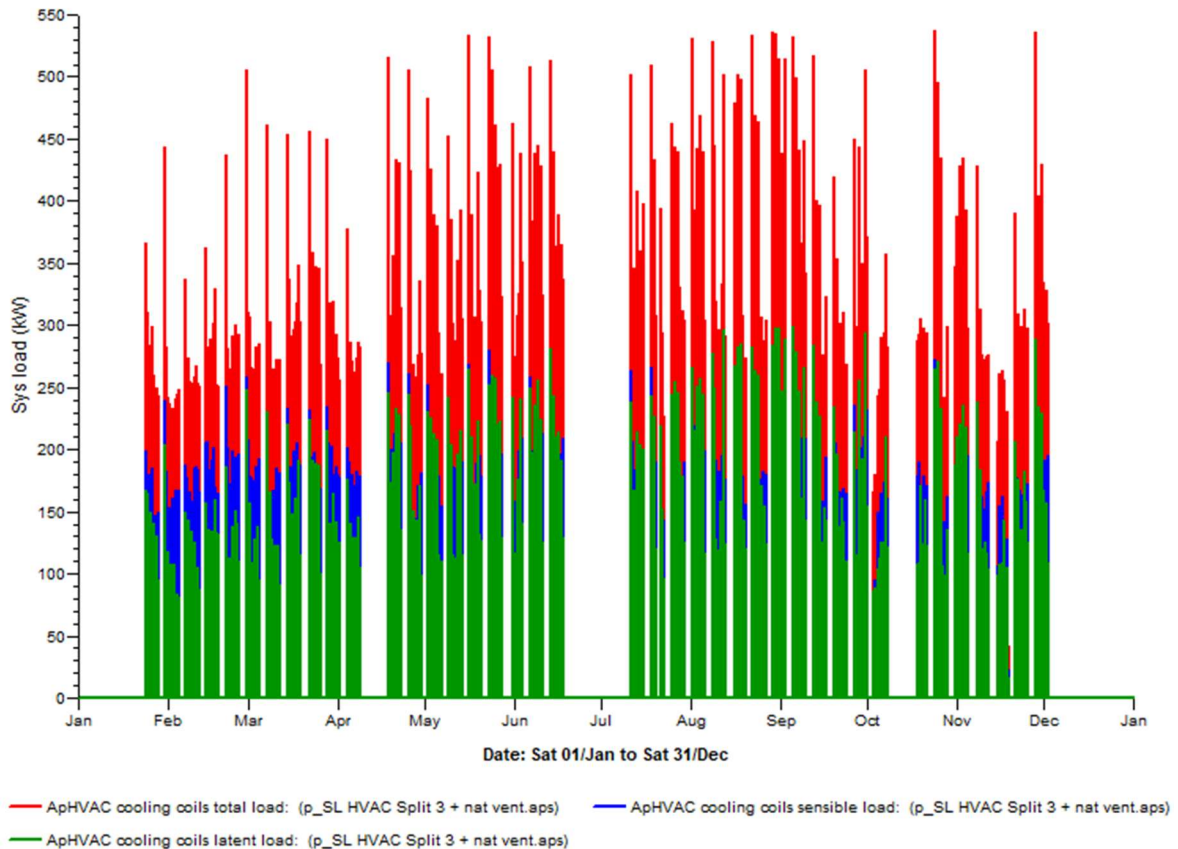


Figure 3-3-36: Total, Sensible, Latent Cooling Loads

In conclusion, it is possible to appreciate in fig 3-37 the compounded electrical consumption of the whole components of the building. It is taken as a reference for the further

dimensioning of the PV system that will be analysed in the next chapter. As seen in the cooling loads graph, also in this graph is possible to notice that the electric peak for the Dx Cooler is coinciding with the cooling loads peak of the 16th of May. The black line spikes of the lighting electricity consumption evidence how the lighting system is switched on only in some days/hour of the year when the solar light is not enough. Regarding the equipment energy it is constant and in line of the occupancy profile of the building. To conclude the distribution fan energy modulates in function of the ventilation demand of the rooms and is relatively stable for the whole operation period of the air conditioning system.

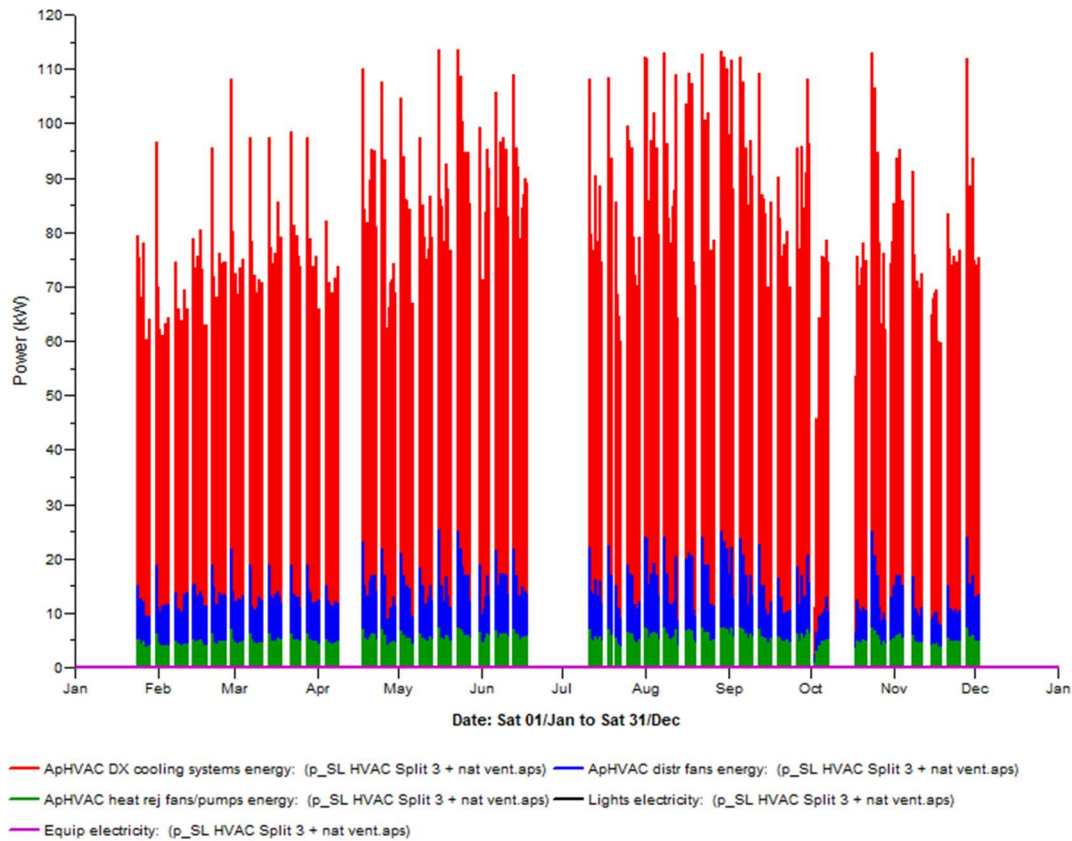


Figure 3-3-37: Electrical Consumption Breakdown

3.7.4. Comparison between AHU & Split system

In this chapter are highlighted the main positive and negative aspect of both the two systems with a final explanation of the reason why one system could be alternative to the other one and which kind of compromise we have to accept if we choose a system instead of the other one.

Positive aspects of Centralized AHU with fan Coil:

- Fresh outdoor air usage implies low levels of CO₂ in the room
- Centralized system implies the acquisition of only one cooling machine

- Constant thermal and IAQ conditions, precise control is possible by use of high-class controls. Close range of Temperature ($\pm 0.15^{\circ}\text{C}$) and Humidity ($\pm 0.5\%$) can be achieved.
- Effective Room air distribution and Ventilation is possible under widely varying load conditions
- Centralized AHU with fan Coils present great opportunities for Energy conservation such as heat recovery wheels
- AHU which is a complete package can be remotely located, well away from conditioned spaces. It helps to reduce noise levels in occupied spaces

Negative aspects of Centralized AHU with fan Coil:

- No personalized control system
- Unavailability of the system compromise the cooling system for all the classrooms
- Invasive construction intervention for the installation of the duct as large space is required in false ceiling to lay the ducts
- Since systems are quite large in size, require separate spaces like AHU Room. It reduces use of effective floor space
- Testing, Adjusting, Balancing may be very difficult task in case of VAV systems

Positive aspect of traditional split system:

- Simultaneous heating and cooling are possible in air-water system
- Lot of space is saved, as only the split system has to be installed in each room together with its condenser cooling unit
- Economic control of individual zones is possible using room thermostats
- Servicing, Repair, Replacement, Maintenance works etc. are relatively easier than Centralized AHU with fan Coils

Negative aspect of traditional split system:

- Constant supply of fresh air is not possible. This imply that to keep CO₂ levels low natural ventilation of 4 l/s/person have to be guaranteed. This imply the rise of cooling consumption due to injection of outdoor air.
- Management of the condense could be difficult especially in high humid environment like tropics
- The acquisition of high number of split systems could be costly if compared to a centralized system
- Noise of the condenser cooling unit could be a problem
- No energy recovery system is possible to be used

To conclude it was proposed two different system because each of them have a different characteristic and according to the energy simulation also different energy expenditure. For

sure the adoption of a split system guarantee a less complexity in terms of installation, and maintenance. Furthermore, the classroom has to be ventilated manually opening windows and doors in order to reduce the carbon dioxide levels. This implies a huge increase of the calculated loads, variation of the thermal conditions inside the rooms that will struggle to remain in the defined temperature and humidity ranges defined.

On the other hand, the all-air system have no problem from this point of view and handling mainly outdoor air guarantee constant low CO₂ levels.

In conclusion the all-air system guarantees all the requisite form thermal and IAQ point of view paying an higher energy cost and installation and maintenance complexity. On the contrary split system are easily to be installed, have a less energy expenditure and could guarantee main of the thermal and IAQ standards but not all.

4 PV system

The main goal of this chapter is to describe the preliminary design of a stand-alone photovoltaic system installed on the rooftop of the primary school in Santa Lucia, Atlántico, Colombia.

4.1. Location and main characteristics of the system

The “Institución Educativa Santa Lucia” is located at latitude 10.321°N and longitude -74.95 °E in the department called Atlántico, in the coast of Colombia at 30m over the sea level. The orientation of the building is 255° from the north direction.



Figure 4-4-1: Top view of Institución Educativa Santa Lucia

The perimeter of the school has a rectangular shape composed by two main side long 120m x 55m. The tilt of the rooftop is 0°. On the roof are present skylights that for sake of simplicity and to adapt the structure to host the pv panels will be erased in order to have available the biggest total roof area. In order to calculate the total floor area, it is possible to decompose the building in different parts. In the next table are condensed all the main dimensions and total area of the roof of the related parts of the building.

Room	Quantity	Length [m]	Wide [m]	Total area [m ²]
Classrooms	14	7.98	7.665	887.94
Bathroom 1	1	7.81	6.3	49.2
Bathroom 2	1	6.88	6.15	42.32
Building 1	1	31.83 + 8.58	15.34 + 12.94	599,35
Building 2	1	30,4 + 7,5	13,594 + 8	473,33

In conclusion, the available total surface area of the roof is 2052,11 m². The azimuth angle is -28° towards East.

The position of the panels will be comprehensive of the norm EN 1991-1-4 (Eurocode 1), which imposes a certain distance (proportional to the dimension of the house) between the modules and the edges of the roof, because of wind loads. Regarding tilt and azimuth angle, they are the same for the entire system because the modules are installed on the roof. According to a simulation made with the free tool of European commission, "PVGIS 5.2" (49) the optimum value for the PV module slope angle is 14°.

		Solar altitude (deg.)
Date	Time	COL_ATL_Barranquilla-Cortissoz.Intl.AP.80028
Wed, 21/Dec	00:30	0.0
	01:30	0.0
	02:30	0.0
	03:30	0.0
	04:30	0.0
	05:30	0.0
	06:30	2.9
	07:30	16.1
	08:30	28.6
	09:30	40.1
	10:30	49.5
	11:30	55.0
	12:30	54.8
	13:30	49.0
	14:30	39.4
	15:30	27.9
	16:30	15.2
	17:30	2.0
	18:30	0.0

Figure 4-4-2: Solar altitude the 21st of December

In order to define the number of panels installable on the roof keeping the optimum module slope angle, two considerations have to be made. To determine the distance between the modules row to avoid shading between them, an analysis of the solar altitude data of the 21st of December from fig 4-2 have to be made because it is supposed to be the shortest day

with available sunlight. The aim of the system is to work as long as possible during the day, for this reason shaded panels have to be avoided for the operativity of our panels. If we consider a panel height of 1 m, according to the lowest value of solar altitude, 2° , the space needed between the rows of the pv panels have to be 7.89 m, if we consider the 1-hour earlier value 15.2° the necessary distance between rows decay to 1.86 m. Furthermore, according to the free tool of European commission, "PVGIS 5.2" (49) the yearly PV energy production for a crystalline silicon technology with an overall system loss of 14% and an installed pv peak power of 1 kWp with 14° panel slope (the optimized one) is 1538,42 kWh per year, instead with 0° panel slope it is 1507,8 kWh per year. The change in the energy production is 1,99%. To conclude, in order to avoid any kind of shading between panels and populate the roof with as much panels as possible in order to maximize the energy production, choosing to have a 0° panel slope could be the best option. Furthermore, no adjacent buildings or vegetation are taller than the school roof so the value of η_{sha} is unitary and will not affect the system efficiency.

In order to determine the number of panels installable on the roof, a pv panel model have to be chosen. It was decided to adopt one of the most common panels on the market, the ALEO SOLAR P23L325 and its technical specification are shown in the fig. 4-3.

DATI ELETTRICI (STC)		P23L320	P23L325	DATI DI BASE MODULO	
Potenza nominale	P_{MPP} [W]	320	325	Lungh. x largh. x alt.	[mm] 1716 x 1023 x 35
Tensione nominale	U_{MPP} [V]	32,8	33,0	Peso	[kg] 19,3
Corrente nominale	I_{MPP} [A]	9,75	9,85	Numero di celle	60
Tensione a vuoto	U_{OC} [V]	40,3	40,5	Dimensioni cella	[mm] 158,75 x 158,75
Corrente di cortocircuito	I_{SC} [A]	10,22	10,31	Materiale cella	Si-mono, PERC
Efficienza	η [%]	18,2	18,5	Numero di bus bars	5
Valori elettrici in condizioni di prova standard (STC): 1000 W/m ² ; 25°C; AM 1,5					
DATI ELETTRICI (NMOT)		P23L320	P23L325	Vetro frontale	Vetro solare (VST)
Potenza	P_{MPP} [W]	236	240	Rivestimento posteriore	Pellicola polimerica, bianco
Tensione	U_{MPP} [V]	30,4	30,6	Materiale cornice	Lega di Al, color argento
Corrente	I_{MPP} [A]	7,78	7,85		
Tensione a vuoto	U_{OC} [V]	37,7	37,9		
Corrente di cortocircuito	I_{SC} [A]	8,24	8,31		
Efficienza	η [%]	16,8	17,1		

Figure 4-4-3: Main characteristic of PV module

With a length of 1,716 m and a width of 1,023 m, it was possible to install 696 PV panels on the roof surface of the building giving an offset from the perimeters of 0.5 m and without utilizing the building shading structures. In fig. 4-4 is possible to see the disposition of the modules. It is possible to notice that where possible the panels were distributed using 24 times a main block of 24 PV panels arranged in 6 rows of 4 modules, for 3 times a block of 16 PV panels arranged in 4 rows of 4 modules, for 3 times a block of 20 PV panels arranged in 5 rows of 4 panels and only one time a block of 12 PV panels arranged in 6 rows of 2 panels. In total the PV modules occupy a roof area of 1221,80 m², the 59,53% of the total roof surface area.

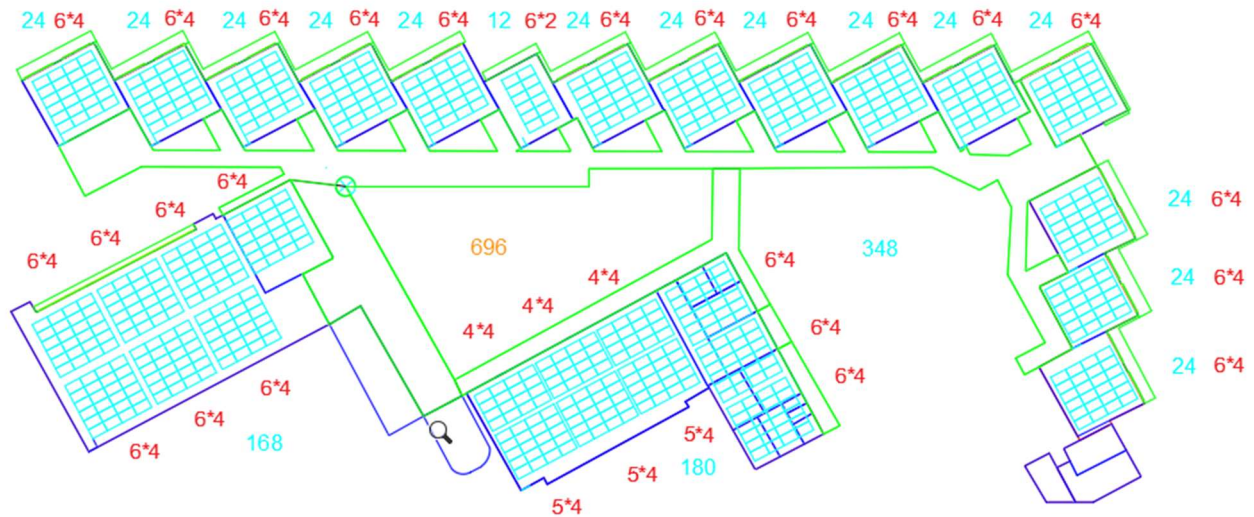


Figure 4-4-4: PV system architecture

The nominal power is 325 W. To summarize, in the following table, the main parameters of the system are reported:

Module tilt	0°
Module azimuth	-28° (towards East)
Number of modules	696
PV installed power	226200kW
Expected PV energy production	368192 kWh/year
Expected energy consumed	329287 kWh/year
Max/Min ambient temperature	36,6 °C/ 22 °C

Table 4-1: Main parameters of the system

The expected PV energy production has been computed with the following formula:

$$E_{year} = H_{year} \left[\frac{kWh}{m^2 \cdot year} \right] * \eta_{plant} * \frac{1}{G_{ref}} \left[\frac{m^2}{kW} \right] * P_{plant} [kW] = 1888.1 \left[\frac{kWh}{m^2 \cdot year} \right] * \quad (4.1)$$

$$0.8621 * 1 \left[\frac{m^2}{kW} \right] * 226.2 [MW] = 368192 \left[\frac{kWh}{year} \right]$$

Where:

- H_{year} has been taken from PVGIS (49)
- η_{plant} has been computed as in Chapter 0
- P_{plant} has been set following constraints on available surfaces

4.2. Electric loads definition

According to the chapter 3-6 and 3-7, all the electrical loads have been simulated by IESve software for the two different cooling system. To design the pv system, an appropriate loads definition is a crucial point. The energy simulation has been performed with a time span of 6 minutes, so it is possible to design the system with a high level of precision taking into account all the possible peak loads present during the operation of the cooling system. The consumption profile depends strongly on the student occupancy of the school that populate the school each weekday of the week from 7:00 to 17:00.

To resume, the main yearly electrical consumptions are reported below.

Load Source	AHU Electrical Energy [kWh]	AHU Electrical Use Demand [kW]	Split Electrical Energy Use [kWh]	Split Electrical Demand [kW]
Dx cooling	157002	115,93	126886,39	113,61
Lights	230.5	23.8	230.5	23.8
Distribution Fan/Pumps	28543,97	14,52	17992,01	25,2
Heat rejection Fan	13317,61	9,46	8099,13	7,25
Room Equipment	37047.1	19.20	37047.1	19.20
Total	329287		190255,2	
Operative days	256			

Table 4-2- Appliances of the school

Only the classroom equipment has a steady operative cycle at a certain nominal power during the day, the others follow a specific operative cycle related to the indoor and outdoor thermal conditions.

4.3. Electric generation and consumption

The solar panel chosen is the Aleo P23L325, from a well-known manufacturer. In the following table, the main characteristics taken from the datasheet are shown.

DATI ELETTRICI (STC)		P23L320	P23L325	DATI DI BASE MODULO	
Potenza nominale	P_{MPP} [W]	320	325	Lungh. x largh. x alt.	[mm] 1716 x 1023 x 35
Tensione nominale	U_{MPP} [V]	32,8	33,0	Peso	[kg] 19,3
Corrente nominale	I_{MPP} [A]	9,75	9,85	Numero di celle	60
Tensione a vuoto	U_{OC} [V]	40,3	40,5	Dimensioni cella	[mm] 158,75 x 158,75
Corrente di cortocircuito	I_{SC} [A]	10,22	10,31	Materiale cella	Si-mono, PERC
Efficienza	η [%]	18,2	18,5	Numero di bus bars	5
Valori elettrici in condizioni di prova standard (STC): 1000 W/m ² ; 25°C; AM 1,5					
DATI ELETTRICI (NMOT)		P23L320	P23L325	Vetro frontale	Vetro solare (VST)
Potenza	P_{MPP} [W]	236	240	Rivestimento posteriore	Pellicola polimerica, bianco
Tensione	U_{MPP} [V]	30,4	30,6	Materiale cornice	Lega di Al, color argento
Corrente	I_{MPP} [A]	7,78	7,85		
Tensione a vuoto	U_{OC} [V]	37,7	37,9		
Corrente di cortocircuito	I_{SC} [A]	8,24	8,31		
Efficienza	η [%]	16,8	17,1		

Figure 4-4-5: Main characteristics of PV module

The overall efficiency η_{plant} has to be computed taking into account many components of the system:

Efficiency	Value	Comments
$\eta_{dev\ STC}$	0,974	It depends on the way of installation of the modules: in order to be more conservative, the value of the case with low ventilation has been chosen.
η_{ref}	0,98	It considers the losses due to reflection and a typical value has been used.
η_{mism}	0,95	It is the mismatching efficiency. A reasonable value has been considered.
$\eta_{DC\ loss}$	0,98	It considers the DC losses on cables. A typical value has been used.
η_{inv}	0,98	It is the inverters efficiency taken from the datasheet.
η_{dirt}	0,99	It considers the losses because of dirty PV modules.
η_{shad}	1	It is the shading efficiency calculated before.

Table 4-3-System efficiencies

Hence:

$$\eta_{plant} = \eta_{dev\ STC} \cdot \eta_{ref} \cdot \eta_{mism} \cdot \eta_{DC\ loss} \cdot \eta_{inv} \cdot \eta_{dirt} \cdot \eta_{shad} = 86,21\% \quad (4.2)$$

In order to account properly the energy production, the position of the site (latitude and longitude), the azimuth and the panel's orientation are taken under consideration. After giving as input all the information stated before, it was possible to obtain the global irradiance values at every hour of the year utilizing the weather files used also in the energy simulation. The computation wanted to assess the global radiation levels hitting the modules through the following formulas, where each component have been computed in sequence with 1h timespan.

$$E_n[min] = 229.18 * (0.000075 + 0.001868 * \cos\left(360 * \frac{n-1}{365}\right) - 0.03277 * \sin\left(360 * \frac{n-1}{365}\right) - 0.014615 * \cos\left(2 * 360 * \frac{n-1}{365}\right) - 0.04080 * \sin(2 * 360 * \frac{n-1}{365}))$$

$$\Phi_{std}[^{\circ}] = STZ * 15$$

$$t_s[h] = t[h] + \frac{\Phi_{long}[^{\circ}] - \Phi_{std}[^{\circ}]}{15} + \frac{E_n[min]}{60}$$

$$\delta [^{\circ}] = 23.45 * \sin\left(\frac{360}{365} * (n + 284)\right)$$

$$h[^{\circ}] = (0,25 * t_s)$$

$$\sin(\alpha) = \cos(\Phi) = \sin(L) \sin(\delta) + \cos(L) \cos(\delta) \cos(h)$$

$$\cos(\theta) = \sin(L) \sin(\delta) \sin(\beta) - \cos(L) \sin(\delta) \sin(\beta) \cos(Z_s) + \cos(L) \cos(\delta) \cos(\beta) \cos(h) + \sin(L) \cos(\delta) \sin(\beta) \cos(Z_s) \cos(h) + \cos(\delta) \sin(\beta) \sin(Z_s) \sin(h)$$

$$G = (G_{HORI} - G_{DIFF}) * \frac{\cos(\theta)}{\cos(\Phi)} + G_{DIFF} * \frac{1 + \cos(\beta)}{2} \quad (4.3)$$

where:

- n : Time Interval of 1h
- E_n : Equation of time
- Φ_{std} : Standard Time Zone Angle
- $\Phi_{long} = L$: Longitude Angle
- t_s : Solar time
- G : Global radiation
- δ : Declination Angle
- h : Hour Angle
- α : Solar altitude
- θ : Incidence Angle
- Z_s : Solar Azimuth Angle
- G_{HORI} : Global Horizontal Radiation
- G_{DIFF} : Global Diffuse Radiation

According to the previous data, we can compute the power produced by PV system every hour i of the year using the yearly irradiance values.

$$P_{el,i}[W] = G_{tilted,i} \left[\frac{W}{m^2} \right] \cdot S_{PV}[m^2] \cdot \eta_{PV} \cdot \eta_{plant} \quad (4.4)$$

Where:

- $G_{tilted,i}$ is the irradiance value computed by excel
- $S_{PV} = N_{PV,modules} \cdot width \cdot length = 696 \cdot 1,023 \text{ m} \cdot 1,716 \text{ m} = 1221,8 \text{ m}^2$
- $\eta_{PV} = 0,185$ is taken from the datasheet of the PV module

Due to a time step of 1h, the total energy produced in a year E_{year} is calculated as follow:

$$E_{year}[Wh] = \sum_{i=1}^{8760} P_{el,i} [W] \cdot \Delta t_i [h] \quad (4.5)$$

	Days	Electric Produced [kWh]	Energy Consumed AHU [kWh]	Electric Energy Consumed Split [kWh]
Year	365	396950,4	236141	190255,2
Mean Daily		1087,53	868,17	699,47

Table 4-4 Overview of electric production and consumption

Looking to the value summarized in the table above it is possible to highlight the similarity between the expected energy computed in Chapter 44.1 and the one evaluated hour by hour.

Moreover, mean daily values are computed as weighted hourly average on the different distribution of days load. The PV system basically work from 7:00 to 18:00, when the solar energy is available during the day, for this reason the computed mean daily energy production is 1087,53 kWh/day. Furthermore, according to the school calendar and classroom occupancy from 7:00 to 17:00 the mean daily electricity consumptions are respectively 1286,3 kWh/day ,598 kWh/day for the all-air and split system.

4.4. Batteries sizing

The main goal of the pv system is to make the school as much independent as possible from the electric grid. For this reason, the battery system was modelled as the school was not connected to the electrical grid as a stand-alone school. Consequently, the battery sizing play a crucial role because the unique power generation source is the photovoltaic system installed on the rooftop, which allows to produce a good amount of power in the central hours of the day. Anyway, the main loads are also in contemporaneity with the electricity production but in order to don't lose the power produced during the weekend and assure the energy demand at any moment of the day also during the peak loads hours a good storage system such as batteries have been sized, without exceeding in their sizing.

In order to size the storage system, it was decided to choose the B-Box 13.8 of the BYD producer as a reference battery available in the market.


Technical parameters	
	
B-Box 13.8	
Battery type	Lithium iron phosphate (LiFePO ₄)
Battery configuration	B-PLUS 13.8 (13.8 kWh)
Usable capacity ¹	13.8 kWh
Max output power	12.8 kW
Peak output power, 60 sec	13.3 kW
Nominal voltage	51.2 V _{DC}
Voltage range	43.2 - 56.4 V
Ambient temperature ²	-10 °C to +50 °C
Interfaces	RS485/CAN
Round trip energy efficiency	≥ 95.3 %
Warranty	10 years
Certifications and standards	UL1642 for cell, EMC (EN 61 000 chapter 4.2, 4.3, 4.5, 4.6; EN55022), dangerous goods (UN3480, UN38.3)
IP protection class	IP20
Dimensions (W/D/H)	650 x 550 x 880 mm
Weight	175 kg
Compatible inverters	SMA / Goodwe / Solax / Victron, more brands to be announced
Scalable	Extend anytime / up to 32 systems parallel / 441.6 kWh
<small>[1] Test Conditions: 100% DOD, 0.5C discharge @+25°C [2] -10°C to 10°C will be derating</small>	

Figure 4-4-6: Battery Datasheet

4.4.1. Battery sizing for All-air system

The sizing procedure of the batteries capacity consist in different steps, the first simple one is related to this formula, that allowed to have an approximative pre-sizing of the storage system.

$$C_{tot,batteries}[Wh] = \frac{E_{cons,daily}[Wh] \cdot n^{\circ} \text{ days of autonomy}}{DoD_{max} \cdot \eta_{round-trip}} = \frac{219,18 \cdot 5}{0,9 \cdot 0,953} = 1277,7 kWh \quad (4.6)$$

where:

- *n° days of autonomy* : they have been assumed equal to 5 in order to pursue a conservative sizing and assure enough energy for an entire week of operation of the cooling system
- *DoD_{max}*: it has been assumed equal to 0,9 in order to keep, for safety reason, the batteries within their number of cycles for the whole life of the system.
- *η_{round-trip}* : it is picked from the battery datasheet
- *E_{cons,daily}[kWh]* = *E_{PV,daily}* - *E_{loads,daily}* = 1087,35 - 868,17 = 219,18 kWh, where the values are reported in the table 4-4 in the row "Mean Daily".

According to this pre-sizing calculation the number of batteries needed in our storage system are:

$$n^{\circ} \text{ of batteries} = \frac{C_{tot,batteries}}{C_{nom,batteries}} = \frac{1277700 \text{ Wh} / 51,2V}{13800 \text{ Wh} / 51,2V} = \frac{24956 \text{ Ah}}{269,53 \text{ Ah}} = 92,59 \rightarrow 93 \text{ batteries} \quad (4.7)$$

Regarding the number of batteries obtained, an important fact has to be pointed out: the previous formula is based on the assumption that the whole weekly electricity surplus has to be stored in the batteries, but this hypothesis does not match with real operation of photovoltaic system, where a charge controller allows to inject to the grid the extra production and the electrical peak demand variate each day depending to the different daily cooling load so the definition of a mean daily electricity demand is not meaningful .

Going to analyze the overall values of electricity produced and consumed directly from them yearly production/consumption profile it is possible to point out that:

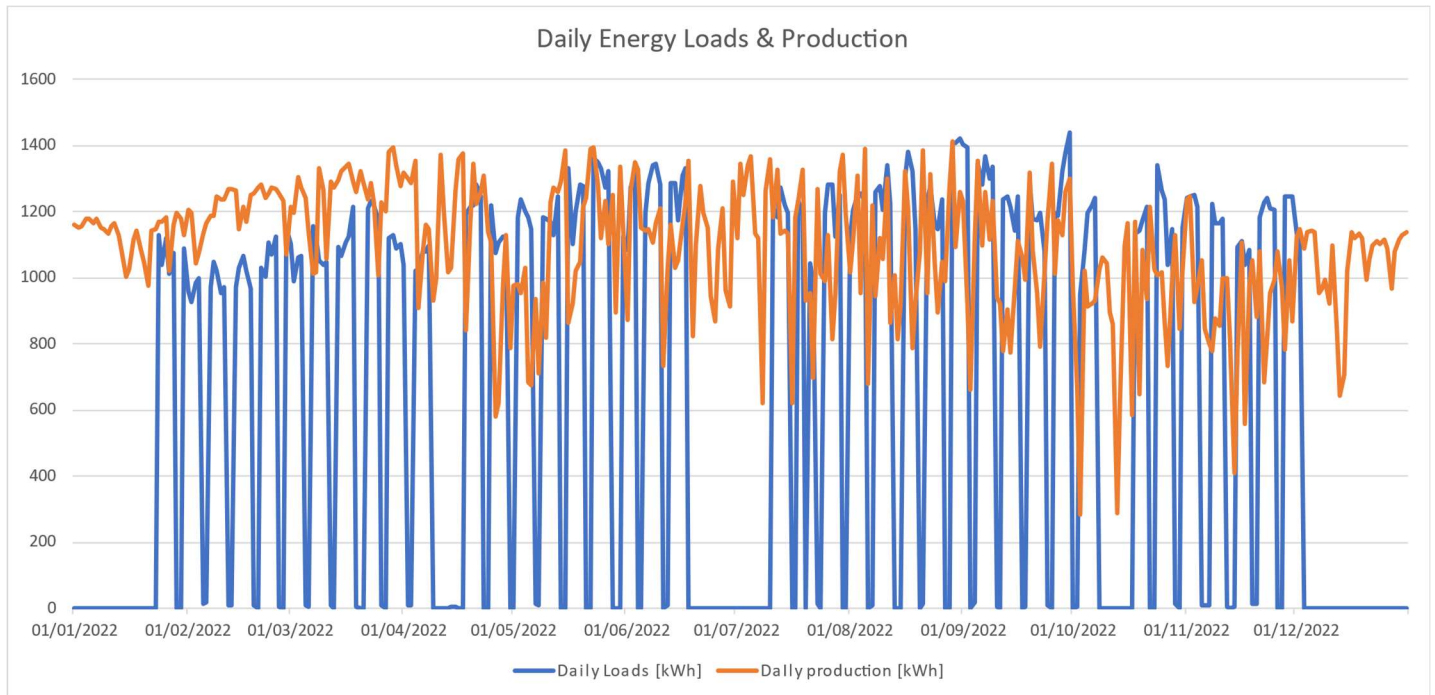


Figure 4-4-7: Daily Energy Loads & Production

- According to the fig 4-7, in some operative day, exactly 123 on 256 the all-air system requires more energy than the produced one. In fact In the best case, in the most profitable day of production it is possible to arrive to generate 1414,42 kWh, instead the day with the less production it is possible to account 285,07 kWh. Regarding the energy demand side, it is possible to observe the highest peak the 29/08 with a 1440,4 kWh demand, instead the lowest demanding day require 929 kWh.
- Overall, in the whole year the energy production is higher with reference to the energy demand and the surplus account for approximately 168,622 MWh.
- The electricity production during the opening days of the school is 212,192 MWh, for this reason it is possible to understand that 23,949 MWh are missing to fulfil the overall energy demand of 236,141 MWh.

The electricity production during the closing days of the school is 184,758 MWh. This implies that it is possible to cover the energy demand, but the number of batteries needed have to be calculated in function of the annual curve difference between production and demand and not on the whole energy that could be produced and saved. According to this consideration, an annual analysis on the energy demand and production has to be performed.

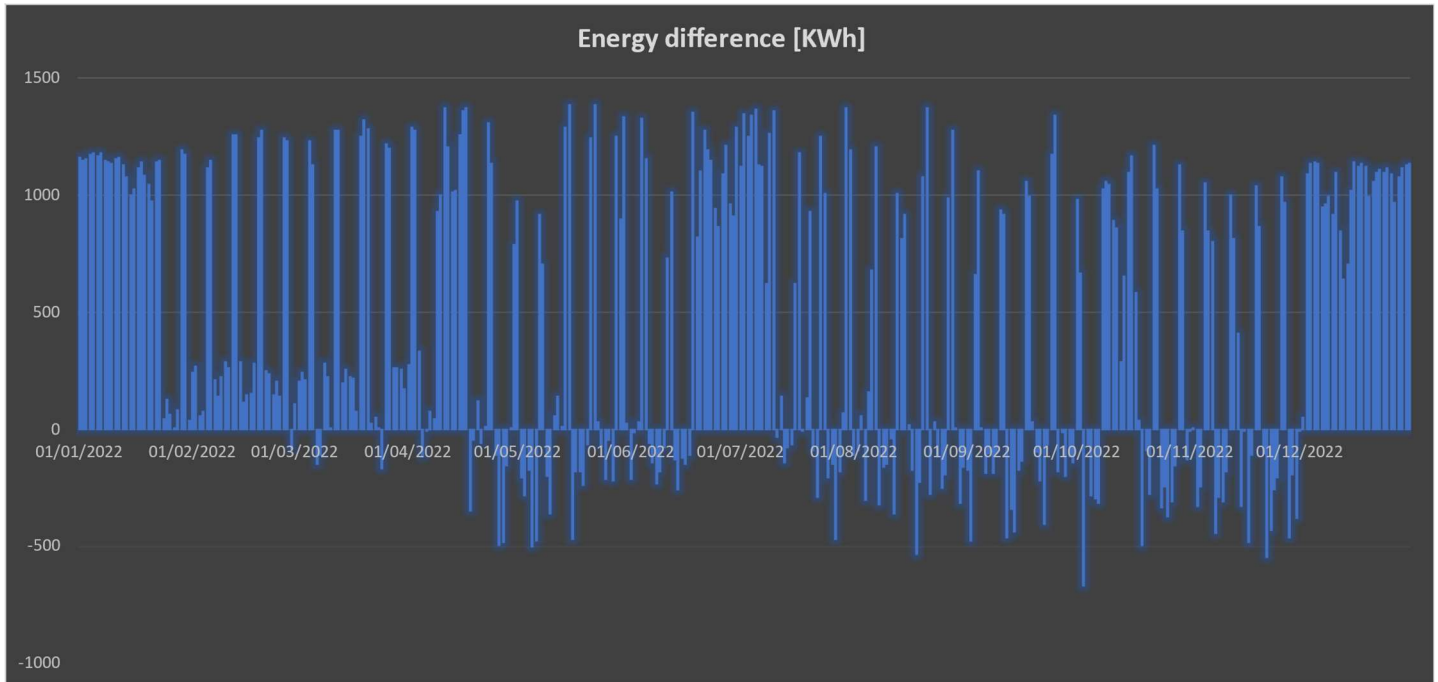


Figure 4-4-8: Production & Demand energy difference

In order to assess the fairness of the battery sizing evaluation, an hourly based annual simulation of electricity produced, of electricity consumed and consequently of the State of Charge has been conducted, considering the following assumptions:

- The electricity consumed has been computed as mentioned in section 4.2, performing a yearly simulation of the all-air system with timespan of 6 minutes.
- The electricity production has been computed considering 696 modules, as mentioned in the previous chapters.
- DOD must not exceed 90% (lithium-based battery).
- The battery starts at SOC of 25%: a conservative value should be assumed since the simulation starts in January (even if at the end of the year an increase of SOC is below demonstrated).
- Roundtrip efficiency set at 95,3% as datasheet.

- Batteries number equal to 141.

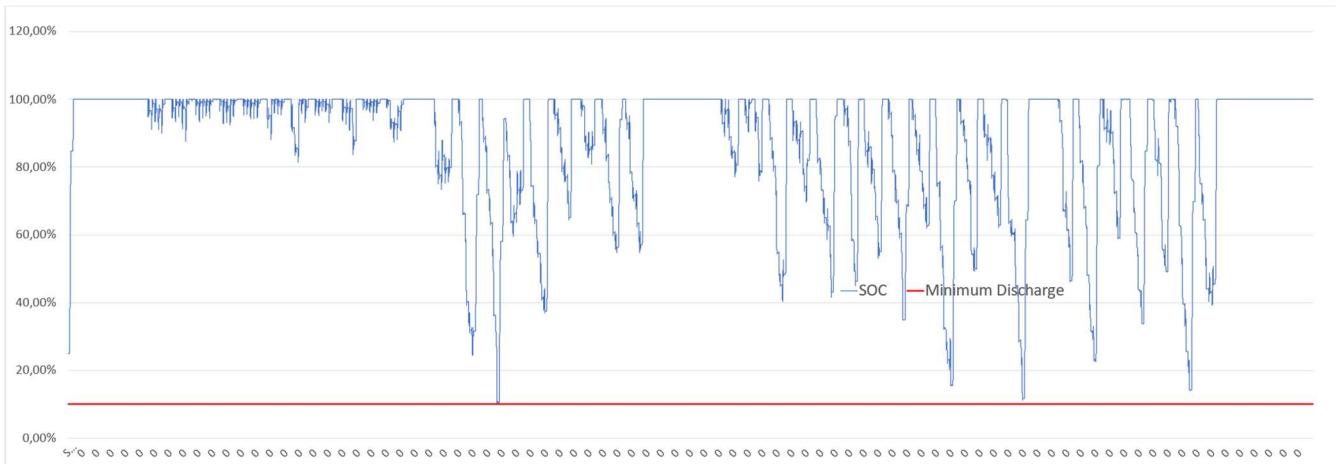


Figure 4-4-9: SOC along the year

In fig 4-9 the State of Charge evolution along the year is reported, where SOC is computed as:

$$SOC = \frac{\text{Energy stored [Wh]}}{\text{Total Capacity of storage system [Wh]}} = 1 - DoD \quad (4.8)$$

From the chart above it is possible to see that SOC is never lower than 10% (apart from the beginning of the year where has been imposed to 25%), this means that the simulation allows to state that the pre-sizing evaluation of the batteries is underestimating the capacity needs. This underestimation of capacity provided by the pre-sizing formula can be explained by considering the pretty big difference between mean daily consumption and real daily consumptions.

The fig 4-9 shows that is possible to install a storage capacity of 1,9458 MWh instead of 1,2834 MWh that is the capacity needed to cover the yearly energy demand during the operative days. This result is obtainable due to the continuative electricity production of the PV system during the year, also in the closing days. Batteries will accumulate the energy in non-operative days in order to keep them state of charge as higher as possible and never go down the settled value of minimum discharge of 10%. During the closing period of the school (all the weekend, the festivity and semester breaks) the storage system can recharge and sustain for the whole year the energy demand, reaching the lowest state of discharge only the last day of operativity of the system.

To conclude, in order to don't lose no electricity produced by the photovoltaic panels, the system was settled to inject all the surplus of energy that don't go to the batteries because are full, directly on the electric grid. This creates the possibility to fulfill part of the residential electric demand of the town of Santa Lucia or get remuneration by the electric provider of the area. The surplus production value injected is equal to 164,25 MWh/year, that hypnotizing a selling price of 100 \$/MWh could be 16425 \$ per year. An amount of revenues that can help to repay the renovation costs and make the school a real electric power plant.

4.4.2. Battery sizing for split system

In this chapter will be shown the battery sizing in the case in which it is decided to adopt the split cooling system that with reference to the annual energy expenditure of all-air system is 57% less. The sizing procedure proceed with the same steps did before. The first one is related to this formula, that allowed to have an approximative pre-sizing of the storage system.

$$C_{tot,batteries}[Wh] = \frac{E_{cons,daily}[Wh] \cdot n^{\circ} \text{ days of autonomy}}{DoD_{max} \cdot \eta_{round-trip}} = \frac{387,88 \cdot 5}{0,9 \cdot 0,953} = 2261,2 \text{ kWh} \quad (4.9)$$

where:

- *n° days of autonomy* : they have been assumed equal to 5 in order to pursue a conservative sizing and assure enough energy for an half of the week the operation of the cooling system
- *DoD_{max}*: it has been assumed equal to 0,9 in order to keep, for safety reason, the batteries within their number of cycles for the whole life of the system.
- *η_{round-trip}*: it is picked from the battery datasheet
- *E_{cons,daily}[kWh]* = *E_{PV,daily}* - *E_{loads,daily}* = 1087,35 - 699,47 = 387,88 kWh, where the values are reported in the table 4-4 in the row "Mean Daily".

According to this pre-sizing calculation the number of batteries needed in our storage system are:

$$n^{\circ} \text{ of batteries} = \frac{C_{tot,batteries}}{C_{nom,batteries}} = \frac{2261200 \text{ Wh} / 51,2V}{13800 \text{ Wh} / 51,2V} = \frac{44164 \text{ Ah}}{269,53 \text{ Ah}} = 163,85 \rightarrow 164 \text{ batteries} \quad (4.10)$$

The previous formula is based on the assumption that the whole weekly electricity surplus has to be stored in the batteries, but this hypothesis does not match with real operation of photovoltaic system, where a charge controller allows to inject to the grid the extra

production and the electrical peak demand variate each day depending to the different daily cooling load so the definition of a mean daily electricity demand is not meaningful.

Going to analyze the overall values of electricity produced and consumed directly from them yearly production/consumption profile it is possible to point out that:

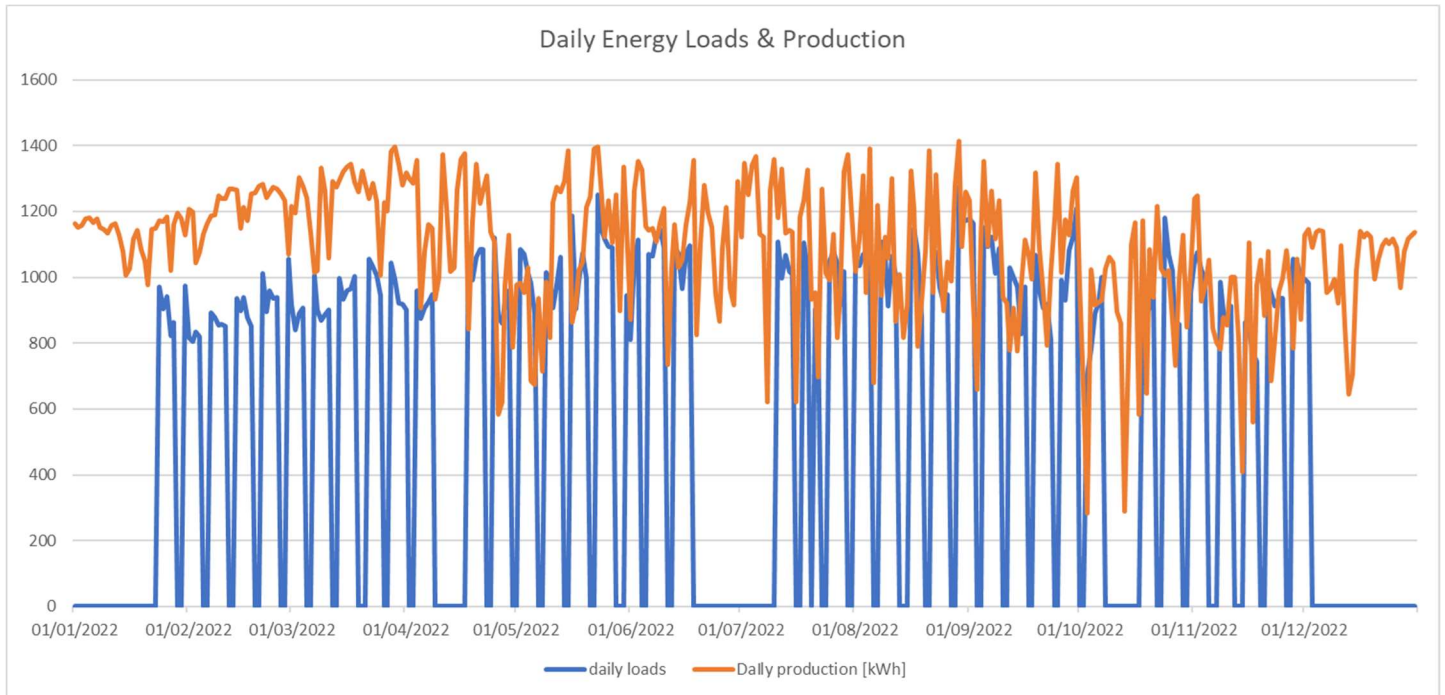


Figure 4-4-10: Daily Energy Loads & Production

- According to the fig 4-11, in most of the operative day the split system requires less energy than the produced one. For this reason, the support of batteries is needed only in some critical days during the year. Regarding the energy demand side, it is possible to observe the highest peak the 29/08 with a 1273,76 kWh demand, instead the lowest demanding day, 03/10 require 702,73 kWh.
- Overall, in the whole year the energy production is higher with reference to the energy demand and the surplus account for approximately 206,9 MWh.

Anyway, the number of batteries needed will be calculated in function of the annual curve difference between production and demand. In order to assess the fairness of the battery sizing evaluation, an hourly based annual simulation of electricity produced, of electricity consumed and consequently of the State of Charge has been conducted, considering the following assumptions:

- The electricity consumed has been computed as mentioned in section 4.2, performing a yearly simulation of the split system with timespan of 6 minutes.
- The electricity production has been computed considering 696 modules, as mentioned in the previous chapters.

- DOD must not exceed 90% (lithium-based battery).
- The battery starts at SOC of 25%: a conservative value should be assumed since the simulation starts in January (even if at the end of the year an increase of SOC is below demonstrated).
- Roundtrip efficiency set at 95,3% as datasheet.
- Batteries number equal to 64.

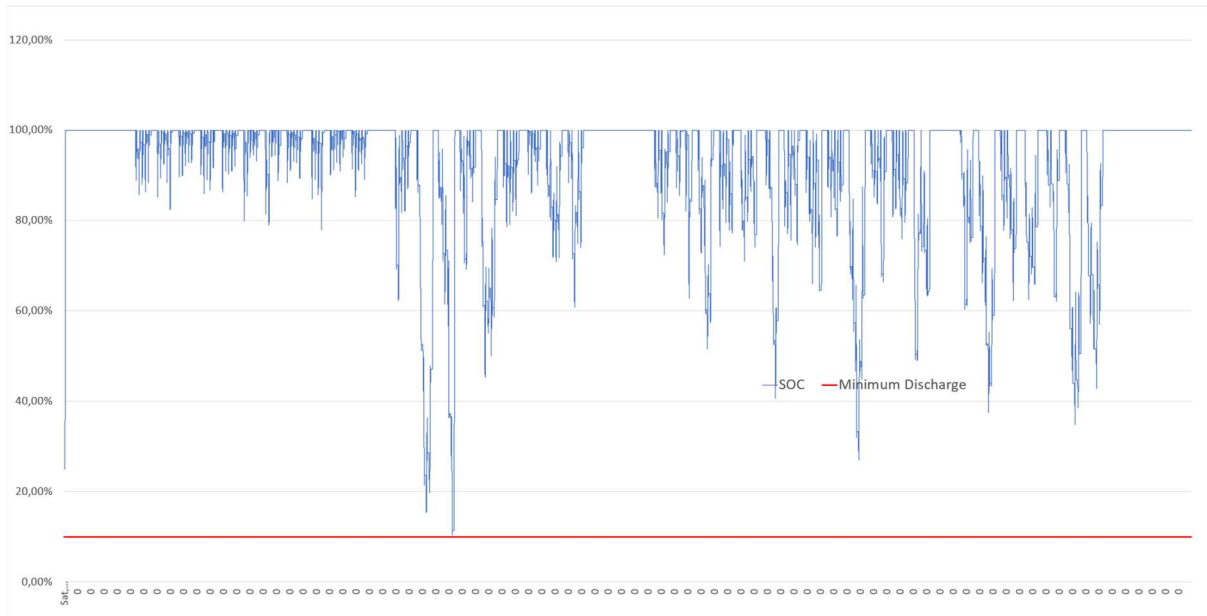


Figure 4-4-11: SOC along the year

From the chart above it is possible to see that SOC is never lower than 10%. This means that the simulation allows to state that the pre-sizing evaluation of the batteries is overestimating the capacity needs. This overestimation of capacity provided by the pre-sizing formula can be explained by considering the pretty big difference between mean daily consumption and real daily consumptions.

The fig 4-12 shows that is possible to install a storage capacity of 883,2 kWh. This result is obtainable due to the continuative electricity production of the PV system during the year, also in the closing days. Batteries will accumulate the energy in non-operative days in order to keep them state of charge as higher as possible and never go down the settled value of minimum discharge of 10%. During the closing period of the school (all the weekend, the festivity and semester breaks) the storage system can recharge and sustain for the whole year the energy demand, reaching the lowest state of discharge only once during the year the 07th May.

To conclude, in order to don't lose no electricity produced by the photovoltaic panels, the system was settled to inject all the surplus of energy that don't go to the batteries because are full, directly on the electric grid. In this case the surplus production value injected is

equal to 203,95 MWh/year, that with the hypothesis of a selling price of 100\$/MWh could generate 20395 \$ per year going to repay the intervention costs and consequently become a real electrical power plant that can produce positive economic benefits for Santa Lucia community.

4.5. Converter selection and matching

The inverter model that has been chosen is HYL-5000 from HUAYU and it comprehends the PV inverter and the battery inverter, so it is able to manage both the PV modules and the batteries. The rated power of the device is equal to 5 kW, but the datasheet claims that it can work with a maximum PV power equal to 6 kW: for this reason, 38 inverters are enough for the installed PV power (that is equal to 226,2 kW). Since the datasheet states that lithium batteries with 51,2 V as nominal voltage can be used, the battery matching is appropriate.

In order to correctly match the inverters to the PV modules, some calculations are required. Firstly, the minimum and maximum number of modules that can be placed in series to form an array have to be determined. These values are computed considering the voltage change in the PV modules (due to the different working conditions) and the allowable voltage limits for the inverter. Secondly, the maximum number of arrays that can be connected to the inverter needs to be determined. This is computed considering the highest short-circuit current for the PV modules and the maximum allowable current for the inverter. The calculations are here reported.

Datasheet	HYL-5000
Output Data	
Rated Power	5000W/5000VA
Parallel Capacity	YES
Normal Output Voltage	230/240, Split Phase 220/110V
Normal Output Frequency	50Hz/60Hz
Surge Power	10000VA
Switch Time	10ms
Waveform	Pure Sine Wave
Battery Data	
Battery Type	Lithium/Lead-Acid
Normal Voltage	51.2V/48V
Max. Charge Voltage	59V
Solar Charger Data	
Max. Recommended PV Power	6000W
MPPT Tracker	2
Max. PV Open Circuit Voltage	480Vdc
MPPT Voltage Range	100V ~ 385V dc
Max. Solar Charge Current(Battery side)	100A
Max. MPPT Efficiency	>98%
Parallel MPPT Charger	YES
AC Charger Data	
Normal Voltage	230V ac
AC Voltage Range	110V ~ 280V ac
Max. Charge Current(Battery side)	60A
Frequency Range	50Hz/60Hz

Figure 4-4-12: Inverter datasheet

- Maximum number of modules per array

It is computed considering the maximum open-circuit voltage $V_{inv,max}$ for the inverter and the maximum open-circuit voltage $V_{OC,max}$ for each PV module.

$$N_{modules,max} = \frac{V_{inv,max}}{V_{OC,max}} \quad (4.11)$$

The maximum open-circuit voltage is the worst voltage condition, and it is reached when the temperature is at the lowest value. From PVsyst database, $T_{amb,min} = 22 \text{ }^{\circ}\text{C}$ has been obtained. Hence:

$$V_{OC,max} = V_{OC,STC} + \beta \cdot V_{OC,STC} \cdot (T_{amb,min} - T_{STC}) = 40,5 - 0,0029 \cdot 40,5 \cdot (22 - 25) = 40,85 \text{ V} \quad (4.12)$$

So, the maximum number of modules is equal to:

$$N_{modules,max} = \frac{V_{inv,max}}{V_{OC,max}} = \frac{480 V}{40,85 V} = 11,75 \rightarrow 11 \text{ modules} \quad (4.13)$$

- Minimum number of modules per array

It is computed considering the minimum allowable voltage $V_{inv,min}$ for the inverter and the minimum MPP voltage $V_{MPP,min}$ for each PV module.

$$N_{modules,min} = \frac{V_{inv,min}}{V_{MPP,min}} \quad (4.14)$$

The minimum MPP voltage is computed taking into account the maximum cell temperature $T_{cell,max}$. From weather database, cell temperatures for each hour are calculated:

$$T_{cell,i} = T_{amb,i} + \frac{NOCT - T_{ref,NOCT}}{G_{NOCT}} * G_i \quad i = 1, \dots, 8760 h \quad (4.15)$$

Where $NOCT = 44,5 \text{ } ^\circ\text{C}$, $T_{ref,NOCT} = 20 \text{ } ^\circ\text{C}$ and $G_{NOCT} = 800 \text{ W/m}^2$, as reported in the PV module datasheet. Hence, the maximum cell temperature occurs at the end of June, at $T_{amb} = 36,3 \text{ } ^\circ\text{C}$ and $G = 1009,83 \text{ W/m}^2$ and it is equal to $T_{cell,max} = 65,56 \text{ } ^\circ\text{C}$.

The minimum MPP voltage $V_{MPP,min}$ is equal to:

$$V_{MPP,min} = V_{MPP,STC} + \beta \cdot V_{OC,STC} \cdot (T_{cell,max} - T_{STC}) = 32,8 - 0,0029 \cdot 40,5 \cdot (65,56 - 25) = 28,04 V \quad (4.16)$$

Hence, the minimum number of modules is equal to:

$$N_{modules,min} = \frac{V_{inv,min}}{V_{MPP,min}} = \frac{100 V}{28,04 V} = 3,57 \rightarrow 4 \text{ modules} \quad (4.17)$$

- Maximum number of arrays

It is computed considering the maximum direct current $I_{inv,max}$ for the inverter and the maximum short-circuit current $I_{SC,max}$ for each PV module.

$$N_{arrays,max} = \frac{I_{inv,max}}{I_{SC,max}} \quad (4.18)$$

The maximum short-circuit current $I_{SC,max}$ occurs at the maximum solar irradiance G_{max} and it is computed as:

$$I_{SC,max} = \frac{G_{max}}{G_{STC}} \cdot I_{SC,STC} \cdot [1 + \alpha \cdot (T_{cell}(G_{max}) - T_{STC})] = \frac{1009,83}{1000} \cdot 10,4 \cdot [1 + 0,0005 \cdot (65,56 - 25)] = 10,7 A \quad (4.19)$$

Hence, the maximum number of arrays that can be connected to an inverter is:

$$N_{arrays,max} = \frac{I_{inv,max}}{I_{SC,max}} = \frac{100 A}{10,7 A} = 9,34 \rightarrow 9 \text{ arrays} \quad (4.20)$$

These electrical constraints permit to choose the expected configuration supposed in the 6-1 chapter using 24 times a main block of 24 PV panels arranged in 6 arrays of 4 modules, for 3 times a block of 16 PV panels arranged in 4 arrays of 4 modules, for 3 times a block of 20 PV panels arranged in 5 arrays of 4 panels and only one time a block of 12 PV panels arranged in 2 arrays of 6 panels.

Moreover, it should be verified if the batteries alone are enough to cover the maximum power required by the household. The maximum load happens the 29/08, as stated before from the energy demand analysis. From the battery datasheet, the maximum output power is equal to 12,8 kW, leading to a maximum discharge current on battery side equal to:

$$I_{batt,max} = \frac{\text{Max output power}}{\text{Min DC voltage}} = \frac{12800 W}{43,2 V} = 296,3 A \quad (4.21)$$

Since this current cannot be handled by the converter, the maximum power that can be recovered from each battery is equal to the product between the maximum current of the converter and the maximum battery voltage:

$$P_{battery,max} = I_{conv,max} \cdot V_{batt,max} = 60 A \cdot 56,4 V = 3384 W \quad (4.22)$$

Since there are 38 converters that can receive power from the battery block, the total instantaneous power that can come from the battery groups is equal to:

$$P_{tot,max} = 38 \cdot P_{battery,max} = 128,6 \text{ kW} < 146,06 \text{ kW} = P_{load,max,Split} \quad (4.23)$$

So, in case of total absence of solar irradiation, the batteries alone cannot cover the maximum instantaneous load power, but over the year some electric power it is partially produced, and it partially goes to compensate the missing one. To be specific and precise, this load power is not an instantaneous power because time ranges of 6 minutes have been considered but it can be considered as instantaneous power.

Regarding the all-air system, the $P_{load,max,HVAC} = 158,49 \text{ kW}$ in the worst day of the year, so the batteries alone cannot cover the maximum instantaneous load power in the case of total absence of solar irradiation.

4.6. Storage systems comparison due to the adoption of two different cooling systems

Starting from the same PV system, the two cooling strategies investigated have different loads profile during the year so the auxiliary storage system needed to cover the loads don't covered by the energy production system differs a lot between them.

Component	HVAC System	Split Sytem
N° of batteries	141	64
Batteries Storage Capacity [kWh]	1945,8	455,4
Electric grid output [MWh]	164,26	193

Table 4-5: Storage system components

Overall, adopting the split system the configuration of the battery storage scheme is easier than in the case of the adoption of Centralized AHU with fan Coil. In the table 4-5 are reassumed all the components of the system for the two different scenarios evaluated.

Financially speaking, the split technology result more convenient for the number of components needed to be fully operative but the main drawback adopting this technology is that high level of CO₂ inside the classrooms imply the use of natural ventilation to keep CO₂ levels under acceptable levels. It is also true that in both cases the difference between

production and energy demand is always positive considering the whole year, for this reason it is also possible to suppose another scenario where the school exchange energy with the electrical grid and no storage system will be needed. In this case, the investment cost will be lowered, and the energy difference will be anyway positive for the whole year but giving a small advantage to the community and furthermore stressing the electrical grid for the continuous electricity exchange in order to cover the loads not covered by the PV system.

5 Building Envelope Improvements and Consequences

An important preamble has to be done. The base building considered for the previous and the following simulations took into account the base building with already installed the PV modules on the roof. The presence of PV modules on the roof have mitigated the solar impact on the roof surface of the building. Furthermore, an initial improvement of the energy performance of the building is solely obtained by installing the panels on the roof. In fact, according to an investigation performed in climate area similar to Colombia as Honduras the research of Ochoa et al (51) found that PV modules decrease up to 24.3% the temperature on the outer roof of the buildings and the heat gain through the roof of 83.8% due to the installation of photovoltaic modules and a reduction of 28.1% in the total gain of the building. This means that the modules influenced the thermal load of the building due to the decrease in temperature on the outside roof. Instead according to the study (52) performed in Shanghai, the daily load of flat and tilted overhead PV roofs were reduced by 77.4% and 69.4%.

5.1. Building Envelop Stratigraphy Improvements

5.1.1. External Wall Stratigraphy Improvement

In order to reduce the thermal load coming from the conduction of the external wall, it was decided to install on the external surface an additional layer of 5mm clay tiles with the aim to reduce the conductive and radiative influence on the building envelope. In the following image is possible to see the properties of the clay tiles layer.

Material	Thickness mm	Conductivity W/(m·K)	Density kg/m ³	Specific Heat Capacity J/(kg·K)	Resistance m ² K/W	Vapour Resistivity GN·s/(kg·m)	Category
[C/T] CLAY TILE	5.0	0.1000	1900.0	800.0	0.0500	200.000	Tiles
[F/B] FELT/BITUMEN LAYERS	2.0	0.5000	1700.0	1000.0	0.0040	15000.000	Asphalts & Other Roofing
[CBL] CONCRETE BLOCK (LIGHTWEIGHT)	150.0	0.1900	600.0	1000.0	0.7895	83.000	Concretes

Figure 5-1: External Wall Stratigraphy

The choice of the material it was related to a local availability and cost of the material and the local construction practices. Regarding the positive effect of the intervention, can be seen in the following graph related to the conduction gain over the whole year and in the following chapter related to the new system loads for the two different technologies evaluated.

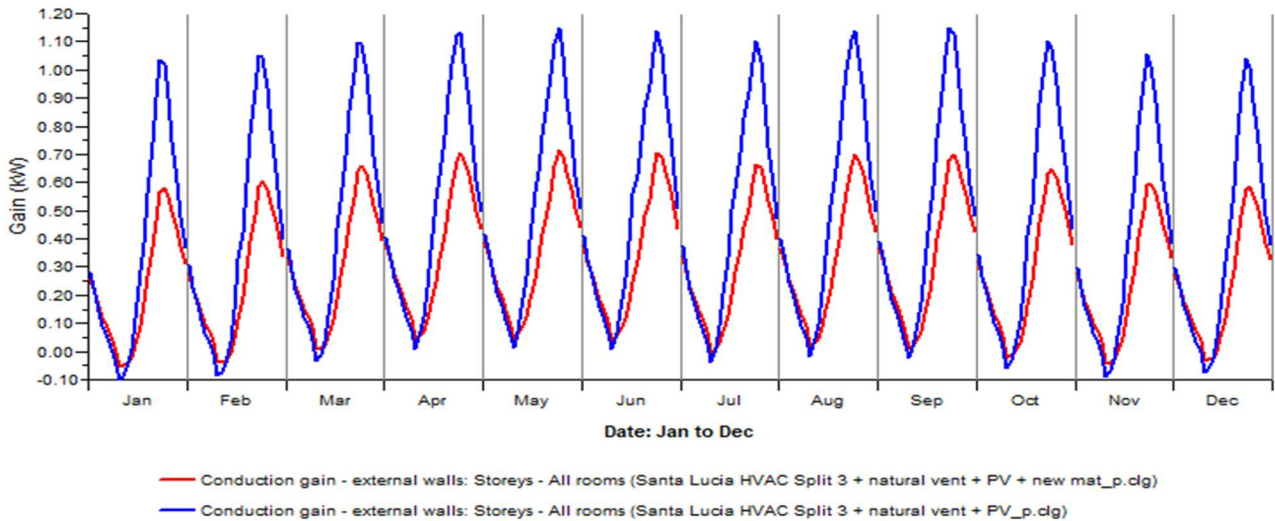


Figure 5-2: External Walls Conduction Gain

5.1.2. Roof Stratigraphy Improvement

In order to reduce the thermal load coming from the conduction of the roof, it was decided to install under the external insulation surface an additional 10 mm fiberboard with the aim to reduce the conductive and radiative influence on the building envelope. In the following image is possible to see the properties of the fiberboard.

Material	Thickness mm	Conductivity W/(m·K)	Density kg/m ³	Specific Heat Capacity J/(kg·K)	Resistance m ² K/W	Vapour Resistivity GN·s/(kg·m)	Category
[STD_PHF] Insulation	6.0	0.0300	40.0	1450.0	0.2000	-	Insulating Materials
[STD_MEM] Membrane	0.3	1.0000	1100.0	1000.0	0.0003	-	Asphalts & Other Roofing
[USFB0000] FIBERBOARD - TILE & LAY-IN PANELS (ASHRAE)	10.0	0.0580	290.0	600.0	0.1724	195.000	Boards, Sheets & Decking
[STD_CC1] Concrete Deck	100.0	2.0000	2400.0	1000.0	0.0500	-	Concretes

Figure 5-3: Roof Stratigraphy

The choice of the material it was related to a local availability and cost of the material and the local construction practices. Regarding the positive effect of the intervention, can be seen in the following graph related to the conduction gain over the whole year and in the following chapter related to the new system loads for the two different technologies evaluated.

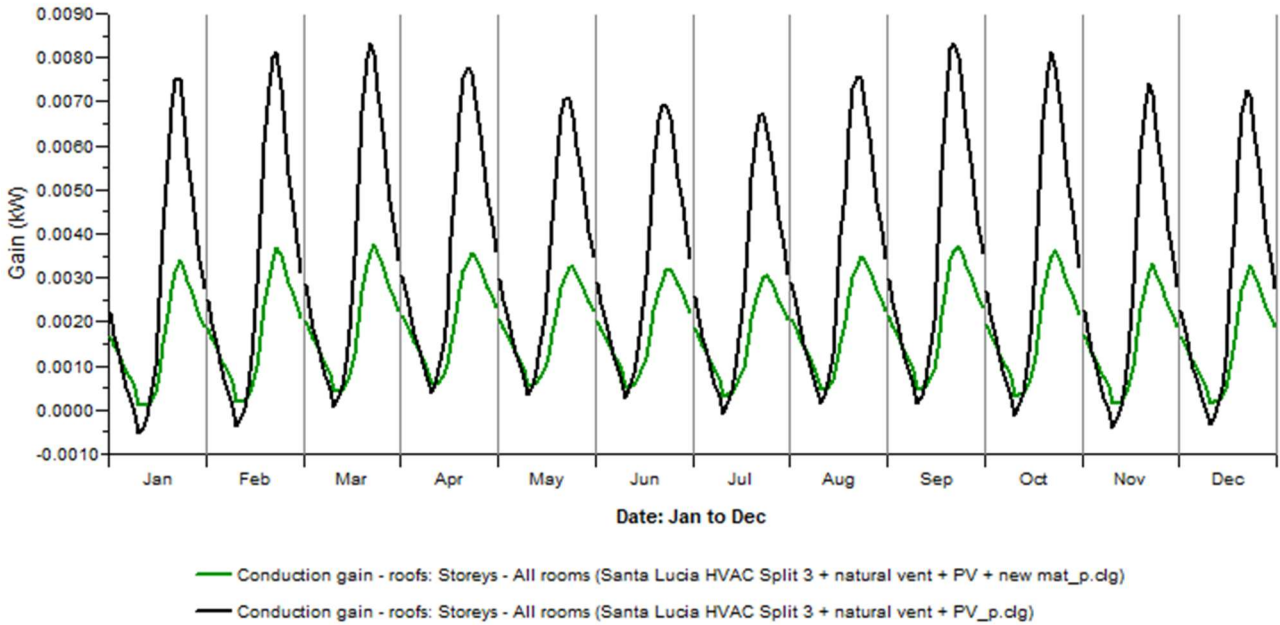


Figure 5-4: Roof Conduction Gain

5.1.3. External Windows Improvement

In order to reduce the thermal load coming from the conduction of the windows and solar gain, it was decided to install a triple glazed window, with the aim to reduce the conductive and radiative influence on the building envelope. In the following image is possible to see the new stratigraphy.

Material	Thickness mm	Conductivity W/(m·K)	Angular Dependence	Gas	Convection Coefficient W/m ² ·K	Resistance m ² ·K/W	Transmittance	Outside Reflectance	Inside Reflectance	Refractive Index	Outside Emissivity	Inside Emissivity	Visible Light Specified
[STD_EXW] Outer Pane	6.0	1.0600	Fresnel	-	-	0.0057	0.409	0.289	0.414	1.526	0.837	0.042	No
Cavity	8.0	-	-	Air	3.1200	0.2999	-	-	-	-	-	-	-
[S6C] STOPSOL 6MM (CLEAR)	6.0	1.0600	Fresnel	-	-	0.0057	0.500	0.250	0.250	1.526	-	-	No
Cavity	8.0	-	-	Air	3.1200	0.1466	-	-	-	-	-	-	-
[STD_INW] Inner Pane	6.0	1.0600	Fresnel	-	-	0.0057	0.783	0.072	0.072	1.526	0.837	0.837	No

Figure 5-5: Windows Stratigraphy

Regarding the positive effect of the intervention, can be seen in the following graph related to the conduction gain over the whole year and in the following chapter related to the new system loads for the two different technologies evaluated.

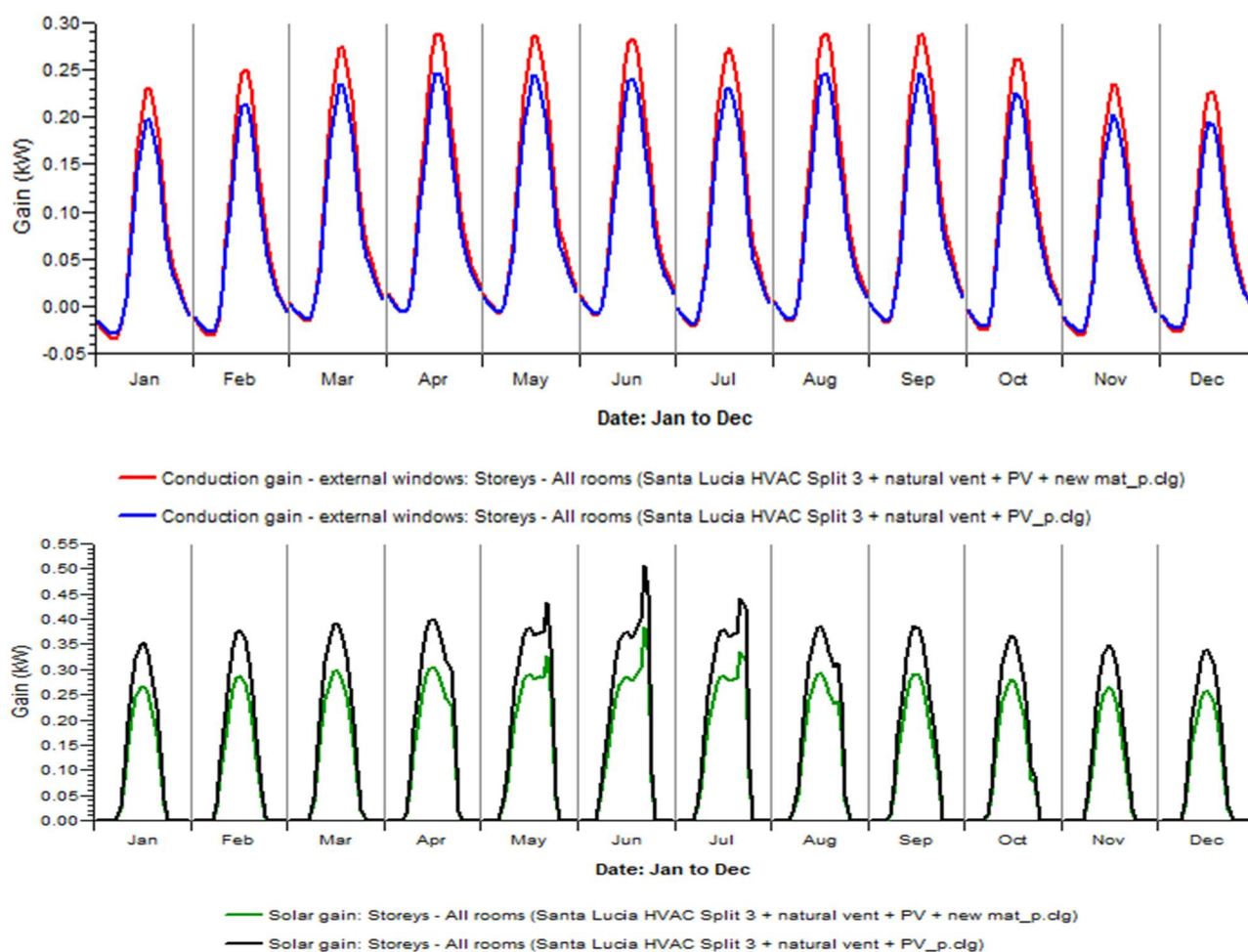


Figure 5-6: Windows Conduction and Solar Gain

5.2. New Split System Loads & Battery System Configuration

5.2.1. System Energy Loads

Firstly, in the fig 5-7 it is possible to appreciate the energy breakdown of the annual energy expenditure of the whole building. Overall, the entire system has an energy expenditure of 182015,46 kWh per year, 4,33% less than the base case previously analysed. The reduction in terms of heat conduction through the envelope is way bigger, but due to the 4 l/s/person of natural ventilation necessary to keep the CO₂ levels in the room under 1200 ppm,

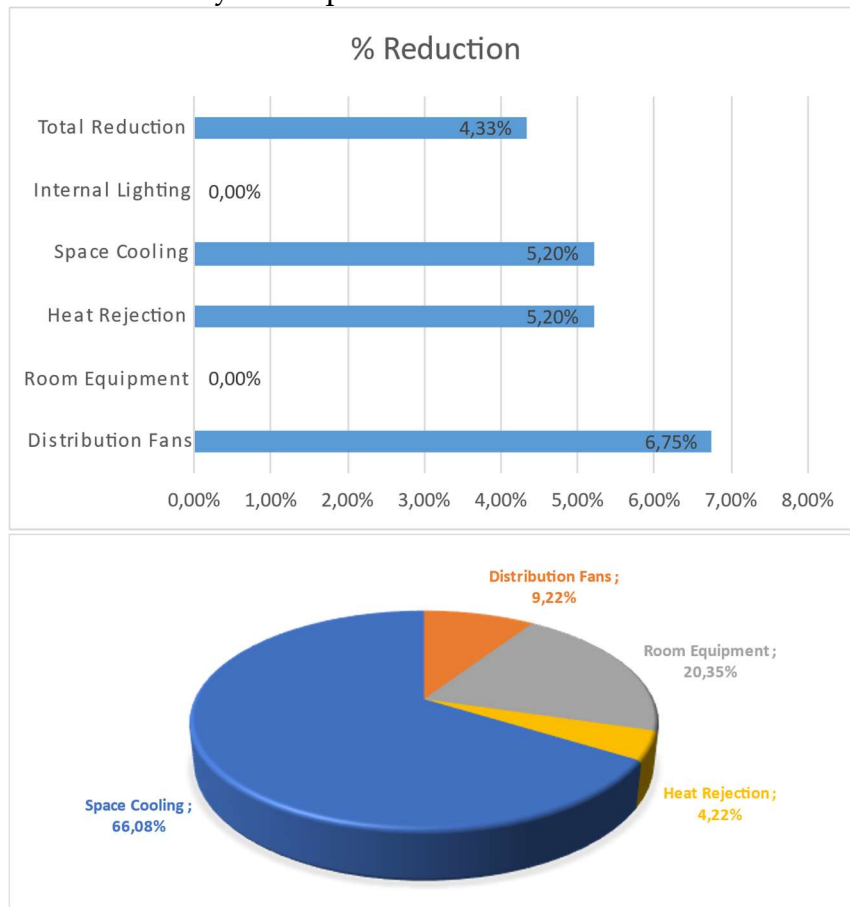


Figure 5-7: Energy Breakdown + % reduction of consumption with new envelope

a lot of the benefits of the envelope improvements are wasted. Possible advantages can be seen on the HVAC system due to smarter usage of the outdoor air.

Secondly, in the fig. 5-8, it is possible to appreciate how the cooling loads are overall reduced, and it is interesting how the peak values are hugely reduced. Comparing them it is possible to account a 15% reduction of the peak values. It could have positive impacts on the battery discharge rate and them consequential number necessary to guarantee a year of complete operation.

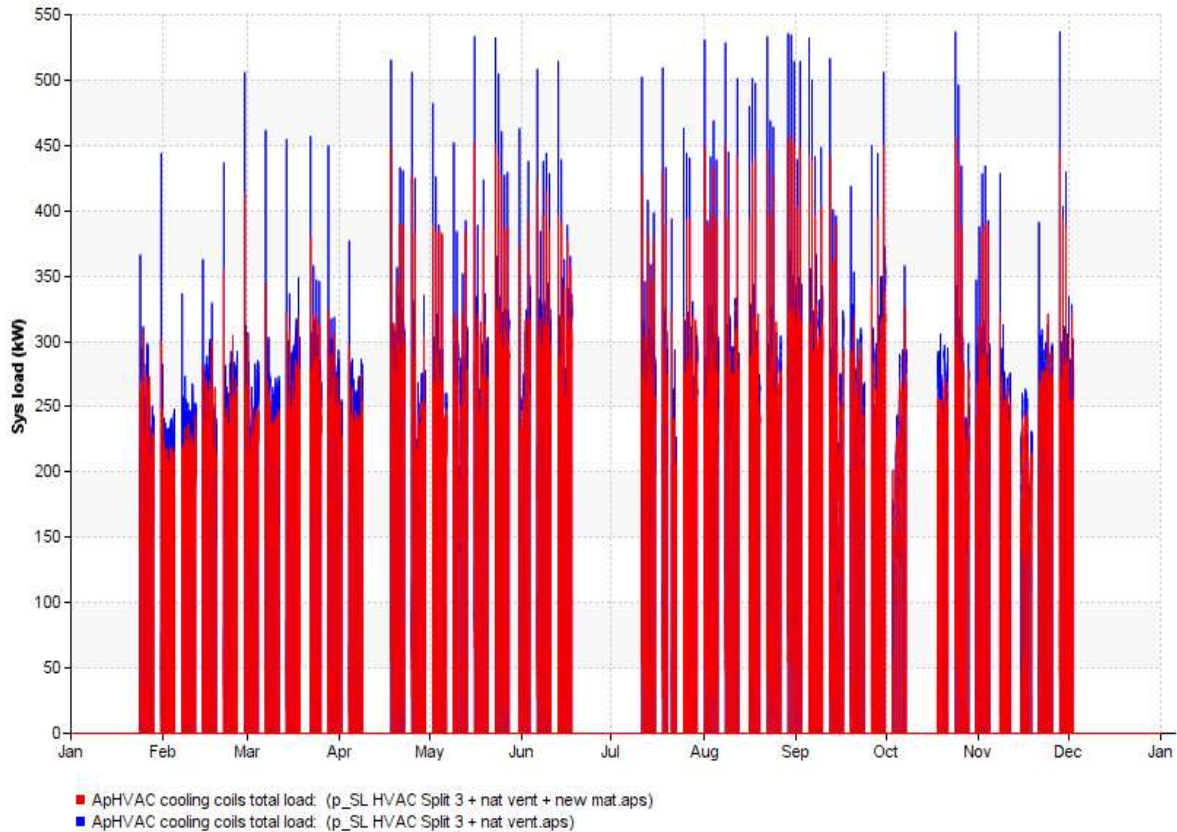


Figure 5-7: Total Cooling Loads

In fact, performing an annual simulation taking into account the energy produced and required by the building, the overall number of batteries decrease from 64 to 54. Additionally, in the following battery discharge graph it is possible to appreciate how the mitigation of peak loads reduces the moment in which the SoC value of the battery pack during the year are critical.

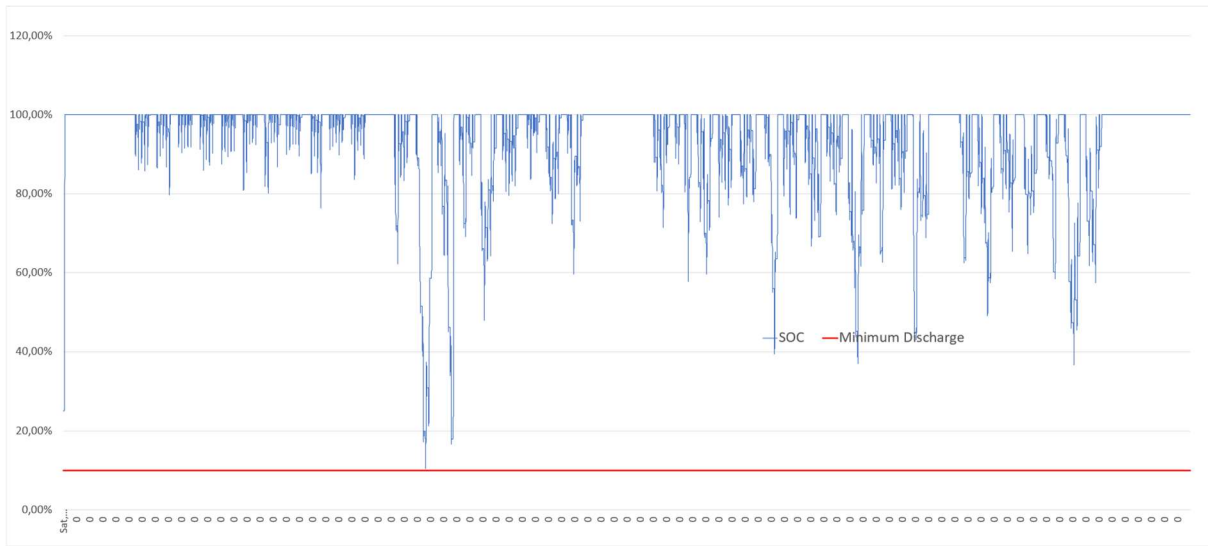


Figure 5-9: Yearly battery SoC

5.3. New HVAC System Loads & Battery System Configuration

5.3.1. System Energy Loads

Firstly, in the fig 5-10, it is possible to appreciate the energy breakdown of the annual energy expenditure of the whole building. Overall, the entire system has an energy expenditure of 227954,9132 kWh per year, 3,47% less than the base case previously analysed. The reduction in terms of heat conduction through the envelope is way bigger, but its appreciable the amount of energy consumption reduction related to the distribution fan and the pumps.

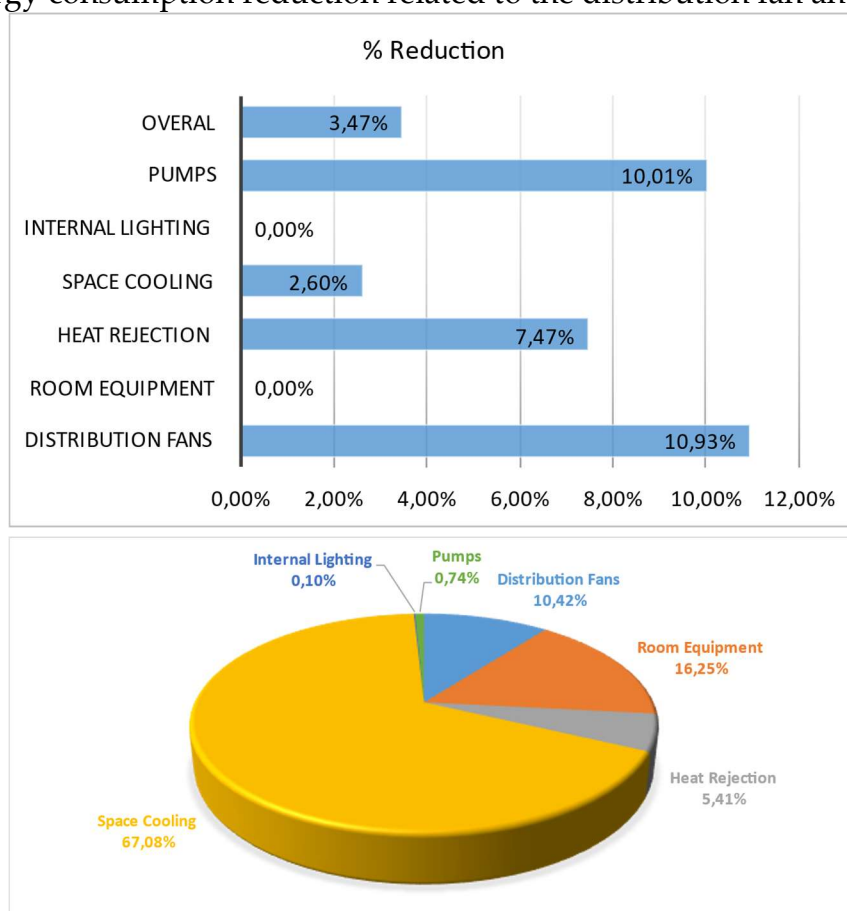


Figure 5-10: Energy Breakdown + % reduction of consumption with new envelope

Secondly, in the fig. 5-11, it is possible to appreciate how the cooling loads are overall reduced, and it is interesting how the peak values are reduced but not so consistently as in the split case. Comparing them it is possible to account a 2,6% reduction of the peak values.

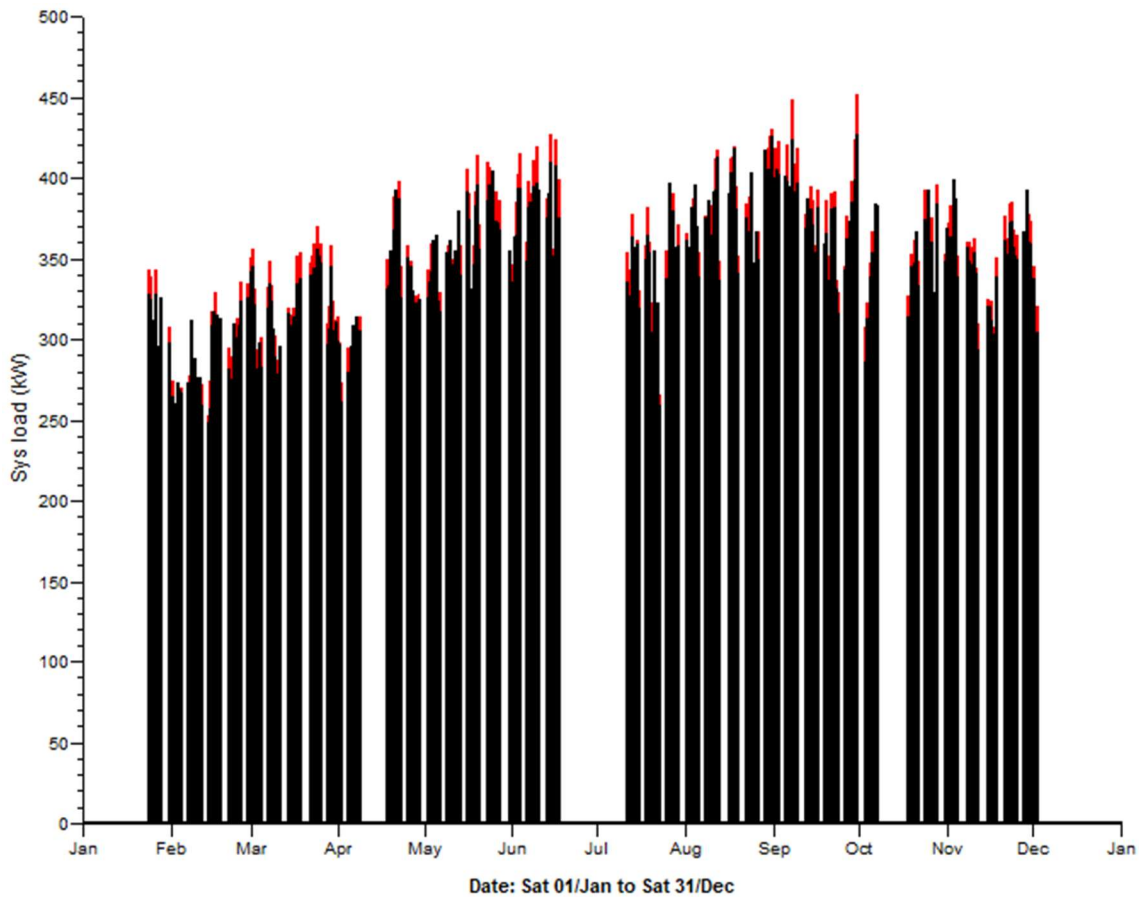


Figure 5-11: Total Cooling Loads

It could have positive impacts on the battery discharge rate and then consequential number necessary to guarantee a year of complete operation.

In fact, performing an annual simulation taking into account the energy produced and required by the building, the overall number of batteries decrease from 141 to 128. Additionally, in the following battery discharge graph it is possible to appreciate the moment in which the SoC value of the battery pack during the year are critical remain similar to the base case and not consistent improvements are seen.

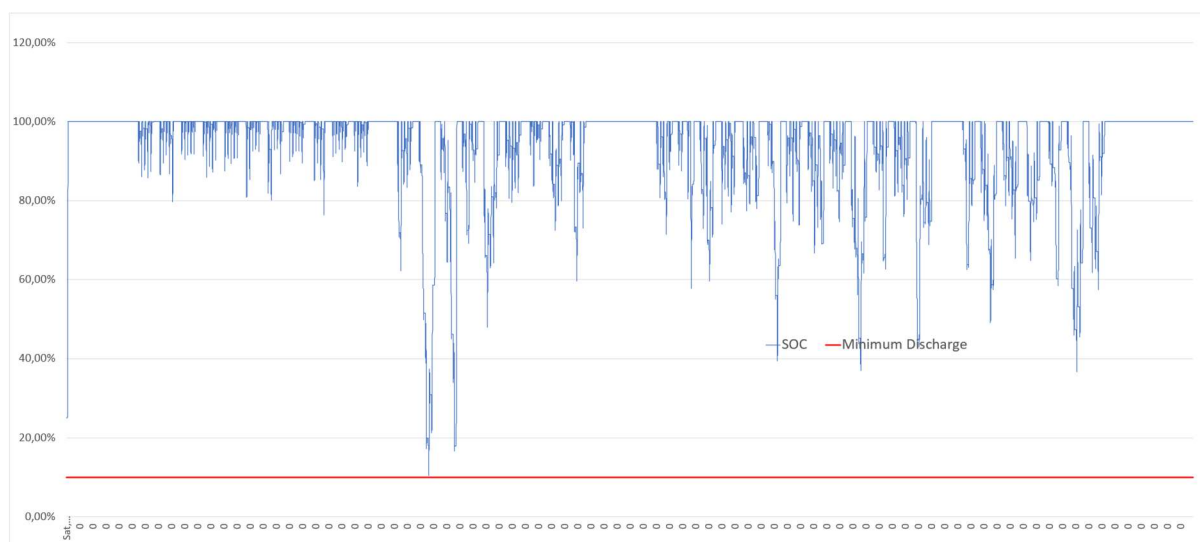


Figure 5-12: Yearly battery SoC

5.4. Final Comparison

	AHU + Fan Coil	% variation	Split System	% variation
Overall Energy Expense [KWh]	227954,9	-3,47%	182015,46	-4,33%
Energy sold on the electric grid [MWh]	164,26	+ 3,93%	203,95	+ 4,74%
N of Batteries	128	-13 batteries (-9,22%)	54	-10 batteries (-15,62%)

In conclusion, after the envelope improvements, the system that benefit with bigger advantages is the Split one, but the main drawback of natural ventilation remains. It will not guarantee the perfect thermal comfort and IAQ continuously during the class hours and the aperture of windows and doors cannot be controlled in a automatized way. Furthermore, the AHU + Fan Coil result more expansive in terms of energy and capital expenditure but it will be perfectly suited for the scope of the intervention with the cons of higher installation complexity.

6 Conclusion

In conclusion, after the envelope improvements, the system that benefit with bigger advantages is the Split one, but the main drawback of natural ventilation remains. It will not guarantee the perfect thermal comfort and IAQ continuously during the class hours and the aperture of windows and doors cannot be controlled in an automatized way. Furthermore, the AHU + Fan Coil result more expansive in terms of energy and capital expenditure but it will be perfectly suited for the scope of the intervention with the cons of higher installation complexity. Anyway, the additional costs could be justified expanding the list of improvements that overall this intervention could provide. It is important to consider that, as cited in the first chapter, the perfect thermal conditions and IAQ bring to reduced absenteeism of students in the classroom due to illness problems. Consequently, also the families or people that live with the students of Santa Lucia will be positively affected from a health point of view and the whole community will benefit. Additionally, the energy surplus produced and sold injecting it in the electrical grid could be an amazing economical source to sustain the huge initial investment for a country like Colombia and could promote the electrification of the houses of Santa Lucia, in which families live in very poor conditions and the capability to afford a fridge, tv or air conditioner is not obvious. This intervention could be used as a case study for the adoption of it as a model to apply in the whole country to improve the condition of rural but huge town like Santa Lucia.

Bibliography

1. *Perceived air quality, sick building syndrome (SBS) symptoms and productivity in an office with two different pollution loads.* **P. Wargocki, D. Wyon, Y. Baik, G. Clausen, P. Fanger,.**
2. *The Effects of Outdoor Air Supply Rate in an Office on Perceived Air Quality, Sick Building Syndrome (SBS) Symptoms and Productivity.* **PAWEL WARGOCKI, DAVID P. WYON, JAN SUNDELL, GEO CLAUSEN, P. OLE FANGER.**
3. *Subjective perceptions, symptom intensity and performance: A comparison of two independent studies, both changing similarly the pollution load in an office.* **Wargocki P., Lagercrantz L., Witterseh T., Sundell J., Wyon D.P., Fanger P.O.**
4. *The effects of indoor air quality on performance and productivity.* **Wyon, DP.**
5. *Effects of pollution from personal computers on perceived air quality, SBS symptoms and productivity in offices.* **Z, Bakó-Biró.**
6. *Indoor air quality and academic performance.* **N, Tess M. Stafford.**
7. *The Effects of Outdoor Air Supply Rate and Supply Air Filter Condition in Classrooms on the Performance of Schoolwork by Children.* **Wyon, Pawel Wargocki David P.**
8. *The Effects of Moderately Raised Classroom Temperatures and Classroom Ventilation Rate on the Performance of Schoolwork by Children.* **Wyon, Pawel Wargocki David P.**
9. *Identifying the K-12 classrooms' indoor air quality factors that affect student academic performance.* **Adel Kabirikopaei, Josephine Lau, Jayden Nord, Jim Bovaird.**
10. *Ten questions concerning thermal and indoor air quality effects on the performance of office work and schoolwork.* **Pawel Wargocki, David P. Wyon.**
11. **DONALD K. MILTON, P. MARK GLENCROSS, MICHAEL D. WALTERS. Risk of Sick Leave Associated with Outdoor Air Supply Rate, Humidification, and Occupant Complaints.**
12. *The impact of school building conditions on student absenteeism in upstate New York.* **Simons E Hwang S. Fitzgerald E.F, Kielb C. Lin S.**

13. *Classroom Carbon Dioxide Concentration, School Attendance, and Educational Attainment.* **Santosh Gaihre MSc, Sean Semple PhD, Janice Miller MBChB, Shona Fielding PhD, Steve Turner MD.**
14. *Associations between classroom CO₂ concentrations and student attendance in Washington and Idaho.* **D, Shendell D.G. Prill R. Fisk W.J. Apte M.G. Blake D. Faulkner.**
15. *The effects of bedroom air quality on sleep and next-day performance.* **P. Strøm-Tejsen, D. Zukowska, P. Wargocki, D. Wyon.**
16. *Do Indoor Pollutants and Thermal Conditions in Schools Influence Student.* **Mark J. Mendell, Garvin A. Heath.**
17. *Would removing indoor air particulates in children's environments reduce rate of absenteeism.* **Rosen, K. G., and G. Richardson.**
18. *The synergistic effect of PM_{2.5} and CO₂ concentrations on occupant satisfaction and work productivity in a meeting room.* **Wu, J., Weng, J., Xia, B., Zhao, Y., Song, Q.**
19. *Children exposure to atmospheric particles in indoor of Lisbon primary schools.* **Almeida, S.M., Canha, N., Silva, A., Do Carmo Freitas, M., Pegas, P., Alves, C., Evtugina, M., Pio.**
20. *Particulate matter and student exposure in school classrooms in Lublin, Poland.* **Polednik, B.**
21. *Indoor environment in schools: Pupils' health and performance in regard to CO₂ concentrations.* **Myhrvold, A. N., E. Olsen, and O. Lauridsen.**
22. *The effects of moderate heat stress on mental performance.* **Wyon DP, Andersen I, Lundqvist GR.**
23. *Creative thinking as the dependent variable in six environmental experiments: A review.* **D.P., Wyon.**
24. *Room air temperature affects occupants' physiology, perceptions and mental alertness.* **Kwok Wai Tham, Henry Cahyadi Willem.**
25. *Individual microclimate control: Required range, probable benefits and current feasibility.* **D.P., Wyon.**
26. *Studies of Children under Imposed Noise and Heat Stress.* **WYON, D. P.**
27. *Experimental and numerical research to assess indoor environment quality and schoolwork performance in university classrooms.* **Ioan Sarbu, Cristian Pacurar.**

28. *Effects of classroom ventilation rate and temperature on students' test scores.* **U. Haverinen-Shaughnessy, R. Shaughnessy.**
29. *Temperature, Test Scores, and Educational Attainment.* **Park, Jisung.**
30. *Indoor environmental effects on productivity .* **Wyon, D.**
31. *Effects of thermal discomfort in an office on perceived air quality, SBS symptoms, physiological responses, and human performance.* **L. Lan, P. Wargocki, D. Wyon, Z. Lian.**
32. *Thermal comfort in classroom: constraints and issues.* **Marzita Puteh, Mohd Hairy Ibrahim, Mazlini Adnan, Che Nidzam Che Ahmad, Noraini Mohamed Noh.**
33. *More Than An Education, Leadership for Rural School-Community Partnerships.* **Kilpatrick, S., Johns, S., Mulford, B., Falk, I., & Prescott, L.**
34. *The Rural Economic Capacity Index (RECI): A benchmarking Tool to Support Community-Based Economic Development.* **Simms, A., Freshwater, D., & Ward, J.**
35. *Community Economic Development in Utah.* **Wrigley, W.N., Lewis C.**
36. *Policy Versus Place Luck: Achieving Economic Prosperity.* **Reese, L.A., Ye, M.**
37. *The Economic and Social Contribution of the Public Sector to Rural Saskatchewan.* **Martz, J.F., & Sanderson, K.**
38. *Conference Report: First National Research Conference on Children's Environmental Health. Network), CEHN (Children's Environmental Health.*
39. *School facilities: America's schools report differing conditions.* **Office., General Accounting.**
40. *Indoor temperature, relative humidity and CO2 levels assessment in academic buildings with different heating, ventilation and air-conditioning systems.* **Ayesha Asif, Muhammad Zeeshan, Muhammad Jahanzaib.**
41. *A comparative study of thermal comfort in learning spaces using three different ventilation strategies on a tropical university campus.* **Stephen Siu Yu Lau, Ji Zhang, Yiqi Tao.**
42. *Air movement acceptability limits and thermal comfort in Brazil's hot humid climate zone.* **C.Cândido, R.J.de Dear, R.Lamberts, L.Bittencourt.**
43. *Thermal and visual comfort of schoolchildren in air-conditioned classrooms in hot and humid climates.* **Lumy Noda, Amanda V.P. Lima, Jullyanne F. Souza, Solange Leder, Luana M. Quirino.**

44. *Thermal Comfort in Tropical Classrooms*. Kwok, Alison G.
45. *Adaptive thermal comfort in university classrooms in Malaysia and Japan*. S.A. Zaki, S.A. Damiaty, H.B. Rijal, A. Hagishima, A. Abd Razak.
46. *Comfort temperature prediction according to an adaptive approach for educational buildings in tropical climate using artificial neural networks*. L.A. López-Pérez, J.J Flores-Prieto, C. Ríos-Rojas.
47. *Experimental study on thermal environment in a simulated classroom with different air distribution methods*. Weixin Zhao, Sami Lestinen, Panu Mustakallio, Simo Kilpeläinen, Juha Jokisalo, Risto Kosonen.
48. *Energy Standard for Buildings Except Low-Rise Residential Buildings*. American Society of Heating, Refrigerating.
49. [Online] https://re.jrc.ec.europa.eu/pvg_tools/en/.
50. Guidelines, IES VE. [Online]
51. Sons, John Wiley &. *Mechanical Engineers' Handbook: Energy and Power, Volume 4, Third Edition*. s.l. : Myer Kutz, 2006.
52. *Productivity is affected by the air quality in offices*. Wargocki P., Wyon D.P., Fanger P.O.
53. *Ten questions concerning thermal and indoor air quality effects on the*. Pawel Wargocki, David P. Wyon.
55. *Do School Facilities Affect Academic Outcomes?* Schneider, Mark.
56. *Field study on adaptive thermal comfort in a typical air-conditioned classroom*. Z. Fang, S. Zhang, Y. Cheng, A.M.L. Fong, M.O. Oladokun, Z. Lin, H. Wu.
57. *Evaluation of strategies that improve the thermal comfort and energy saving of a classroom of an institutional building in a tropical climate*. Loyde V. de Abreu-Harbach, Victor L.A. Chaves, Maria Carolina G.O. Brandstetter.
58. [Online] <https://media3.bosch-home.com/Documents/specsheet/it-IT/WAV28MA9II.pdf>.
59. [Online] https://www.lighting.philips.it/api/assets/v1/file/PhilipsLighting/content/fp929001889702-pss-it_it/929001889702_EU.it_IT.PROF.FP.pdf.
60. [Online] <https://media3.bosch-home.com/Documents/specsheet/it-IT/SMV4EDX17E.pdf>.

61. [Online] https://www.download.p4c.philips.com/files/3/32pfs5603_12/32pfs5603_12_pss_itait.pdf?_gl=1*bmqslq*_ga*MTE1MTcyMTE1MC4xNjM0NzE5OTE2*_ga_2NMXNNS6LE*MTYzNDcxOTkxNS4xLjEuMTYzNDcxOTkyMy41Mg..&_ga=2.230672927.244468814.1634719916-1151721150.1634719916.
62. [Online] <https://www.samsung.com/it/cooking-appliances/ovens/compact-oven-nq50t8939bk-et/>.
63. [Online] PF_CNPesf 4613 001 21_it_IT.pdf (liebherr.com).
64. [Online] <https://www.lg.com/it/microonde/lg-MJ3965BPS>.
65. [Online] https://eu.dlink.com/it/it/-/media/consumer_products/dsl/dsl-3788/dsl_3788_b2_datasheet_eu_it.pdf.
66. [Online] <https://www.ariete.net/script/product-sheet/id/Jet-Force-2791-cyclonic-vacuum-cleaner>.
67. [Online] multi_srk-skm_R32.pdf (mitsubishi-termal.it).
68. [Online] https://www.philips.it/c-p/GC4537_70/azur-ferro-da-stiro.
69. [Online] <https://www.hp.com/it-it/shop/product.aspx?id=W5D55AA&opt=ABZ&mastersku=W5D55AA&masteropt=ABZ&sel=ACC&>.
70. [Online] <https://www.apple.com/it/shop/product/MGN13ZM/A/alimentatore-usb-apple-da-5w?fnode=40e91c148ad679952cf1d295bec47898e3cadb5c8a1eb869d05a212fbdd6cef2bab4a6cfbb5e1785b93d8a8fc0eae550a2a2a2ef6b16c4fff699fab5e6402796992bc9cb156f21c6fb336d7eea3141611f375209dda9>.
71. [Online] DYSON SUPERSONIC GENTLE AIR | Euronics.
72. <https://www.mdpi.com/1996-1073/11/3/607>. *The Determination of Load Profiles and PowerConsumptions of Home Appliances*. s.l.: Fatih Issi , Dand Orhan Kaplan, 2018.
73. [Online] https://www.researchgate.net/publication/260523367_Load_Profiles_of_Selected_Major_Household_Appliances_and_Their_Demand_Response_Opportunities.
74. https://www.aleo-solar.com/app/uploads/sites/6/2016/02/P23_320-325W_IT_web.pdf.

75. [Online] <https://www.europe-solarstore.com/download/byd/BYD-Battery-Box-Pro-13.8-datasheet.pdf>.

76. [Online] <https://www.huayu-solar.com/off-grid/5kw-off-grid-solar-inverter/5kw-off-grid-home-battery-solar-inverter.html>.

List of Figures

Figure 1-1-1: Experimental relationship between air supply rate x child and classroom performance of schoolwork.....	13
Figure 1-1-2: How IAQ affect cognitive performance	14
Figure 1-1-3: Casual link between academic performance and poor IAQ	15
Figure 1-1-4: Metabolic heat production according to ANSI/ASHRAE Standard 55-1992	17
Figure 1-1-5: Comfort zone according to ASHRAE 55-1992.....	18
Figure 1-1-6 : Air temperature and thermal sensation vote relation with performance	19
Figure 1-1-7: Temperature and academic performance correlation.....	20
Figure 2-2-1: Top view of Institución Educativa Santa Lucia	29
Figure 2-2-2: Localization of Santa Lucia in Colombia	29
Figure 2-2-3: Köppen-Geiger classification.....	30
Figure 2-2-4: Dry-bulb temperature	31
Figure 2-2-5: Dry bulb temperature from 17/05 to 23/05.....	32
Figure 2-2-6: Relative humidity color gradient chart	32
Figure 2-2-7: Global, Direct, Diffused Radiation level	33
Figure 2-2-8: Daily wind data measurement	34
Figure 2-2-9: Wind Speed Distribution.....	35
Figure 2-2-10: Distribution of Wind Direction	36
Figure 2-2-11: Annual Windrose	36
Figure 3-3-1: Top view of Institución Educativa Santa Lucia	37
Figure 3-3-2: Outside view of a classroom	37
Figure 3-3-3: Dwg of second floor	38
Figure 3-3-4: Dwg of first floor	38
Figure 3-3-5: East solar exposure.....	45
Figure 3-3-6: North solar exposure	46
Figure 3-3-7: South solar exposure.....	46

Figure 3-3-8: Planimetry of 1 st and 2 nd floor	47
Figure 3-3-9: Building digital twin created by IES-VE	47
Figure 3-3-10: Concrete block properties	48
Figure 3-3-11: Roof layer properties.....	48
Figure 3-3-12: Internal ceiling roof properties.....	48
Figure 3-3-13: Windows properties.....	48
Figure 3-3-14: Openings dimension	49
Figure 3-3-15: Daily Internal Daily Profile	51
Figure 3-3-16: Daily occupancy profile.....	51
Figure 3-3-17: School Yearly Calendar	51
Figure 3-3-18: Air Handling Unit with Recirculation.....	53
Figure 3-3-19: AHU System Architecture	54
Figure 3-3-20: Sensor logic.....	54
Figure 3-3-21: Week Air Temperature & Humidity inside the classrooms.....	55
Figure 3-22: HP Characteristics	56
Figure 3-23: Water Loop Scheme.....	56
Figure 3-24: Cooling power Characteristics.....	57
Figure 3-3-25: Fan system	58
Figure 3-3-26: Technical characteristic of the fan	58
Figure 3-3-27: Energy Consumption Breakdown	59
Figure 3-3-28: Total, Sensible and Latent Cooling Loads	60
Figure 3-3-29: Electrical Consumption Breakdown.....	61
Figure 3-3-30: Packaged Terminal Air Conditioning System.....	62
Figure 3-3-31: Packaged Air Conditioning System Architecture.....	63
Figure 3-3-32: Control logic of humidity and temperature sensors	64
Figure 3-3-33: DX Cooler characteristic	67
Figure 3-3-34: Technical characteristic of the fan	69
Figure 3-3-35: Energy Consumption Breakdown	70
Figure 3-3-36: Total, Sensible, Latent Cooling Loads	71

Figure 3-3-37: Electrical Consumption Breakdown.....	72
Figure 4-4-1: Top view of Institución Educativa Santa Lucia	75
Figure 4-4-2: Solar altitude the 21 st of December	76
Figure 4-4-3: Main characteristic of PV module.....	77
Figure 4-4-4: PV system architecture	78
Figure 4-4-5: Main characteristics of PV module	80
Figure 4-4-6: Battery Datasheet.....	84
Figure 4-4-7: Daily Energy Loads & Production.....	86
Figure 4-4-8: Production & Demand energy difference.....	87
Figure 4-4-9: SOC along the year.....	88
Figure 4-4-11: Daily Energy Loads & Production.....	90
Figure 4-4-12: SOC along the year.....	91
Figure 4-4-13: Inverter datasheet.....	93
Figure 5-1: External Wall Stratigraphy.....	98
Figure 5-2: External Walls Conduction Gain	99
Figure 5-3: Roof Stratigraphy.....	99
Figure 5-4: Roof Conduction Gain	100
Figure 5-5: Windows Stratigraphy.....	100
Figure 5-6: Windows Conduction and Solar Gain.....	101
Figure 5-9: Energy Breakdown + % reduction of consumption with new envelope	102
Figure 5-10: Total Cooling Loads	103
Figure 5-11: Yearly battery SoC.....	104
Figure 5-11: Yearly battery SoC.....	107

List of Tables

Table 1-1 Contaminant levels permitted according to EPA standards.....	11
Table 4-1: Main parameters of the system	78
Table 4-2- Appliances of the school	79
Table 4-3-System efficiencies	80
Table 4-4- Overview of electric production and consumption	83
Table 4-5: Storage system components.....	96

Acknowledgments

I want to thank my family for the unconditioned support.

I want to thank Professor Antonio Bula to make this thesis project possible. I want to thank Professor Marcello Aprile to believe in me and to support. I want to thank all the Politecnico di Milano students that I meet during this journey, who shared with me the pain, the suffer and difficulties during the various project and exams. I want to thank the person with who I lived and spent most of the time with since I started my master that now is no more in my life. I want to thank me to have been able to arrive until the end despite all the moment I was thinking to quit.

